ADVANCES IN PHYSICS

A QUARTERLY SUPPLEMENT of the PHILOSOPHICAL MAGAZINE

VOLUME 10 JANUARY 1961 NUMBER 37

PRICE per part 25*s.* plus postage
PRICE per annum £4 15*s.* 0*d.* post free

PRINTED AND PUBLISHED BY TAYLOR & FRANCIS, LTD
RED LION COURT, FLEET ST., LONDON E.C.4

CONTENTS

The Ordinary Transport Properties of the Noble Metals. By J. M. Ziman, Cavendish Laboratory, University of Cambridge . . . 1

The Many-body Theory of Electrons in Metal or Has a Metal Really Got a Fermi Surface? By L. M. Falicov and V. Heine, Royal Society Mond Laboratory, Cambridge 57

ADVANCES IN PHYSICS
A QUARTERLY SUPPLEMENT
of the
PHILOSOPHICAL MAGAZINE

VOLUME 10 1961 NUMBER 37

The Ordinary Transport Properties of the Noble Metals

By J. M. ZIMAN
Cavendish Laboratory, University of Cambridge

" *Only connect . . .* "
E. M. Forster.

CONTENTS

§ 1. THE NEED FOR A QUANTITATIVE THEORY.
§ 2. THE OBSERVED FERMI SURFACE.
§ 3. THE ENERGY SURFACES.
§ 4. NECK DIMENSIONS AND ENERGY GAP.
§ 5. DENSITY OF STATES.
§ 6. OPTICAL MASS.
§ 7. HALL EFFECT.
§ 8. MAGNETORESISTANCE.
§ 9. ELECTRICAL CONDUCTIVITY
§ 10. THERMAL CONDUCTIVITY
§ 11. THERMOELECTRIC POWER: THE ' DIFFUSION ' TERM.
§ 12. THERMOELECTRIC POWER: PHONON DRAG.
§ 13. SOME UNDOUBTED FACTS AND UNCERTAIN THEORIES.
ACKNOWLEDGMENTS.
REFERENCES.

ABSTRACT

The Fermi Surfaces in Cu, Ag and Au are now known to be greatly distorted, with thick ' necks ' passing through the zone boundaries. In this paper we enquire whether such an electronic structure is quantitatively consistent with the observed transport coefficients. The mathematical model is quite simple; the shape of the Fermi surface is made to depend on a single parameter which can be interpreted as the pseudo-potential of the {111} atomic planes acting on an orthogonalized plane wave, giving rise to an energy gap of 5–10 ev at the zone boundaries. Various integrals over the Fermi surface can then be evaluated by elementary methods, and compared with the corresponding experimental quantities. The electronic specific heat and optical mass in the pure metals are consistent with the model. The galvanomagnetic effects are shown to depend a great deal on the anisotropy of the electron relaxation time, whose variation with energy is also probably the main determinant of the sign of the thermoelectric power. A better theory of electron–phonon interaction is needed before this, and the electrical and thermal conductivities, can be calculated accurately. Generally speaking there is no evidence which directly contradicts the rigid band model, except perhaps the effect of alloying on the optical absorption edges and on the electronic specific heat, but there are still many experimental and theoretical gaps in our knowledge.

§ 1. The Need for a Quantitative Theory

The free-electron model of a metal has an interesting history. Once upon a time it threw a brilliant light upon the properties of metals, and was the basis of the whole theory. Then the ideas of Bloch and of Brillouin were developed and attempts were made to calculate everything in terms of zones and bands and localized atomic orbitals. Now more recent work has suggested (Phillips and Kleinman 1959, Harrison 1959) that a single orthogonalized plane wave, with nearly the energy of a free electron, may be a remarkably good representation of the electron wave function except for wave vectors very near to the boundary of a Brillouin zone. Thus, we may return to a Fermi surface approximating to a sphere, in the extended zone scheme, with modifications and changes of connectivity only in the neighbourhood of the zone boundary planes.

If we apply this principle to the monovalent metals, we expect to find very simple Fermi surfaces; a perfect sphere with one electron per atom does not even touch the zone boundary in the body-centred and face-centred structures. This is not what is observed. Na, true, seems to be very close to the free-electron model, but even for the other alkali metals there is indirect experimental evidence (Cohen and Heine 1958, García-Moliner 1958a, Ziman 1959a) that the Fermi surface is quite distorted, and perhaps touches the zone boundary, in Li, Rb and Cs. Unfortunately these metals are not easily studied: it is difficult to make single crystals, there is a phase transformation at low temperatures, and 'doping' with suitable impurities is not easy. For the noble metals, however, the evidence is incontrovertible: the anomalous skin effect (Pippard 1957), the de Haas–van Alphen effect (Shoenberg 1960), high field magnetoresistance (Alekseevskii and Gaidukov 1959, Priestley 1960), cyclotron resonance (Langenberg and Moore 1959), ultrasonic attenuation (Gavenda and Morse 1959), all show that the Fermi surface touches the zone boundaries in the [111] directions, with an appreciable area of contact. The magnetic phenomena are, indeed, absolute in that they show the existence of small minimal cross-sections at the Fermi surface corresponding to cuts through the 'necks' passing through the zone faces. One can also demonstrate that the Fermi surface must be multiply-connected, for electrons in 'open' orbits are also observed. These methods are capable of giving 'topological' data about the Fermi surface, and show that is very far from a simple sphere.

The information from all these experiments is very valuable, but it has some serious limitations; in every case the specimen must be extremely pure, and must be at extremely low temperatures in order that the relaxation time of the electrons, for scattering by lattice waves or impurities, shall not be too short. One is inevitably restricted to a small region in the corner of the phase diagram of the metal and its alloys. This is unfortunate, for we have no guarantee that the electronic energy surfaces in **k**-space remain unchanged when other metals are added to a noble metal, or when the lattice is strongly perturbed by thermal

vibrations. Indeed, Cohen and Heine (1958) have specifically proposed that this 'rigid band' hypothesis must be abandoned if we are to understand certain properties of the alloys of the noble metals. It would obviously be valuable to have an independent check on this point.

At the same time, there are many published measurements of the more 'ordinary' transport coefficients of the noble metals. Thus, we have data on the electrical and thermal conductivities, thermoelectric power, Hall coefficient, magnetoresistance, residual resistance per impurity atom, etc., at all temperatures and for a wide variety of specimens—pure metals, single crystals, cold-worked wires, alloys, etc. There are also observations of the optical properties, the Knight shift, and of the electronic specific heats, which are not confined to the special conditions of the 'topological' techniques.

Now all these experimental results have one feature in common—they do not fit at all neatly into a free-electron model. The coefficients are often of the wrong sign, show anomalies of functional behaviour with temperature and impurity content, do not satisfy similarity conditions like Matthiessen's Law and Kohler's Rule and are certainly very seldom in quantitative agreement with theory. Of course we have now an easy way out; we attribute the anomalies to the complicated shape of the Fermi surface. Thus, we say that the positive thermoelectric power is due to the 'hole' states near the contact region, and that the large magnetoresistance is due to the large distortion of the Fermi surface. But it is very necessary to make these arguments quantitative and precise if we are to construct a consistent picture of the electronic states in the metal. Not all the phenomena are even properly understood in principle, so that we do not know whether we can get by with the rigid band model or whether we must, indeed, invoke the Cohen and Heine hypothesis in order to explain what we see in alloys. The matter is still very much open to discussion.

The main purpose of this review is to give a quantitative numerical framework to these problems. We use a particular model of the energy surfaces in the noble metals, soundly based on theory, consistent with the topological results, but sufficiently simple that many important physical parameters can be computed by schoolboy calculus. Each of the properties is reviewed in turn, and comparison made between the theory and the actual observations. In this way, one can bring out the really difficult points, and show where there are still serious discrepancies. It is hoped that a quantitative theory may encourage further careful and reliable experiments; it is not at all easy to be sure that some of the reported phenomena are not due merely to accidental impurities in the specimens; for example it would be extremely profitable to make measurements of a number of different transport properties on the same specimen, at the same temperature, to avoid random errors from this source. A number of interesting theoretical problems are also raised. Near the 'necks' the electron energy surfaces are hyperboloidal, rather

than ellipsoidal, and this requires an entirely new technique in such problems as scattering by impurities. It will be suggested that much may depend on the anisotropy of the relaxation time of the electrons; we need a good theory of this effect. These problems are not treated in this review, but obviously merit study.

I have one further, personal, motive. Having just written a book (Ziman 1960—to be referred to as E & P) on the theory of the transport properties of metals in general, I am interested in applying this theory in detail to a particular group of metals and, where necessary, modifying and extending the general argument. To avoid unnecessary formal theory and its bibliographical background, reference will be made to this book for many points which are there completely documented.

§ 2. The Observed Fermi Surface

The noble metals crystallize in the face-centred cubic structure with the lattice constants given in table 1. From the atomic volume alone, using the simple free electron model, one can deduce certain theoretical parameters, which are also recorded here for reference.

Table 1

Metal	Cu	Ag	Au
Lattice constant a (Å at 20°C)	3·608	4·078	4·070
Atomic radius (Å)	1·41	1·59	1·59
Fermi energy, for free electrons (ev)	7·04	5·51	5·51
Electronic specific heat parameter (γ) for free electrons (millijoules/mol (°K)^2)	0·502	0·644	0·644
Hall constant for free electrons $=(Ne\boldsymbol{c})^{-1}$ (cm^3/coulomb)	$-7{\cdot}45\times10^{-5}$	$-10{\cdot}65\times10^{-5}$	$-10{\cdot}60\times10^{-5}$

The reciprocal lattice is body-centred cubic, with the Brillouin Zone shown in fig. 1. This has eight hexagonal faces, with normals in the {111} directions and six square faces which are the {200} planes. For our purposes, the most important scale parameter in this figure is p, the distance ΓL from the origin to the midpoint of a hexagonal face. In terms of this distance,

$$\Gamma X=(2/\sqrt{3})p=1{\cdot}155p\,;\quad \Gamma K=\Gamma U=\sqrt{(\tfrac{3}{2})}p=1{\cdot}225p\,;$$
$$\Gamma W=\sqrt{(\tfrac{5}{8})}p=1{\cdot}290p,$$

and the side of one of the squares or hexagons is $\sqrt{(\frac{2}{3})}p = 0{\cdot}817p$. Thus L is the symmetry point on the zone boundary nearest to the origin, followed by X, K and U, and W, in that order.

The volume of the zone is $(32/3\sqrt{3})p^3 = 6{\cdot}16p^3$. If there is but one electron per atom, the Fermi surface must enclose just half this volume. If the electrons were free, the sphere would have a radius

$$(4/\pi\sqrt{3})^{1/3}p = 0{\cdot}902p.$$

This sphere approaches, but does not touch the zone boundary even at the centre of a hexagonal face. Thus, it takes a substantial perturbation,

Fig. 1

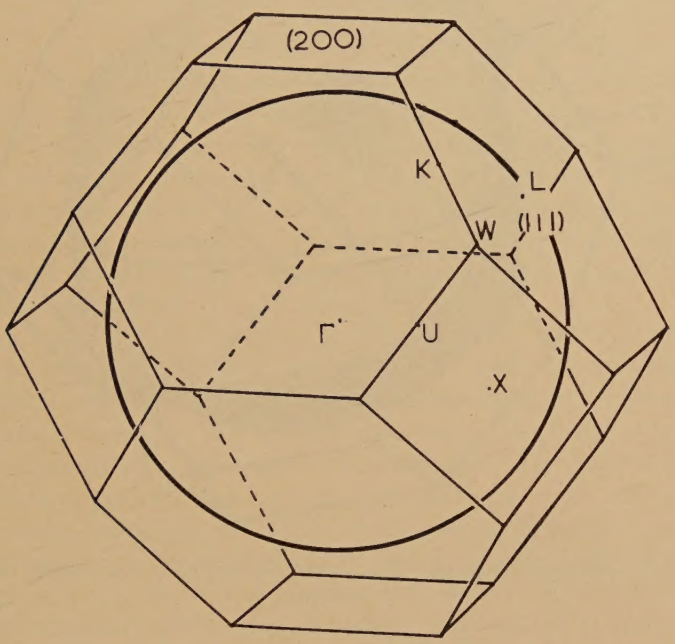

The Brillouin zone for a face-centred cubic lattice, showing a sphere containing one electron per atom.

of the single orthogonalized plane waves to change the noble metals from ideal free-electron systems; there is no direct geometrical necessity, as in a polyvalent metal, for the Fermi surface to cut the zone boundary at all.

The actual situation seems to be as in fig. 2. The Fermi surfaces in all three metals are drawn to the zone boundaries, and make contact. The diameter of the 'neck' formed between the surface in one zone and its image across the zone boundary is quite appreciable; Shoenberg (1960) gives the values in table 2 from his direct measurements of the de Haas–van Alphen periods of orbits encircling these necks. These data

are consistent with the results of ultrasonic-attenuation experiments (Gavenda and Morse 1959) and with the magnetoresistance work on single crystals (Alekseevskii and Gaidukov 1959, Priestley 1960).

Fig. 2

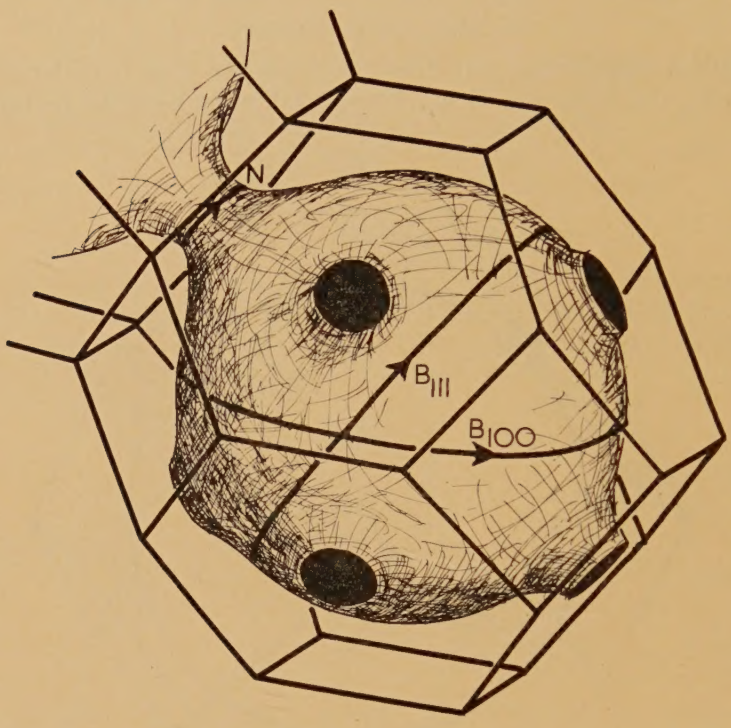

A sketch of the Fermi surface of a noble metal, showing 'neck' and 'belly' orbits.

Table 2

	Cu	Ag	Au
Neck radius, r	$0{\cdot}18p$	$0{\cdot}13p$	$0{\cdot}16p$
Effective masses, m_H* (Free-electron mass units)	1·30–1·38 (belly)	0·7 (belly)	1·2 (belly) 0·5 (neck)

Other finer details of the shape of the Fermi surface are still in dispute. Thus, the 'belly' circuits in the {111} and {103} planes, as observed by the de Haas–van Alphen effect, do not seem quite to agree with Pippard's measurements (1957) on the anomalous skin effect. The experiments

also give rough estimates of the 'effective masses' of the electrons on some of the orbits—i.e. the cyclotron masses

$$m_H^* = \frac{\hbar^2}{2\pi}\frac{d\mathscr{A}(k_z)}{d\mathscr{E}} \quad . \quad . \quad . \quad . \quad . \quad . \quad . \quad (2.1)$$

where $\mathscr{A}$ is the area of the cross section, normal to the magnetic field, of the surface of energy $\mathscr{E}$. For Cu, these dynamical data are more or less consistent with the direct cyclotron resonance measurements of Langenberg and Moore (1959). It is obvious that further experiments using these various techniques will soon make these data more precise, and perhaps give a definite shape to the Fermi surface in each of the noble metals; for the moment we shall accept the figures in table 2 without comment.

§ 3. The Energy Surfaces

Our problem is to find an analytical function for surfaces having the shape shown in fig. 2, with the parameters of table 2. It would be agreeable if we could simply take over some calculation of the electronic structure from first principles, but (E & P, p. 112) the attempts that have been made so far do not accord at all with the experimental results that we have just considered. We must fall back on some phenomenological model which takes certain parameters from observation, and interpolates suitable surfaces between them.

There is a well-known interpolation formula due to Slater and Koster (1954), which is an explicit analytic function, with the proper symmetry and periodicity at all points in the repeated zone scheme. García-Moliner (1958 b) has shown that the surface proposed by Pippard (1957) can be fitted quite closely by a few terms of this formula. However, this formula has disadvantages for numerical computations, and its theoretical interpretation, based on the tight-binding approximation, is not very sound (although it can be thought of simply as a Fourier expansion of the energy in **k**-space, without physical significance in detail).

The contemporary philosophy of energy-band theory is quite different; free electrons have come back into fashion. Our model is going to be based on the 'nearly-free electron' approximation, which would have us write

$$\psi_{\mathbf{k}}(\mathbf{r}) = \sum_{\mathbf{g}} \alpha_{\mathbf{k}+\mathbf{g}} \phi_{\mathbf{k}+\mathbf{g}}(\mathbf{r}) \quad . \quad . \quad . \quad . \quad . \quad . \quad (3.1)$$

where **g** are the reciprocal lattice vectors, and the $\phi_{\mathbf{k}+\mathbf{g}}(\mathbf{r})$ are basically plane waves. In the original formulation of this method (E & P, § 2.2), they were simple plane waves,

$$\phi_{\mathbf{k}+\mathbf{g}}(\mathbf{r}) = \exp\left[i(\mathbf{k}+\mathbf{g})\,.\,\mathbf{r}\right], \quad . \quad . \quad . \quad . \quad . \quad (3.2)$$

and one found the coefficients $\alpha_{\mathbf{k}+\mathbf{g}}$ by substituting in the Schrödinger equation, and solving the set of linear equations

$$(\mathscr{E}_{\mathbf{k}+\mathbf{g}}{}^0 - \mathscr{E}_{\mathbf{k}})\alpha_{\mathbf{k}+\mathbf{g}} + \sum_{\mathbf{g}'} \mathscr{U}_{\mathbf{g}'}\alpha_{\mathbf{k}+\mathbf{g}+\mathbf{g}'} = 0 \quad . \quad . \quad . \quad . \quad (3.3)$$

for all values of $\mathbf{g}$. Here, of course, $\mathscr{E}_{\mathbf{k}}$ is the energy of the electron state $\psi_{\mathbf{k}}$, $\mathscr{E}_{\mathbf{k}}^{0}$ is the energy of the unperturbed state $\phi_{\mathbf{k}}$, and

$$\mathscr{U}_{\mathbf{g}} = \frac{1}{V}\int \mathscr{U}(\mathbf{r})\exp(-i\mathbf{g}.\mathbf{r})\,\mathbf{dr} \quad . \quad . \quad . \quad . \quad . \quad (3.4)$$

that is, it is a Fourier coefficient of the lattice potential which is causing the mixing of the simple plane wave states.

Although (3.1)–(3.4) constitute a formal Fourier expansion of the wave functions and a corresponding Fourier transform of the Schrödinger equation, this was thought to be an unsatisfactory method in practice because the series (3.1) converges so slowly. There is obviously little value in an interpolation formula for $\mathscr{E}_{\mathbf{k}}$ which depends on a large number of coefficients like $\mathscr{U}_{\mathbf{g}}$ through the solution of a secular equation of high order. But this judgement is too pessimistic.

The justification of the method comes from the theory of energy bands. It has long been known that in most metals a single orthogonalized plane wave is quite a good approximation to the wave function for values of $\mathbf{k}$ well inside the zone. In other words, if we take for $\phi_{\mathbf{k}+\mathbf{g}}(\mathbf{r})$ a suitable set of OPW's, instead of simple plane waves like (3.2), the expansion of $\psi_{\mathbf{k}}$ in (3.1) may converge very rapidly. Each OPW has already the rapid oscillations required to fit it into the atomic core with the correct number of nodes; there is no need to bring in a large number of higher Fourier components in order to represent this part of the wave function. We expect most of the coefficients that would then appear in place of (3.4) to be quite small and easily manageable by perturbation methods.

This point has been tested explicitly by Phillips and Kleinman (1959) who have shown that the orthogonalization condition is equivalent to a repulsive pseudo-potential which is spherically symmetrical and which balances out most of the real attractive potential due to the ordinary Hartree–Fock field of the ion. This cancellation seems to be almost complete inside the core; only a few of the lowest Fourier components, corresponding to the long range part of $\mathscr{U}(\mathbf{r})$, are at all important.

In our monovalent metals we know that the Fermi surface keeps well away from all the zone boundaries except the $\{111\}$ planes. This means that the effects, on the energy, of all coefficients of the lattice potential except $\mathscr{U}_{111}$ will be small. We can approximate to these effects by perturbation theory, writing

$$\mathscr{E}_{\mathbf{k}} \sim \mathscr{E}_{\mathbf{k}}^{0} - \sum_{\mathbf{g}\neq\{111\}} \frac{|\mathscr{U}_{\mathbf{g}}|^2}{\mathscr{E}_{\mathbf{k}-\mathbf{g}}^{0} - \mathscr{E}_{\mathbf{k}}^{0}} . \quad . \quad . \quad . \quad . \quad . \quad (3.5)$$

Roughly speaking, this gives rise to an increase of the effective mass by a more or less constant factor, and leaves us still with a nearly spherical Fermi surface. The really important parameter in determining the *shape* of the surface is $\mathscr{U}_{111}$, which causes the energy splitting on the $\{111\}$ faces at the zone, and hence fixes the amount of contact with those faces.

Thus, if we put into (3.1) a set of OPW's in place of the simple plane waves (3.2), then we may solve (3.3) for our energy function with only $\mathscr{U}_{111}$ and perhaps $\mathscr{U}_{200}$ not negligibly small. This should give us a range of interpolation functions, with only these two parameters to be fixed by appeal to experiment.

Even this is too complicated for our present purpose; we wish to represent the Fermi surface by a simple analytical function depending only on a single parameter whose value will be fixed by the size of the all-important 'necks' passing through the {111} faces. It is obvious that $\mathscr{U}_{111}$ is the key to this. Moreover, in the neighbourhood of a *particular* hexagonal face—the one bisecting the reciprocal lattice vector **g**, say—

Fig. 3

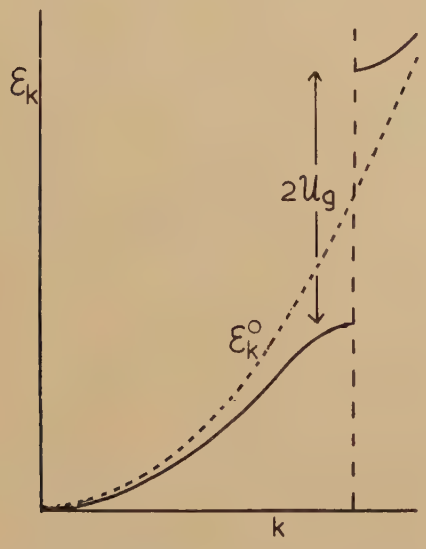

The energy gap at the zone boundary.

we may neglect all the terms in (3.1) except the two which are nearly degenerate when $\mathbf{k} \sim \frac{1}{2}\mathbf{g}$. The secular equation then reduces to a quadratic, whose lower root lies below $\mathscr{E}_{\mathbf{k}}^{0}$, by the amount

$$\mathscr{E}_{\mathbf{k}}^{0} - \mathscr{E}_{\mathbf{k}} = \tfrac{1}{2}\sqrt{\{(\mathscr{E}_{\mathbf{k}-\mathbf{g}}^{0} - \mathscr{E}_{\mathbf{k}}^{0})^2 + 4\mathscr{U}_{\mathbf{g}}^{2}\}} - \tfrac{1}{2}(\mathscr{E}_{\mathbf{k}-\mathbf{g}}^{0} - \mathscr{E}_{\mathbf{k}}^{0}). \quad . \quad (3.6)$$

At the zone boundary itself, this tends to $|\mathscr{U}_{\mathbf{g}}|$, so that the Fourier coefficient is just half the value of the 'energy gap' (at this point in **k**—space) between the two bands that are split by the action of the lattice potential (fig. 3). But as we go away from the zone boundary, we soon find that this expression is well approximated by the perturbation formula (3.5).

This formula is the basis of our model. *We assume that* $\mathscr{E}_{\mathbf{k}}$ *deviates from the spherically symmetric function* $\mathscr{E}_{\mathbf{k}}^{0}$ *by the amount* (3.6), *where* $\mathbf{g}$ *is the reciprocal lattice vector corresponding to the nearest hexagonal face of the zone.* The depression of the energy levels is thus greatest at points near the centres of the zone faces, so that the energy surfaces bulge out in these directions. In the neighbourhood of each {111} face, they are surfaces of revolution, with fairly simple geometrical and analytical properties. The shape of the necks depends only on the parameter $\mathscr{U}_{\mathbf{g}}$, i.e. $\mathscr{U}_{111}$, in (3.6), which is therefore fixed, for each metal, by the radius r in table 2. Thus, our model has no adjustable parameters to tempt us into melting the theory and pouring it into the mould of the facts! Similar models have been used previously for the analysis of particular phenomena (Jones 1957, Ziman 1959b; Suffczynski 1960), but this is the first comprehensive study of all the transport properties on the same basis.

There is one further mathematical approximation that is extremely convenient. The part of the Fermi surface that 'belongs' to a particular hexagonal face is certainly a surface of revolution, but its boundary—i.e. the frontier between two such regions—is a complicated curvilinear polygon. It would obviously be much more satisfactory if this boundary were simply a circle, as if each region of the Fermi surface were the cap of a circular cone with vertex at the centre of the zone and axis to the centre of a hexagonal face. Unfortunately one cannot map out the whole 4π solid angle in this way with circular cones facing along the {111} directions; some parts are left uncovered whilst other parts lie in intersecting cones (fig. 4). But in those regions where cones intersect the Fermi surface is nearly spherical, and its transport properties will not be very different from those of a portion of a sphere. The same is true of the regions which are left out (see fig. 5). Thus, so long as we make the total cap area and total volume of our eight cones equal to the total area and volume of the surface, it will cause very little error if we count some of these border lands twice over and leave out others altogether. The overall cubic symmetry of the figure saves us from any difficulty about the exact direction into which these bits of surface face. In other words we choose the vertex angle of each cone so that it subtends one-eighth of a whole solid angle, i.e. $\pi/2$ steradians, and ignore the fact that they will not all pack properly together without overlap. The enormous gain in mathematical simplicity more than balances the small errors introduced by this approximation.

As we have seen, there is good theoretical ground for our present standpoint. Nevertheless, (3.6) is only an approximation, and one might wish to improve the model for a very exact numerical computation. For example, what happens when we are near a [110] direction—the point K in fig. 1. We are in the neighbourhood of two hexagonal faces, both of which will exert their influence on the energy surfaces. For points in the plane of symmetry containing the zone edge KW, one can

Fig. 4

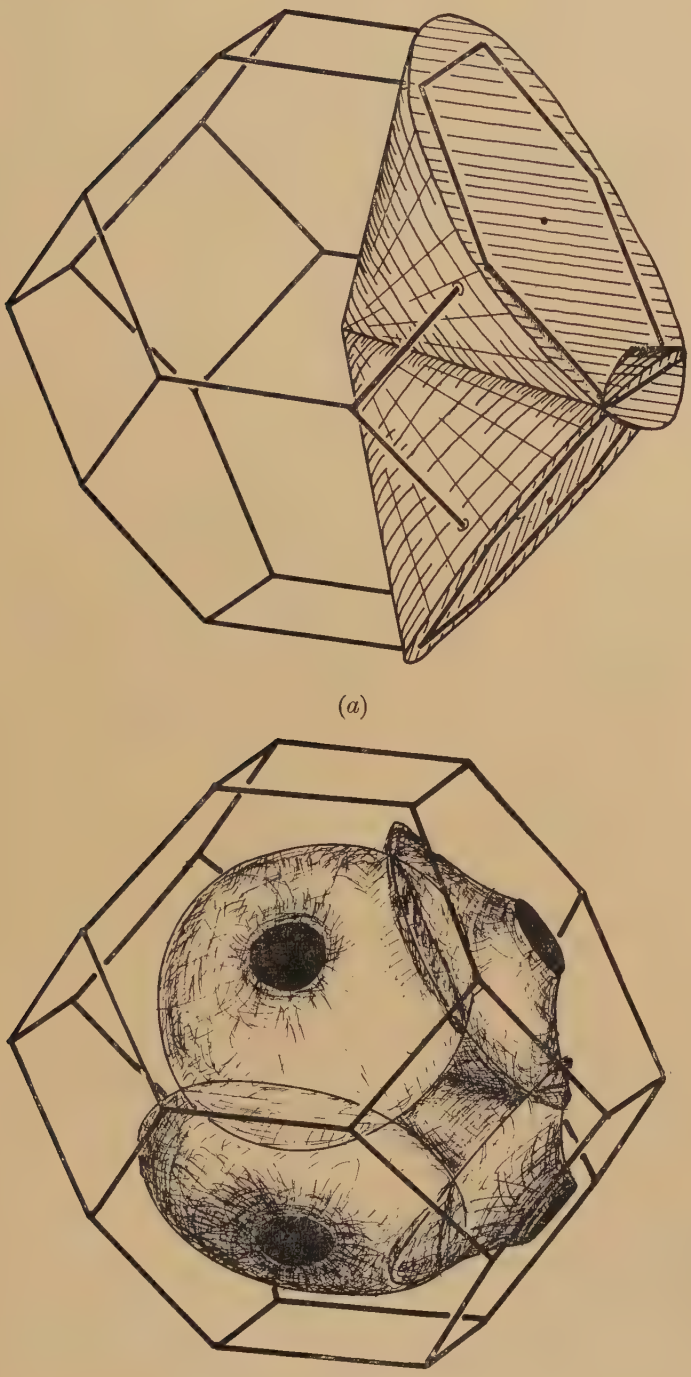

(*a*)

(*b*)

Eight cones cannot be fitted together without intersecting.

solve the secular equation; it turns out that one must double the value of $\mathscr{U}_g^2$ in (3.6), and hence increase, by a factor $\sqrt{2}$, the energy gap there. As shown in fig. 5, this pulls the surfaces out a bit towards these edges, without materially changing them from a nearly spherical form.

Again, we expect the [200] component of the equivalent potential to be comparable with $\mathscr{U}_{111}$. This will cause the surfaces to bulge a little towards the square faces of the zone—the regions which are not covered by the cones in fig. 4. But the distances from a Fermi sphere to these faces weakens this effect. As shown in fig. 5 (where we have taken $\mathscr{U}_{200} = \mathscr{U}_{111}$), there is

Fig. 5

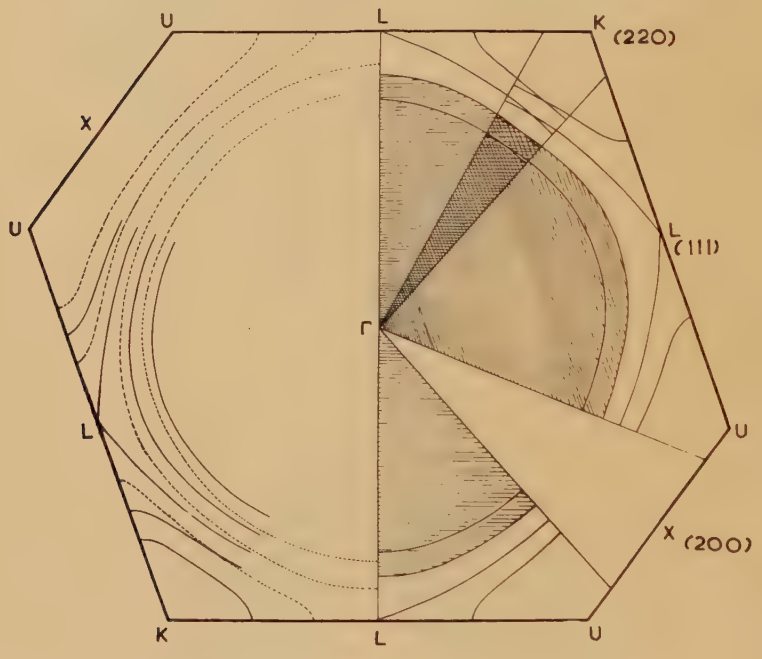

Energy contours in a section of the zone.
———— as used in the 8-cone model; – – – – allowing for the effects of the two {111} faces near K and of the {200} faces near X.
The regions where cones interest, or that are left out, are shown on the right.

little deviation from a spherical form, and the calculated value of a transport coefficient would not depend very much on the value of $\mathscr{U}_{200}$. Incidentally, this may be the clue to the difficulty noted by Shoenberg (1960), that the belly circuits normal to (100) seemed to have a larger area than those normal to (111). By increasing $\mathscr{U}_{200}$, one could pull out the surfaces a bit towards the square faces, where they are traversed by the former circuits (see fig. 2), without altering the shape in the other regions.

Finally, we must say something about the form of $\mathscr{E}_{\mathbf{k}}^{0}$, the energy of a single OPW before it has been influenced by the pseudo-potential of the lattice. This is not necessarily the energy of a simple free-electron, although it is probably spherically symmetrical. We shall assume

$$\mathscr{E}_{\mathbf{k}}^{0} = \hbar^2 k^2 / 2m^* \quad . \quad . \quad . \quad . \quad . \quad . \quad . \quad . \quad (3.7)$$

where m^* is an 'effective mass' parameter, which is not known *a priori*. In other words, we introduce this as an adjustable parameter, which fixes the energy scale of the band structure in each metal. However, the experimental data are sufficient to determine m^* in various ways, so that a consistency check is possible. In principle, m^* can be calculated directly if one knows the core potential etc, but this is a lengthy and difficult computation except for an atom of small atomic number. We have already noted in (3.5) that the apparent value of m^* will depend also on the lattice pseudo-potential, $\mathscr{U}_{\mathbf{g}}$, as a perturbation effect from all the distant zone boundaries. We shall, of course, always quote m^* in units of the free-electron mass.

§ 4. Neck Dimensions and Energy Gap

The differential geometry of the cones is surprisingly simple. Each cone must subtend the solid angle $4\pi/8$, so that its vertex angle is $\cos^{-1}(\frac{3}{4})$ (fig. 6). The axis of the cone is a vector, $\frac{1}{2}\mathbf{g}$, to a [111] face, and this we take to be of length p, and as the local z axis. It is convenient to introduce dimensionless coordinates $x \equiv k_x/p$, $y \equiv k_y/p$, $z \equiv k_z/p$, and to measure energy in terms of the dimensionless variable

$$\epsilon \equiv \mathscr{E}_{\mathbf{k}}/(\hbar^2 p^2/m^*). \quad . \quad . \quad . \quad . \quad . \quad . \quad . \quad (4.1)$$

For the Fourier component of the lattice pseudo-potential we introduce the parameter

$$u \equiv \mathscr{U}_{111}/(\hbar^2 p^2/m^*). \quad . \quad . \quad . \quad . \quad . \quad . \quad . \quad (4.2)$$

The energy surfaces defined by (3.6) and (3.7) are now given by

$$\epsilon = \tfrac{1}{2}(x^2+y^2) + f(z), \quad . \quad . \quad . \quad . \quad . \quad . \quad . \quad (4.3)$$

where

$$f(z) \equiv \tfrac{1}{2} + \tfrac{1}{2}(1-z)^2 - \sqrt{\{u^2 + (1-z)^2\}}. \quad . \quad . \quad . \quad . \quad (4.4)$$

Each surface terminates on the sloping sides of the cone at some ordinate z_1. Since the cone has the equation

$$x^2 + y^2 = z^2 \tan^2(\cos^{-1}\tfrac{3}{4}) = \tfrac{7}{9} z^2, \quad . \quad . \quad . \quad . \quad . \quad . \quad (4.5)$$

we can find z_1, for a particular value of ϵ, by the relation

$$\epsilon = \tfrac{7}{18} z_1^2 + f(z). \quad . \quad . \quad . \quad . \quad . \quad . \quad . \quad . \quad (4.6)$$

This same energy surface will either cut the z axis at some point z_2 given by

$$\epsilon = f(z_2), \quad . \quad . \quad . \quad . \quad . \quad . \quad . \quad . \quad (4.7)$$

or it will meet the zone boundary, at $z_2 = 1$, on a circle of radius

$$r = p\sqrt{(2\epsilon + 2u - 1)}. \quad . \quad . \quad . \quad . \quad . \quad . \quad . \quad (4.8)$$

Our first problem is to calculate the volume lying inside the cone below a certain energy surface. But this is just the sum of the volume of a right circular cone, of height z_1 and semi-angle $\cos^{-1}(\frac{3}{4})$—i.e. $(7\pi/27)\,z_1^3$—and the volume of the surface of revolution lying between z_1 and z_2, i.e.

$$\pi\int_{z_1}^{z_2}(x^2+y^2)dz = 2\pi\int_{z_1}^{z_2}\{\epsilon - f(z)\}\,dz. \quad . \quad . \quad . \quad . \quad (4.9)$$

These volumes are, of course, in units of p^3, and we must multiply this sum by 8 to get the total volume inside the energy surface ϵ. We know that the whole zone, of volume $(32/3\sqrt{3})p^3$, would hold exactly two

Fig. 6

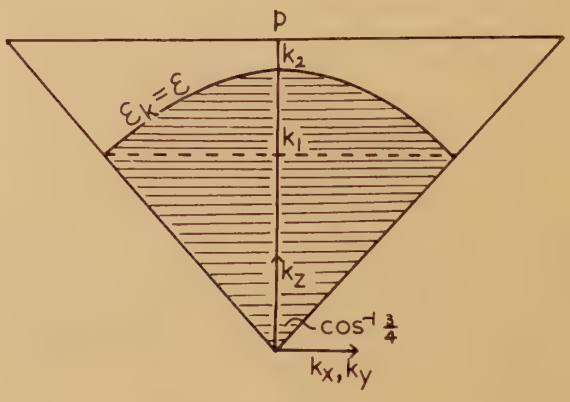

electrons per atom, so that the number of electrons per atom inside this surface is given by

$$\begin{aligned} n &= \frac{3\sqrt{3}}{16}\,.8\,.\pi\left[\frac{7}{27}z_1^3+\int_{z_1}^{z_2}[2\epsilon-1-(1-z)^2+2\sqrt{\{u^2+(1-z)^2\}}]\,dz\right] \\ &= \frac{3\sqrt{3}}{2}\,\pi\left[\frac{7}{27}z_1^3+(2\epsilon-1)(z_2-z_1)-\tfrac{1}{3}\{(1-z_1)^3-(1-z_2)^3\}\right. \\ &\quad +[(1-z_1)\sqrt{\{u^2+(1-z_1)^2\}}-(1-z_2)\sqrt{\{u^2+(1-z_2)^2\}}] \\ &\quad \left.+u^2\ln\left\{\frac{(1-z_1)+\sqrt{\{u^2+(1-z_1)^2\}}}{(1-z_2)+\sqrt{\{u^2+(1-z_2)^2\}}}\right\}\right]. \quad . \quad . \quad . \quad . \quad . \quad . \quad (4.10) \end{aligned}$$

We have given this formula in full to show that the integrations are quite elementary and all the algebraic operations are easily handled on a desk calculating machine. There is only one difficulty: z_1 and z_2 depend on ϵ through (4.6) and (4.7), so that we cannot just fix n and find u and ϵ. It is necessary to proceed in the following order: fix u and choose a value of z_1; calculate ϵ from (4.6); solve (4.7) for z_2 (if $z_2<1$); substitute for u, z_1, z_2 and ϵ in (4.10) and hence find n.

In this way we can construct a table of corresponding values of ϵ and n for a given value of u; we have found the relation between the energy and the volume of the surfaces for a given lattice potential. In the pure

metal, $n=1$; by graphical interpolation one can find the corresponding value of ϵ, and, from (4.8), the radius of the neck at the zone boundary. As we increase u, we get a series of surfaces of this sort, all of the same volume but more and more distorted. Thus, we establish a relation (fig. 7) between the lattice potential, u, and the size of the necks on the Fermi surface of an exactly monovalent metal.

It will be seen that the radius r is very sensitive to the value of the lattice potential, and increase rapidly once contact has been established. For a given value of u, it is also quite sensitive to the number of electrons in the system, as indicated by the curve for $n=1{\cdot}1$,—it might be for an alloy of a noble metal with a polyvalent metal.

Fig. 7

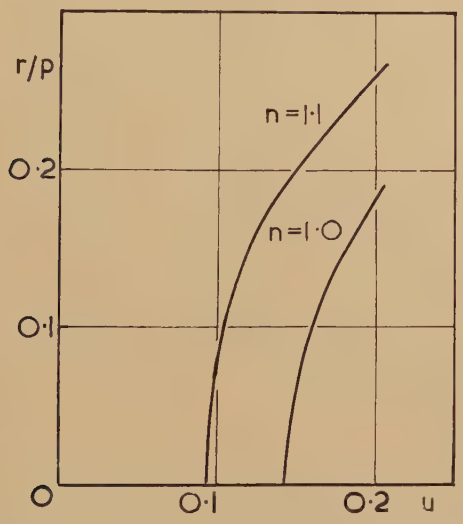

Calculated variation of ' neck ' radius r with energy-gap parameter u, for 1 and for 1·1 electrons per atom.

Now the de Haas–van Alphen experiments have given us quite accurate estimates of r in the pure metal. From table 2, and fig. 7 we can read off values of u, and hence, with (4.2), estimate the Fourier component $\mathscr{U}_{111}$. These data are shown in table 3.

We notice at once that the appropriate values of u are not very different in the three metals and that they correspond to quite large splitting of the energy levels; the depression of energy at the zone face is between $\frac{1}{3}$ and $\frac{2}{5}$ of the kinetic energy of the electron at that point. These values of u can be translated into absolute electron energy by the definition (4.2)—but this requires a knowledge of m^*. Yet even taking for m^* the free-electron mass, we find that $2\mathscr{U}_{111}$, the energy gap at the zone face, must be of the order of 5–7 ev in all three metals. If, as will appear later, m^* is actually smaller than 1, these estimates must be raised further.

This is a far cry from the values—all less than 1·5 ev—proposed by Cohen and Heine from the splitting of the s and p states of the free atoms. Our values are, indeed, closely in support of Pippard's theoretical estimate of 7·5 ev required to give the shape of Fermi surface which he observed in Cu. The experimental evidence from optical absorption is not at all clear. Biondi and Rayne (1959) talk of a gap of 2·6 ev in a 30% CuZn alloy and their data show this moving up to nearly 5 ev in pure Cu. Suffczynski (1960) has made a more detailed calculation, allowing for the density of states in the lower and upper parts of the conduction band, but finds difficulty in a comparison with experiment.

In § 2 we noted that some of the 'topological' experiments give information about the cyclotron mass on various orbits. Values calculated from our model can be compared with some of these data, if we write, instead of (2.1)

$$m_H^* = \frac{\hbar}{2\pi} \oint \frac{dk}{v_\perp} . \qquad (4.11)$$

Table 3

	Cu	Ag	Au
r/p	0·180	0·126	0·162
u	0·20	0·168	0·188
$\mathscr{U}_{111}$(ev: $m^*=1$)	3·5	2·3	2·5

where $v_\perp$ is the electron velocity normal to the magnetic field. Now the components at the electron velocity are, from (4.3),

$$(v_x, v_y, v_z) = \frac{hp}{m^*}\left(x, y, \frac{\partial f(z)}{\partial z}\right), \qquad (4.12)$$

i.e. z is replaced by $f'(z)$.

It is obvious that a 'neck' orbit, in the plane $z=1$, gives very simply

$$m_H^* = m^*; \qquad (4.13)$$

this experiment should determine the true 'effective mass' parameter for our system. A 'belly' orbit, however, in a [111] or [100] plane, passes near, but not through, the axis of several of the cones (see fig. 2). Thus, $v_\perp$ will have strong contributions from v_z, for which (4.11) and (4.12) suggest

$$m_H^* = mz^*/f'(z). \qquad (4.14)$$

This function which is plotted in fig. 8 (for $u=0{\cdot}2$) rises steeply near $z=1$, i.e. at the zone boundary. Referring to fig. 5, we see that these orbits cut across the zones in the range $0{\cdot}8 < z < 0{\cdot}9$, so that the ratio in (4.14) could lie between 1·5 and 2·5. This is in rough accord with

the quoted ratio of belly to neck masses in Cu and Au (i.e. about 2). But for a precise comparison between theory and experiment we must use a more complete model (e.g. including $\mathscr{U}_{200}$) and make more exact calculations.

Fig. 8

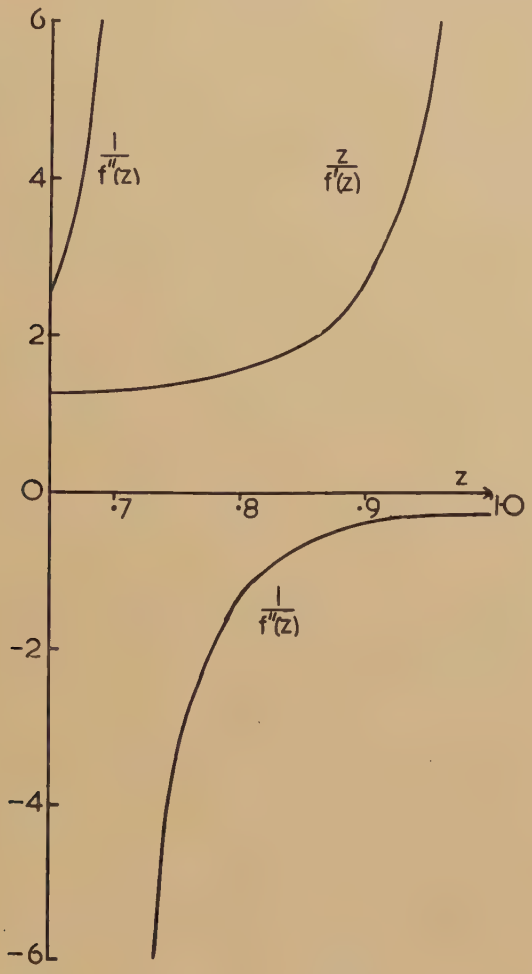

§ 5. Density of States

Several properties of the bulk metal depend mainly on the density of states in energy at the Fermi surface. This is given in general (E & P § 2.11) by the integral

$$\mathscr{N}(\mathscr{E}) = \frac{1}{4\pi^3\hbar}\int \frac{d\mathscr{S}}{v}. \qquad \ldots\ldots \quad (5.1)$$

where v is the electron group velocity on the element $d\mathscr{S}$ of Fermi surface. For our model surface we have (4.12), which a little elementary geometry gives

$$\mathscr{N}(\mathscr{E}) = \frac{4}{\pi^2}\frac{m^*p}{\hbar^2}\int_{z_1}^{z_2} dz. \qquad \ldots\ldots \quad (5.2)$$

Fig. 9

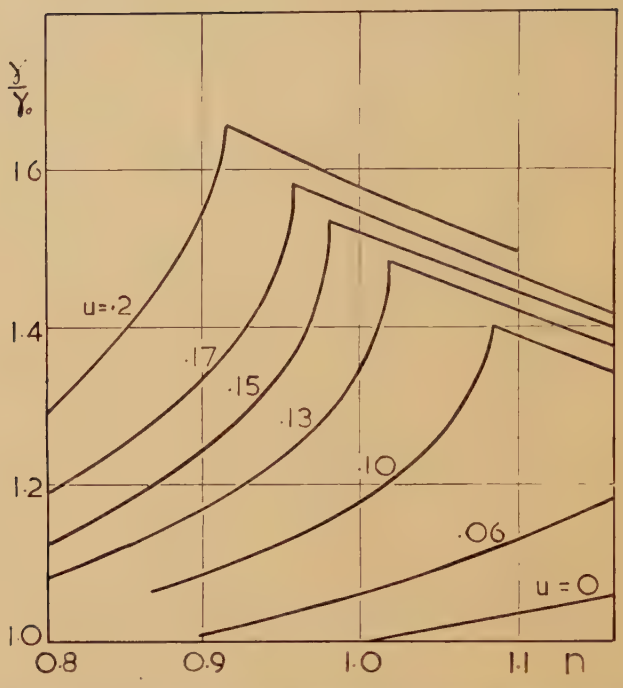

Density of states, as a function of electron density, calculated for various values of u. The peak occurs at the point where the Fermi surface touches the zone boundary.

Fig. 10

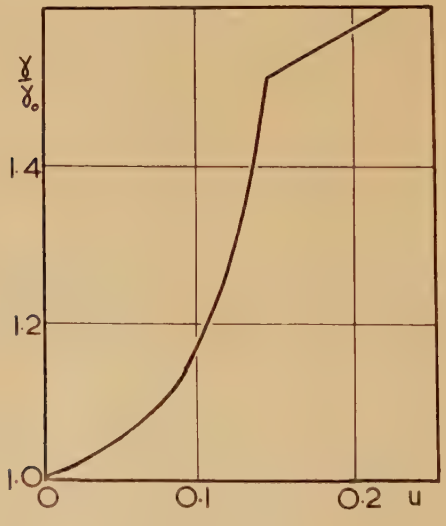

Density of states, as a function of u, for 1 electron per atom.

For comparison we refer to the value of the density of states for a system of electrons of mass m^* on a Fermi sphere of radius $\mathfrak{k}_F$;

$$\mathcal{N}_0(\mathcal{E}) = \frac{1}{\pi^2}\frac{m^*\mathfrak{k}_F}{\hbar^2}. \qquad \ldots\ldots\ldots \quad (5.3)$$

Thus, the ratio of (5.2) to (5.3) can be calculated very easily from the values of z_1 and z_2 already obtained in the previous section, and from $\mathfrak{k}_F = 0{\cdot}902p$. This is the quantity γ/γ_0 plotted in fig. 9, as a function of n, the number of electrons per atom, for various values of the parameter u, and again in fig. 10 as a function of u, for $n=1$. Because v vanishes at the zone boundary there is a singularity in the integrand of (5.1), but this can be integrated, and all that remains is a discontinuity of slope, with a vertical tangent, as a function of n.

We have used the symbol γ because the most direct measure of the density of states is the electronic specific heat. This is not an easy quantity to measure accurately, but the best data for the purest specimens are set out in table 4 (Corak, *et al.* 1955, Rayne 1957a, 1958, Guthrie 1959). This observed value is compared with the value γ_F, calculated for a simple free electron model with $m^*=1$; this ratio is often called the *thermal mass*.

Table 4

	Cu	Ag	Au
γ_{obs} (millijoules/mol (°K)^2)	0·688	0·610	0·743
γ_F (calculated for free electrons)	0·502	0·644	0·644
$m_t = \gamma_{obs}/\gamma_F$	1·37	0·95	1·15
γ_{calc}/γ_0 from fig. 9	1·57	1·54	1·56
Hence $m_t^* = \frac{\gamma_{obs}}{\gamma_F}\frac{\gamma_0}{\gamma_{calc}}$	0·87	0·62	0·73

Now from table 3 we can look up values of u for the three metals, and from fig. 10 extract corresponding values of the ratio γ/γ_0. The two rows do not agree very well. However, there is still the unknown parameter m^*, which occurs in (5.2)—i.e. $\gamma_0/\gamma_F = m^*$. We can adjust our theoretical values of γ and make them agree with experiment by giving m^* the values shown in the final row of table 4 (which we shall label m^*_t). These values are more or less consistent with the data on m_H^* presented in table 2 (for example, they are in the correct order of size) when allowance has been made, as in (4.14), for the fact that belly orbits do not give m^* directly. In § 6 we shall make comparison of m_t^* with an optical mass, m_a^*.

The main point here is that the observed electronic specific heat in the pure metals is quite consistent with our model. But when we study the effect of alloying we run into a thick fog of mystery. Almost all the experiments have been done on Cu, where, as Rayne (1956) pointed out, the reported values of γ could be correlated with the estimated purity of the sample. For example, γ for 99·999% Cu is 0·686–0·688, whereas samples of only 99% purity gave values as high as 0·75–0·8. Thus there were either serious experimental errors or there is some effect which is extremely sensitive to small concentrations of impurity.

Fig. 11

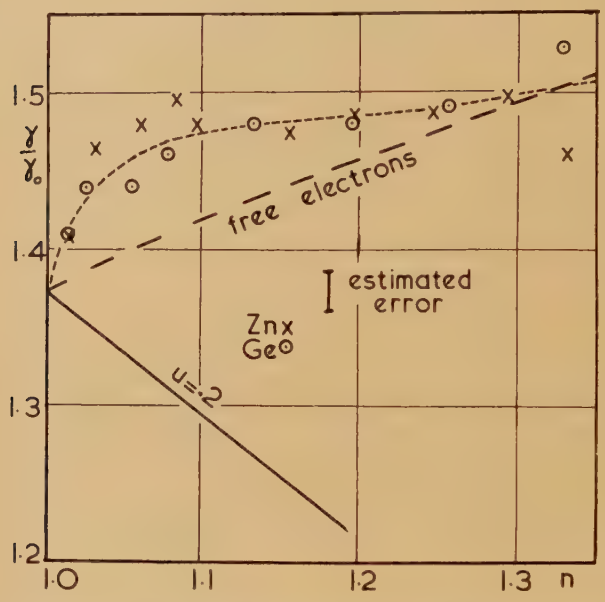

Variation of electronic specific heat with electron density for alloys of Cu with Zn and Ge (Rayne 1957 a, 1958).

This has been to some extent confirmed by more systematic experiments. When Zn, or Ge, are added to Cu, we get the change of γ shown in fig. 11 (Rayne 1957 a, 1958). Although there is a good deal of scatter, one can draw a reasonable curve through these points as if γ depended only on the number of free electrons added with the divalent or tetravalent metal. On a free electron model with a spherical Fermi surface, a general increase of γ with n is quite intelligible; the density of states increases as the Fermi surface swells until it touches the zone boundary in a special little cusp at about 1·32 electrons per atom.

But another experiment spoils this argument. Guthrie (1959) has measured γ for alloys of the type $Cu_{1-2x}Ni_xZn_x$, which should retain $n = 1$.

For $x=0{\cdot}03$, γ increased from 0·686 to 0·844 ($\gamma/\gamma_F=1{\cdot}68$, and for $x=0{\cdot}08$ γ became 0·985 ($\gamma/\gamma_F=1{\cdot}98$), which is much longer than any of the values attained in fig. 10. It seemed, also that the increase could be analysed into contributions as if from the Zn and Ni acting alone, so that it does not depend very much on the concentration of electrons. (On the other hand, in disordered Cu_3Au (Rayne 1957 a), $\gamma=0{\cdot}66$, in spite of a lattice expansion which would have increased the value for a free electron system to about 0·74, so that the effect of alloying may be here to decrease γ).

Our model, also, does not agree with the data of fig. 11. As we increase n, we expect to go *down* the curve, as we leave behind the little peak at the point of contact. As we see in fig. 8, the theoretical trend in γ is always downwards, once we have passed the contact region.

Cohen and Heine (1958) have suggested that the explanation of these discrepancies is to be found in a change of shape of the Fermi surface with alloying. In particular, they propose that the Fermi surface should get more spherical, even breaking away from contact, at least until so many electrons have been added that even a single sphere touches the zone boundary. But it is difficult to fit such a suggestion in our model. Let us suppose that the effect of alloying is simply to change the parameter u, the splitting at the band edge. Then looking at figs. 9 and 11, we see that we could only match the observed rise in γ by making u increase, from 0·2 say, to 0·4—surely an impossibly distorted surface. Sphericizing the surface—reducing u—does not increase γ at all—it makes it fall even more steeply than the theoretical line drawn for $u=$ constant in fig. 11. Thus, our numerical calculation does not at all support the interpretation put forward by Cohen and Heine; it suggests an exactly contrary effect.

There is a further experimental point that may be of relevance. Biondi and Rayne (1959) have measured the shift of the main optical absorption edge in Cu (presumably due to transitions from the top of the d-band to the Fermi level) on the addition of Zn, and compared this with the theoretical shift,

$$\delta\mathscr{E}=\int_1^n \frac{dn}{\mathscr{N}(\mathscr{E})}, \quad \ldots\ldots\ldots \quad (5.4)$$

which can be calculated directly from the electronic specific heat data. There is a considerable discrepancy; the observed shift rises much more slowly than one calculates, and even when the curve becomes linear the slope is only about one third of the value given by (5.4).

In the same experiments the absorption edge which is attributed to transitions across the energy gap into the upper band was less pronounced, and seemed to shift to longer wavelengths as Zn is added. This looks like the same sort of effect—the Fermi level rising towards the lowest state of the upper band. But our model tells us that once contact has taken place the energy gap for 'vertical transitions' in **k**-space remains constant, so that we have here some support for the Cohen and Heine

hypothesis that the band gap decreases on alloying. However the change is not big enough for contact to be lost (consult fig. 9 to see how u would vary with n in the series of surfaces containing more and more electrons but just keeping contact with the zone boundary) and would certainly not help with the problem of understanding the Hume–Rothery rules. The optical data and their theoretical interpretation are still too uncertain for this argument to be accepted without question.

There are a number of points at which one might attack this problem. Is it possible that m^* is radically changed—increased—with alloying? There is no other evidence on this point. Again the alloying may cause a *local* distortion of the Fermi surface near the zone boundary increasing $\mathcal{N}(\mathcal{E})$ there without having much effect on the round belly of the surface. One can show (Mr. W. G. Chambers, work in progress) that there could be different changes of energy at different points on the Fermi surface, due to scattering by impurities but the effect seems to be small. Then Jones (1957) has calculated an effect, that would look like an electronic specific heat, due to the change in the zero-point energy of the lattice waves as the electron distribution varies with temperature. If we thought that we were just about to make contact with the zone boundary, this would be important. Yet again, we know from the work of Pines (1955), that the electron–electron interactions and the plasma oscillations can seriously affect the density of states. It may be that the effect of alloying is to quench this term or to alter it in the way observed. Another possibility lies in Friedel's discussion (1954) of the creation of virtual bound states in the neighbourhood of impurities. Finally, we may find that there is a flaw in the argument which derives the linear specific heat at low temperatures from the density of states in a model of independent electrons.

This problem also merits further experimental study. For example, it would be interesting to check whether Ag and Au show the same anomalies and also to look at a wider range of alloys of Cu.

A phenomenon which is related to the density of states is the Knight shift. Cohen and Heine (1958) have discussed this for alloys of the noble metals, but it is difficult to draw any firm conclusions from the measurement of a quantity which depends on a variety of complex factors. We should only like to make one comment. According to our model, the wave function in the state $\mathbf{k}$ is given by (3.1):

$$\psi_{\mathbf{k}} = \alpha_{\mathbf{k}}\phi_{\mathbf{k}} + \alpha_{\mathbf{k}-\mathbf{g}}\phi_{\mathbf{k}-\mathbf{g}}, \quad \ldots\ldots\ldots \quad (5.5)$$

where, as in (3.3),

$$\alpha_{\mathbf{k}-\mathbf{g}}/\alpha_{\mathbf{k}} = (\mathcal{E}_{\mathbf{k}} - \mathcal{E}_{\mathbf{k}})/\mathcal{U}_{-\mathbf{g}}. \quad \ldots\ldots\ldots \quad (5.6)$$

Thus, at the zone boundary itself, where $\phi_{\mathbf{k}\ \mathbf{g}} = \phi_{\ \mathbf{k}}$, and where $\mathcal{E}_{\mathbf{k}} - \mathcal{E}_{\mathbf{k}} = -|\mathcal{U}_{-\mathbf{g}}|$, the state $\psi_{\mathbf{k}}$ will be s-like or p-like according as $\mathcal{U}_{-\mathbf{g}}$ is $-$ve or $+$ve. A naïve interpretation of the argument of Phillips and Kleinman (1959) would suggest that the residual quasi-potential should be essentially attractive at large distances, so that we might expect $\mathcal{U}_{111}$ to be

−ve, and these states always to be s-like—hence contributing to the Knight shift. However, a recent band-structure calculation by Segal (private communication) shows the p-state lowest in Cu, and some rather circumstantial evidence from the behaviour of the relaxation time (Ziman, to be published) makes it likely that this is the case also for Ag and Au. At this point the deficiencies of the quasi-potential model become apparent; we need proper band-structure calculations to argue in detail about the wave functions.

§ 6. Optical Mass

As pointed out by Cohen (1958), the optical properties of a metal depend in a special way on the shape of the Fermi surface, etc. Under appropriate conditions one finds that the electrons should behave as if they were free particles of mass

$$m_a = 12\pi^3\hbar n N \Big/ \int v \, d\mathbf{S} \quad . \quad . \quad . \quad . \quad . \quad . \quad (6.1)$$

where there are N atoms per unit volume and the integral means an average of the electron velocity over the Fermi surface.

It is not difficult to compute this integral for our 8-cone model. Thus, from (4.12), (5.1) and (5.2),

$$\begin{aligned} \int v \, d\mathbf{S} &= \frac{16\pi p m^*}{\hbar} \int_{z_1}^{z_2} v^2 \, dz \\ &= \frac{16\pi p^3 \hbar}{m^*} \int_{z_1}^{z_2} [2\epsilon - 2f(z) + \{f'(z)\}^2] \, dz, \quad . \quad . \quad . \quad (6.2) \end{aligned}$$

so that

$$\begin{aligned} m_a = m^* n \sqrt{3}\pi \Bigg[& 2\epsilon(z_2 - z_1) + 2u^2 \ln \left\{ \frac{(1-z_1) + \sqrt{\{u^2 + (1-z_1)^2\}}}{(1-z_2) + \sqrt{\{u^2 + (1-z_2)^2\}}} \right\} \\ & - u \left\{ \tan^{-1}\left(\frac{1-z_1}{u}\right) - \tan^{-1}\left(\frac{1-z_2}{u}\right) \right\} \Bigg]^{-1}, \quad . \quad . \quad . \quad (6.3) \end{aligned}$$

which can easily be calculated from values of z_1 and z_2 which have already been tabulated. In fig. 12 we plot m_a/m^* against n, for different values of u. We note that there is no apparent singularity in these curves at the point where the Fermi surface touches the zone boundary; the zero in v^2 cancels the infinity in the integrand of (5.1). In fig. 13, we also plot the optical mass as a function of u, for a strictly monovalent metal.

The experimental data of Schulz (1957) provide the entries in table 5: the optical mass for Cu is much larger than it is for Ag and Au. But we consult table 3 for appropriate estimates of u, and then read off, on fig. 13, theoretical values of m_a/m^*. Thus we have an estimate (m_a*) of m^*, the overall scale parameter of the energy surfaces. These estimates agree quite well with the values of m_l* obtained by trying to match the specific heats; considering the inaccuracy of the experimental values of m_a, this is satisfactory.

Fig. 12

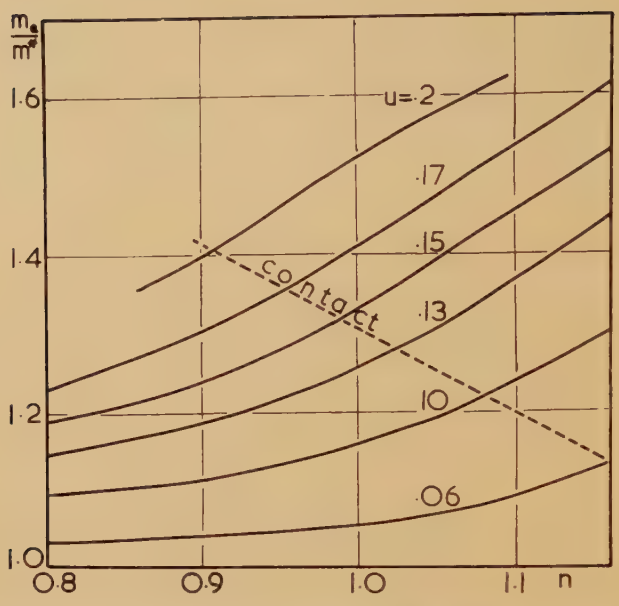

Optical mass, as a function of electron density, calculated for various valus of u.

Fig. 13

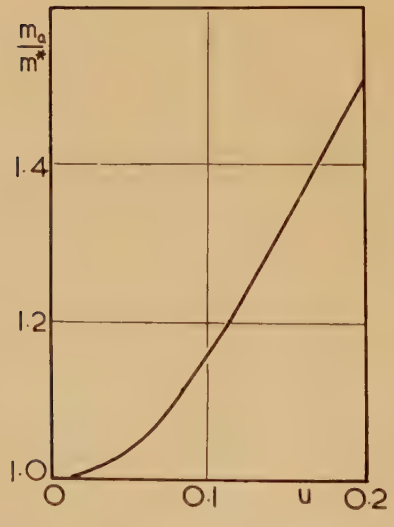

Optical mass, as a function of u, for 1 electron per atom.

It is interesting to make this comparison in a slightly different way by calculating the ratio $m_t/m_a = \gamma/m_a\gamma_F$ which ought to be independent of m^*, but which should depend on the shape of the Fermi surface, etc. It turns out that this ratio does not depend so much on the parameter u as on the actual area of the contact region. One can plot (fig. 14),

Table 5

	Cu	Ag	Au
m_a (obs)	1·45	0·97	0·98
m_a/m^* (theor)	1·52	1·40	1·47
hence m_a^*	0·95	0·68	0·67
m_t^*/m_a^*	0·95	0·99	1·18

Fig. 14

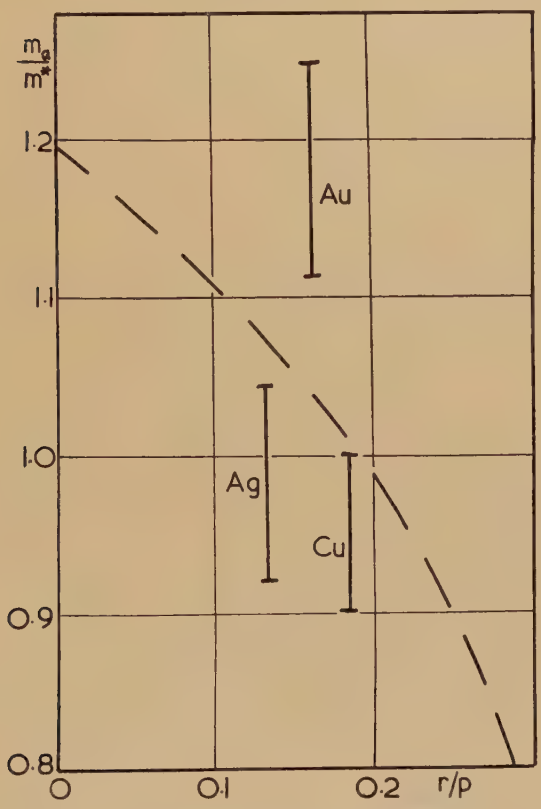

Theoretical relation between optical mass and neck radius compared with experimental values.

m_t/m_a against r/p, the radius of the necks. Since we have values of r/p directly from the de Haas–van Alphen experiment, we can put an experimental point for each metal against this curve. The result is not very good, although the theoretical curve lies nearly within the quoted limits of experimental error. But this calculation certainly confirms the qualitative argument of Cohen for the conditions under which m_t/m_a should be greater or less than unity.

§ 7. Hall Effect

Although a great deal of information about the Fermi surface can be obtained by the study of the effect of a *strong* magnetic field on the transport properties, this information is quite blurred and smudged at high temperatures and in alloys by the scattering of the electrons by lattice waves and impurities, and only the 'low field' phenomena can be observed except in very pure specimens at very low temperatures. Of these, the Hall effect is the strongest (being linear in H) and is relatively easy to measure, being a single scalar parameter in a cubic metal and hence well-defined for a polycrystalline specimen.

For the theory we again refer to E & P (§ 12.5), where we find that

$$R=\sigma_H/\sigma_0^2; \quad \sigma_0=\frac{e^2}{12\pi^3\hbar}\int v\tau_{\mathbf{k}}\frac{d\mathbb{S}}{v}; \quad . \quad . \quad . \quad .(7.1)(7.2)$$

and

$$\sigma_H=\frac{e^3}{4\pi^3 c}\int\left\{\tau_{\mathbf{k}}^2(v_x^2\mathsf{M}_{yy}^{-1}-v_xv_y\mathsf{M}_{yx}^{-1})-\tau_{\mathbf{k}}v_xv_y\left(v_y\frac{\partial\tau_{\mathbf{k}}}{\partial k_x}-v_x\frac{\partial\tau}{\partial k_y}\right)\right\}\frac{d\mathbb{S}}{v}.$$
$$. \quad . \quad . \quad . \quad . \quad (7.3)$$

In other words, σ_0 is the electrical conductivity in zero field, governed by a relaxation time $\tau_{\mathbf{k}}$ which may vary over the Fermi surface. The Hall coefficient, R, obviously depends mainly on the components of the inverse mass tensor of the electrons on the Fermi surface,

$$\mathsf{M}_{yx}^{-1}\equiv\frac{1}{\hbar^2}\frac{\partial\mathscr{E}_{\mathbf{k}}}{\partial k_y\partial k_x} \quad . \quad . \quad . \quad . \quad . \quad . \quad . \quad (7.4)$$

A particular set of rectangular coordinate axes, with the field in the z-direction, is implied in (7.3), but because of the cubic symmetry the answer should be irrespective of their orientation. This symmetry allows us to drop all the terms containing derivatives of $\tau_{\mathbf{k}}$, which vanish on the average over the Fermi surface. Then for a single cone we should choose the axis of the cone as z axis, whereupon M_{yx}^{-1} disappears; the form (4.3) of $\mathscr{E}_{\mathbf{k}}$ is such that the cone axis is automatically a principal axis of the inverse mass tensor at all points on the surface region belonging to that cone. Thus, the value of σ_H is obtainable rather simply as the value of (7.3) for a single cone averaged for all possible orientations relative to the magnetic field, i.e.

$$\sigma_H=\frac{e^3}{3\pi^3\hbar c}\int\tau_{\mathbf{k}}^2(v_x^2+v_y^2)\mathsf{M}_{zz}^{-1}+(v_y^2+v_z^2)\mathsf{M}_{xx}^{-1}+(v_z^2+v_x^2)\mathsf{M}_{yy}^{-1}\frac{d\mathbb{S}}{v}.$$
$$. \quad . \quad . \quad (7.5)$$

Unfortunately, we do not know τ_k. But, if it were a constant, it would vanish from (7.1). Let us make this assumption for the moment. Then (7.5) can be evaluated by the same techniques as were used in (6.1)–(6.3).

Fig. 15

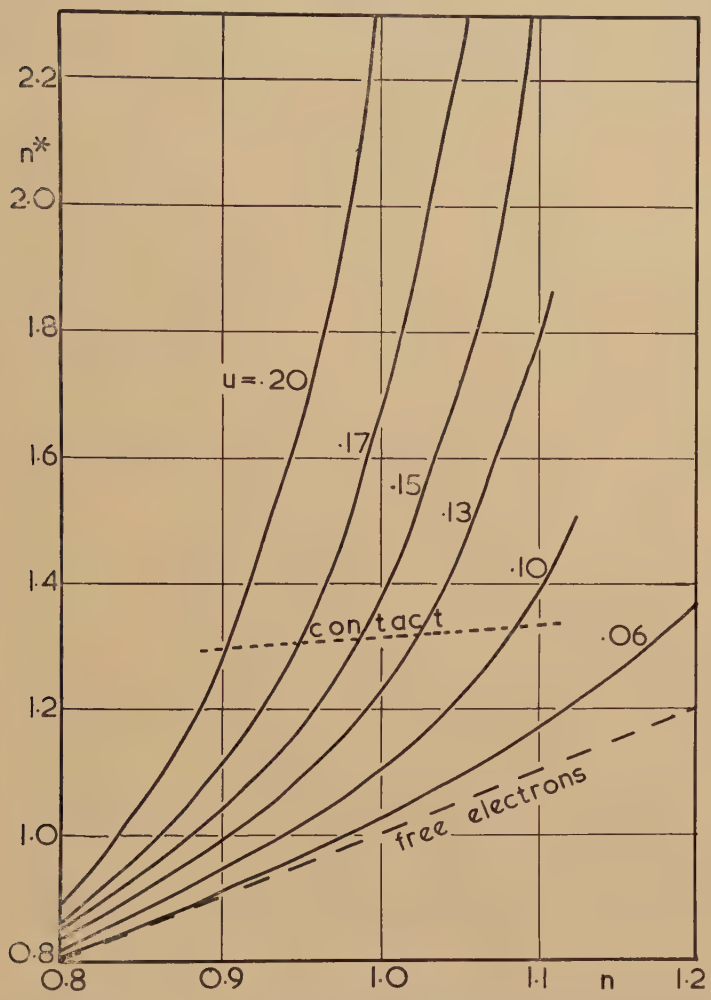

Inverse Hall coefficient as a function of electron density, calculated for various values of u.

We note from (4.3) that

$$\mathsf{M}_{xx}^{-1}=\mathsf{M}_{yy}^{-1}=1/m^*, \quad \mathsf{M}_{zz}^{-1}=f''(z)/m^* \quad . \quad . \quad . \quad (7.6)$$

and by a little algebraic manipulation we obtain

$$R=\frac{1}{nN\mathbf{e}c}\frac{m_a}{m^*}\left[3-\frac{2m_a}{m}-\frac{7\pi}{3\sqrt{3}}\frac{m_a z_1^{\,2}}{m^* n}\left\{\frac{(1-z_1)}{\sqrt{\{u^2+(1-z_1)^2\}}}-1\right\}\right], \quad (7.7)$$

which can be computed quite simply for different values of u and for different energy surfaces.

We note at once that

$$R \to \frac{1}{nNec} \quad . \quad . \quad . \quad . \quad . \quad . \quad . \quad . \quad (7.8)$$

when $m_a = m^*$ and $u = 0$. This is, of course, the standard result for free carriers, the sign of R being determined by the sign of e. We see that R does not depend on m^*, but on the shape and volume of the Fermi surface. It is conventional and convenient to re-interpret (7.7) in the spirit of (7.8), and to write

$$n^* = \frac{1}{NecR}. \quad . \quad . \quad . \quad . \quad . \quad . \quad . \quad . \quad (7.9)$$

Fig. 16

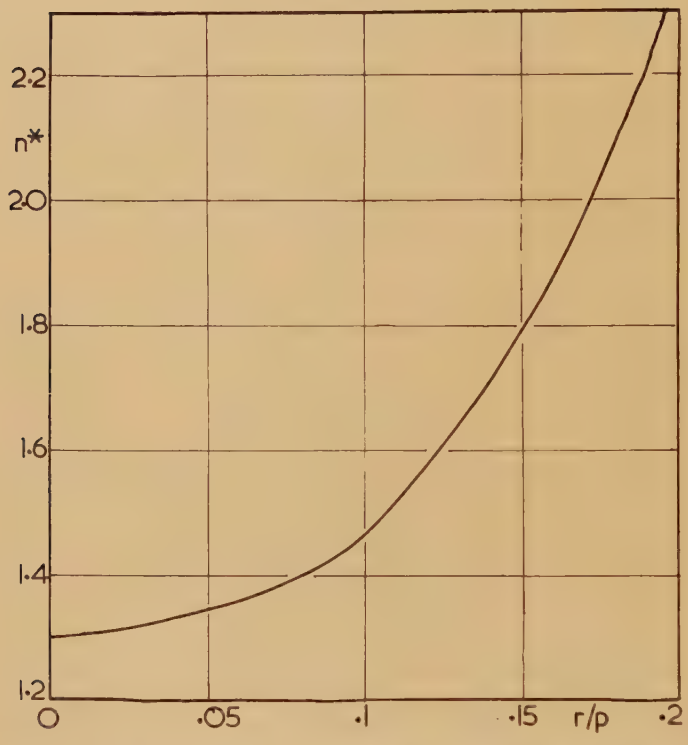

Inverse Hall coefficient calculated as a function of neck radius.

as if the Hall coefficient gave the effective number of free electrons per atom. This is the quantity which is plotted in fig. 15, against n, the actual number of electron states per atom available inside the Fermi surface, for various values of u.

There are several features of interest in this figure. The Hall coefficient is obviously rather sensitive to the shape of the Fermi surface; n^* can be as large as 2, even for a surface with one electron per atom, for values of u in the range suggested in table 3. But we may also note that, on

each curve, n^* is about 1·3 when the surface just touches the zone boundary. This suggests, as indicated in fig. 16, that n^* depends mainly on the size of the necks, and not on the shape of the broad belly of the surface. We can plot a single curve which represents quite accurately a simple relation between n^* and r/p, independently of the total volume inside the surface.

What makes n^* increase thus—or, more directly, what causes $|R|$ to decrease as the Fermi surface expands? In semiconductor physics R is the balance of a contribution (conventionally negative) from electrons, and a contribution of opposite sign (i.e. positive) from 'holes'. Thus, we should say that "the number of holes is increasing as the Fermi surface makes contact and pushes outwards over the zone boundaries". This sort of statement is often made, but it is slightly misleading in the present case. To achieve a true 'hole' carrier, we need to go right into a corner of a zone, where all the components of the effective mass tensor are negative. Only then can we construct wave-packets corresponding to the absence of an electron from a given state—wave-packets which behave like particles with positive charge and mass. The situation on the necks is more complicated. The components M_{xx}^{-1} and M_{yy}^{-1} in (7.6) are certainly positive—i.e. 'electron'-like—but the value of M_{zz}^{-1} is negative. Thus, from (4.4),

$$f''(z)=1-\frac{u^2}{\{u^2+(1-z)^2\}^{3/2}}\rightarrow\left(1-\frac{1}{u}\right)\text{as}\,z\rightarrow 1, \quad . \quad . \quad (7.10)$$

and is negative for $u<1$ over the greater part of the range of z on the Fermi surface. (It is interesting to compare $1/f''(z)$, which is a sort of 'component of effective mass in the z-direction', with the cyclotron-mass component (4.14). As we see in fig. 8, they have quite different properties.) That is to say, the effective mass tensor is *hyperbolic*, and a wave packet will obey rather strange dynamical laws, unlike those of a simple classical particle. It is true that we can distinguish between 'electron-like' and 'hole-like' orbits in a strong magnetic field according to whether the orbits enclose full or empty regions in $\mathbf{k}$-space, but a given electron state can participate in either type, according to the orientation of the magnetic field. Returning to (7.5), we see that the sign of the contributions to R will depend on the orientation of the electron velocity to the magnetic field. The thicker the necks, the greater can be the contribution from negative values of M_{zz}^{-1}, and hence the smaller the value of $|R|$. But that is not quite the same thing as saying that the number of 'holes' has increased.

Now for the observed values of the Hall coefficient. Table 6 shows a comparison between theory and experiment. As shown in fig. 17, there is a good deal of uncertainty about the behaviour of R at low temperatures —probably because this parameter also is sensitive to impurities—but the room temperature data are fairly well defined (Onnes and Beckman 1912, Wortman 1933, Chambers 1956, Frank 1957, Blue 1959). From

the observed value of R we calculate n^* as in (7.9). For comparison we refer directly to fig. 16, using values of r/p from table 2 to read off appropriate theoretical estimates of n^*.

It is at once evident that there is a large discrepancy between theory and experiment; for all three metals, the observed value of n^* is too small by something like 20%. The theoretical value is independent of m^* so that we have not this parameter to play with, and the observations are quite accurate enough to rule out experimental error as the source of the discrepancy.

Table 7

	Cu	Ag	Au
R_{obs} (cm^3/coulomb $\times 10^{-5}$)	$-4{\cdot}9 \rightarrow -5{\cdot}2$	$-8{\cdot}0 \rightarrow -8{\cdot}5$	$-7{\cdot}0 \rightarrow -7{\cdot}2$
$R_F = (Ne\boldsymbol{c})^{-1}$ (free electrons)	$-7{\cdot}45$	$-10{\cdot}65$	$-10{\cdot}60$
n^*_{obs}	$1{\cdot}52 \rightarrow 1{\cdot}43$	$1{\cdot}33 \rightarrow 1{\cdot}25$	$1{\cdot}52 \rightarrow 1{\cdot}48$
n^*_{calc}	2·05	1·58	1·87

Fig. 17

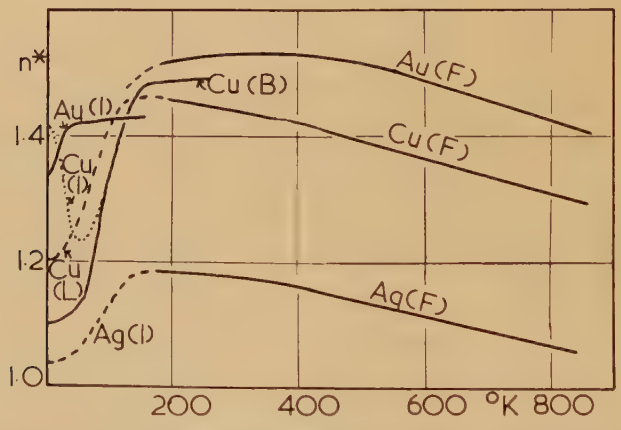

Variation of inverse Hall coefficient with temperature. References (F) Frank 1957; (B) Berlincourt 1958; (L) Love 1959; (I) Fukuroi and Ikeda 1959.

One line of thought (Ziman 1959b) is to suppose that the thermal scattering of the electrons has to some extent sphericized the Fermi surface, so that at room temperatures the necks in Cu and Au are reduced to $r/p \sim 0{\cdot}1$, whilst in Ag contact has been lost with the zone boundary. This is what we should need if we wanted to obtain the observed values

of n^* from fig. 16. But other evidence is against it. Thus, the measurements of optical mass (§ 6) made at room temperature are in good agreement with the specific heat data and the shape of Fermi surface found at low temperature by the 'topological' experiments. The change of Hall coefficient with temperature (fig. 17) is also inconsistent with this hypothesis, which would require n^* to rise to the high calculated values of table 6 as we go down to low temperatures; we observe instead a low peak, and an irregular fall to smaller values in the residual resistance range.

Fig. 18

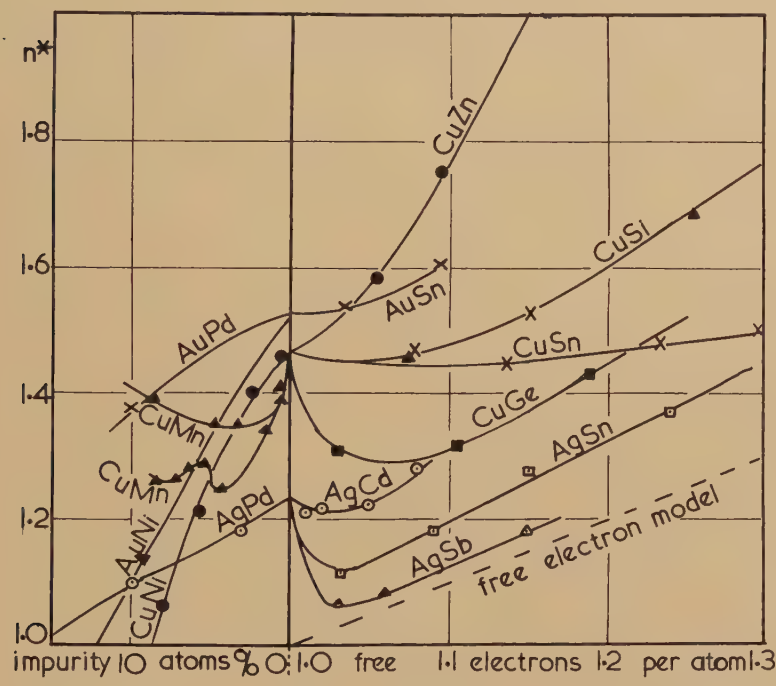

Inverse Hall coefficient in alloys. Data taken from Andrewartha and Evans (1941), Blue (1959), Dorfman and Zhukova (1939), Flanagan and Averbach (1956), Frank (1955), Schindler and Pugh (1953); Wortman (1933).

These irregularities in n^* at low temperatures suggest that the Hall coefficient is sensitive to impurity type and concentration. When we actually study the effect of alloying, we find a bewildering confusion of phenomena. Figure 18, taken from various miscellaneous sources, shows how the room temperature Hall coefficient can be changed by 10 or 20% by the addition of one or two atoms per cent of a polyvalent metal such as Sb or Ge. Moreover, this change is often in the wrong direction. Our theory would predict that n^* should rise along one of

the curves $u =$ constant in fig. 15, as the electron concentration increases; the typical behaviour is a steep drop, followed by a steady rise which is more or less parallel to the line for 'free electrons', but displaced from it by varying amounts for various types of impurity. On the side of the transition metals it is true, we find n^* falling as it might due to electrons being swallowed by the d-shells, but the agreement with theory is only qualitative.

Of course we may try to explain these phenomena also as the effects of 'spericizing' by the impurities. But the arguments of Cohen and Heine would suggest that each curve in fig. 17 should drop steadily down to the free electron line, and follow this up to the Hume-Rothery phase boundary at about 1·3 electrons per atom. There is no allowance in their theory for the necks in $Cu_{90}Si_{10}$, say, being thicker than in pure Cu—which is what seems likely from fig. 16 and fig. 18. Moreover, the specific heat data of fig. 11 indicate a close similarity between **Cu**Zn and **Cu**Ge, when plotted in terms of electrons per atom; the effects of these two metals on the Hall coefficient are quite different.

A more likely explanation is that put forward by Coles (1956) and by Cooper and Raimes (1959): the relaxation time $\tau_{\mathbf{k}}$ is by no means isotropic, and cannot simply be cancelled from (7.1), (7.2) and (7.5). In these expressions it occurs as a weight function—to the first power in (7.2), but squared in (7.5). Since our Fermi surface is highly anisotropic, there is a good reason to expect the electron scattering probability to be very different on the necks, say, from what it is on the bellies. Suppose, for example, that τ is smaller near the zone boundary then it is on the main, nearly spherical part of the surface. The contributions of the neck regions in (7.5) will be reduced—and these are the parts where M_{zz}^{-1} has its large negative values which make $|R|$ smaller than it would be for free electrons. Thus this anisotropy in τ would have the effect of increasing the theoretical value of the Hall coefficient bringing it nearer to the simple free-electron value. That is, n^* will be decreased towards unity. In crude terms, the 'mobility' of the 'holes' is less than that of the 'electrons', and they contribute proportionately less to the Hall effect.

This is our interpretation of the discrepancy between theoretical and experimental values of n^* in table 6; $\tau_{\mathbf{k}}$ for phonon scattering of electrons at room temperature must have just this sort of anisotropy, and our estimate of n^* is to be reduced accordingly. Now, following Cooper and Raimes, we can imagine that the functional form of $\tau_{\mathbf{k}}$, is different for impurity scattering from its form for phonon scattering. When impurities are added we first get a rapid change of n^* as the residual resistance of the impurity becomes dominant over the 'ideal' resistance due to the phonons (one can check that the minima in fig. 18 came at about this point). Thereafter there is a steady rise in n^* along a line characteristic of this form of $\tau_{\mathbf{k}}$, due simply to the swelling of the Fermi surface as more and more electrons are added to the alloy.

Unfortunately it is difficult, as yet, to make a quantitative theory of this effect. The calculation of Cooper and Raimes is not applicable in detail, since it refers to a Fermi surface which is simply-connected and deformed only moderately from a sphere. But we can make a number of comments on the data. Evidently the degree of anisotropy of τ_k is different for impurity scattering by different metals. It looks as if

Fig. 19

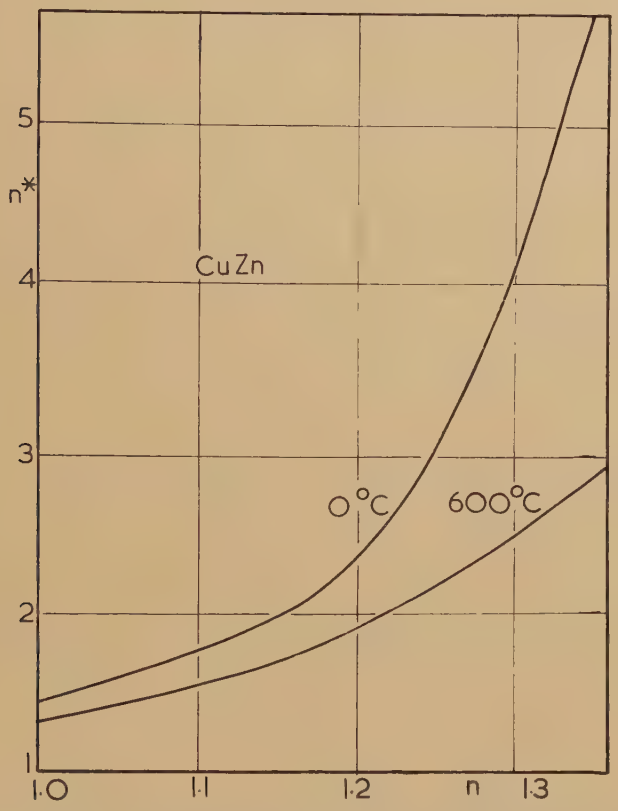

Variation of inverse Hall coefficient with electron density in CuZn alloys (Frank 1955).

the anisotropy for scattering by Zn in Cu is actually less than for phonon scattering. This is confirmed by the curves of fig. 19 showing how n^* is systematically less at 600°C than at 0°C, for the **Cu**Zn alloys; at higher temperatures the phonon scattering is relatively more important, and tends to keep n^* down. Generally speaking there is a tendency for the anisotropy to be greater (n^* smaller) as the valence difference between solute and solvent increases; thus **Cu**Zn and **Ag**Cd lie above **Cu**Ge and **Ag**Sb. The observations on alloys of the noble metals with one

another are also most interesting. According to Onnes and Beckman (1912) in the AuAg system (fig. 20) where there are no disturbing changes of volume, n^* rises at low temperatures to a high peak—above even the theoretical value already calculated for isotropic τ_k. This peak is somewhat muted at room temperature, but is still quite remarkable,

Fig. 20

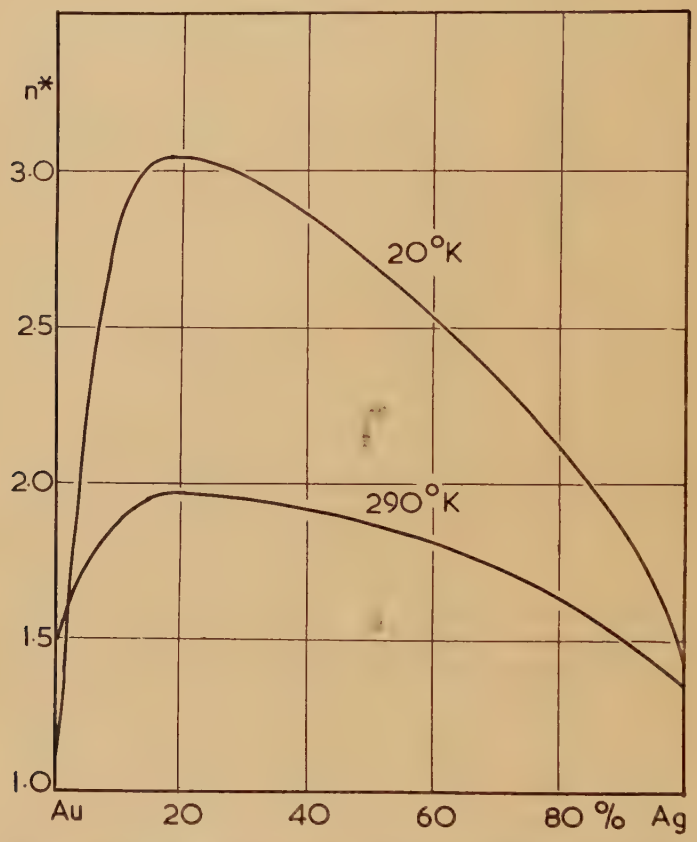

Variation of inverse Hall coefficient in the AuAg system (Onnes and Beckman 1912).

considering that the number of electrons is constant. We can only assume that the functional form of τ_k for scattering by Ag in Au is quite different—is, say, larger on the necks than on the belly—from its shape for phonon scattering. However, the data of Flanagan and Averbach (1956) do not show such a large effect in AuAg, and in CuAu there appears a slight minimum in the plot of against concentration. Here is a point requiring careful experimental confirmation.

There is independent evidence for the anisotropy of τ over the Fermi surface. Rayne (1959) has measured the infra-red absorptivity of Cu as a function of temperature, and in order to explain his results requires that

$$\langle\tau\rangle\langle 1/\tau\rangle \sim 1{\cdot}64 \quad . \quad . \quad . \quad . \quad . \quad . \quad . \quad (7.11)$$

in which we mean that

$$\langle\tau\rangle \equiv \int \tau_{\mathbf{k}} v \, d\mathfrak{S} \Big/ \int v \, d\mathfrak{S} \quad . \quad . \quad . \quad . \quad . \quad . \quad (7.12)$$

and $\langle 1/\tau\rangle$ is a similar average of $1/\tau_{\mathbf{k}}$ on the Fermi surface. Since this quantity is identically unity for isotropic relaxation time, we must conclude that $\tau_{\mathbf{k}}$ varies considerably over the surface—by a ratio of 5 to 1 or more. (7.11) refers to electron–phonon scattering. Similar experiments on **Cu**Zn alloys (Biondi and Rayne 1959) give

$$\langle\tau\rangle\langle 1/\tau\rangle \sim 1{\cdot}3 \quad . \quad . \quad . \quad . \quad . \quad . \quad . \quad (7.13)$$

which suggests that the anisotropy of scattering by Zn is smaller than by phonons, in qualitative agreement with our deduction from the Hall effect. Although the theoretical deduction of (7.11) from the optical data is not quite complete, it would obviously be of great interest to do the same sort of experiment on alloys like AuAg, or like **Cu**Ge, where we expect the anisotropy of τ to be entirely different.

§ 8. Magnetoresistance

The theory of the galvanomagnetic effects of second order is much more complicated, even for low magnetic fields where the method of Jones and Zener can be applied. Referring to E & P (§ 12.5) we find the following formulae:

In a polycrystalline specimen there are only two independent magnetoresistance coefficients, the longitudinal and transverse coefficients in the relation

$$\frac{\Delta\rho}{\rho_0} = B_l H^2 \sin^2\theta + B_t H^2 \cos^2\theta \quad . \quad . \quad . \quad . \quad . \quad (8.1)$$

for the relative change of resistance in a wire at an angle θ to the field H. These in turn are defined by

$$B_l = \rho_1^{(2)} + \tfrac{32}{105}\rho_2^{(2)}; \quad B_t = \rho_1^{(2)} + \tfrac{3}{5}\rho_2^{(2)} + \rho_3^{(2)} \quad . \quad . \quad . \quad . \quad (8.2)$$

in terms of the three quadratic-field coefficients for a cubic crystal, i.e. the coefficients in the formula

$$\frac{\Delta\rho}{\rho_0} = \frac{H^2}{\rho_0}\{\rho_1^{(2)} + \rho_2^{(2)}\textstyle\sum_\alpha j_\alpha^2 h_\alpha^2 + \rho_3^{(2)}(\sum_\alpha j_\alpha h_\alpha)^2\} \quad . \quad . \quad . \quad (8.3)$$

(where j_α, h_α are the direction cosines of the electric current and the magnetic field referred to the cube axes of the crystal).

Now the coefficients in (8.3) can be calculated from the following relations:

$$\left.\begin{aligned}\rho_1^{(2)} &= -\rho_0^2\{\sigma_{1122}+\rho_0\sigma_H^2\},\\ \rho_2^{(2)} &= -\rho_0^2\{\sigma_{1111}-\sigma_{1122}-\sigma_{1212}-\sigma_{1221}\},\\ \rho_3^{(2)} &= -\rho_0^2\{\sigma_{1212}+\sigma_{1221}-\rho_0\sigma_H^2\},\end{aligned}\right\} \quad . \quad . \quad . \quad (8.4)$$

where σ_H is given by (7.5), and the other symbols are the components of a tensor of the fourth rank:

$$\sigma_{\alpha\beta\gamma\delta} = -\epsilon_{\rho\gamma\nu}\epsilon_{\mu\delta\sigma}\frac{e^4}{4\pi^3c^2\hbar^3}\int\tau_{\mathbf{k}}v_\alpha v_\rho\frac{\partial}{\partial k_\nu}\left\{\tau_{\mathbf{k}}v_\mu\frac{\partial}{\partial k_\sigma}(\tau_{\mathbf{k}}v_\beta)\right\}\frac{d\mathfrak{S}}{v} \quad . \quad (8.5)$$

(The symbols $\epsilon_{\rho\gamma\nu}$, etc. are, of course, the standard totally anti-symmetric tensors of the third rank arising out of the vector products between magnetic field and electron velocity in the equation for the Lorentz force.)

These formulae are quite intractable unless we know the functional form of $\tau_{\mathbf{k}}$. Suppose we make the simplifying assumptions of § 7—that τ is constant and that the energy surfaces are of our model form. For the components of (8.5) that we need in (8.4) we find

$$\sigma_{1111}=\sigma_{1212}=0, \quad . \quad . \quad . \quad . \quad . \quad . \quad . \quad (8.6)$$

$$\sigma_{1122}=\frac{e^4}{3\pi^3\hbar c^2}\int\tau^3\{v_x^2\mathsf{M}_{xx}^{-1}(\mathsf{M}_{yy}^{-1}+\mathsf{M}_{zz}^{-1})+\ldots\text{cyclic perms}\}\frac{d\mathfrak{S}}{v} \quad (8.7)$$

$$\sigma_{1221}=\frac{-2e^4}{3\pi^3\hbar c^2}\int\tau^3\{v_x^2\mathsf{M}_{yy}^{-1}\mathsf{M}_{zz}^{-1}+\ldots\text{cyclic perms}\}\frac{d\mathfrak{S}}{v} \quad . \quad . \quad (8.8)$$

These expressions are relatively simple because, as previously remarked, the inverse mass tensor has the same principal axes over the whole of a cone, so that all off-diagonal components of $\mathbf{M}^{-1}$ can be made to vanish.

Since all the terms in (8.7) and (8.8) can be expressed as algebraic functions of z, the integrations can all be done analytically. But this calculation would be much less realistic than for the Hall effect, because of the anisotropy of $\tau_{\mathbf{k}}$. There is a very simple test. Add the relations (8.4):

$$\rho_1^{(2)}+\rho_2^{(2)}+\rho_3^{(2)}=-\rho_0^2\sigma_{1111} \quad . \quad . \quad . \quad . \quad . \quad . \quad (8.9)$$

which by (8.6) should be zero. The experimental evidence (Olsen and Rodriguez 1957) is that this sum is not zero for any of the noble metals; but is comparable in magnitude with each of its separate terms. Thus, our model is not in agreement with experiment on an important general point.

It may be that the shape of Fermi surface that we are studying is not near enough to the actual shape. A sufficient condition for (8.6) is that

$$\mathscr{E}_{\mathbf{k}}=f_1(k_x)+f_2(k_y)+f_3(k_z) \quad . \quad . \quad . \quad . \quad . \quad (8.10)$$

over the whole cap of a cone. This is only approximately true; as we go outwards from L towards K, say, in fig. 1, we shall notice the influence

of the contact region of the next hexagonal face, and this will tip the axes of the inverse mass tensor. Going towards U, on the other hand, we enter the realm of the more distant square face, which may not be so important. Thus, the surface loses the local rotational symmetry about each (111) axis, and there will be contributions to σ_{1111} from off-diagonal elements of $\mathbf{M}^{-1}$ relative to this axis.

A more likely explanation rests upon the anisotropy of $\tau_{\mathbf{k}}$. Not only does this occur as a weight factor in the galvanomagnetic tensor (8.5); its derivatives in k-space should appear explicitly in the integrals. Looking at σ_{1111}, for example, we find in the integrand terms like

$$v_x^2 v_y^2 \left\{ \tau_{\mathbf{k}} \frac{\partial^2 \tau_{\mathbf{k}}}{\partial k_z^2} + \left(\frac{\partial \tau_{\mathbf{k}}}{\partial k_z} \right)^2 \right\} \quad . \quad . \quad . \quad . \quad . \quad (8.11)$$

which certainly need not vanish, even in cubic symmetry. If the anisotropy of τ is really as large as has been suggested in § 7 (e.g. (7.11) and (7.13)), then we must expect important contributions from such terms. The calculations of Olsen and Rodriguez (1957) are quite unreliable quantitatively in these circumstances, except in confirming that the Fermi surface touches the zone boundaries.

This interpretation can be correlated with the observation of de Launay *et al.* (1959) that Kohler's Rule is not exactly obeyed in Cu. When $\Delta\rho/\rho_0$ is plotted against H/ρ_0, the points corresponding to different temperatures or specimens containing different impurities do not fall precisely on a single curve. The fundamental condition for the validity of Kohler's Rule is that the functional form of $\tau_{\mathbf{k}}$ should be the same under all conditions, even though its magnitude may vary with temperature etc. We have already seen that this is unlikely from the Hall data; it seems that in Cu the anisotropy of $\tau_{\mathbf{k}}$ (e.g. the value of $\langle\tau\rangle\langle 1/\tau\rangle$) is least for scattering by Zn, is larger for phonon scattering at room temperature and greatest for scattering by polyvalent impurities such as Ge. We might expect this variation to be reflected in deviations from Kohler's rule. In particular, B_l, the longitudinal magnetoresistance in a polycrystalline specimen, seems from (8.2) and (8.9) to be rather sensitive to the value at σ_{1111}, and hence to the form of $\tau_{\mathbf{k}}$. It is interesting that B_l is a bit smaller at room temperature than it is at 78°K, as if the anisotropy of τ had decreased and also that B_l is not at all constant from specimen to specimen at 4·2°K, where the residual resistance probably arises from various atomic species as impurities.

§ 9. Electrical Conductivity

The theory of the basic transport coefficients is complicated, and it is difficult to say much quantitatively about the result of assumed deviations from a simple free-electron system. Thus, we need to know more about the electron–phonon interaction, more about the electron wave functions, more about the lattice spectrum, and more about how

to solve the Boltzman equation before we can assign definite effects to the anisotropy of the Fermi surface, or can calculate in detail the anisotropy of the relaxation time. The following remarks are not, therefore tied down quantitatively to our 8-cone model, but are concentrated on some points of difference between the observed conductivities and some of the conventional results for free-electron models.

The magnitude of the 'ideal' electrical resistivity in the noble metals is not anomalous. When allowance has been made for the velocity of sound, the atomic weight, density, etc., of the solid, the reduced resistivity $\mathfrak{R}$ (E & P, § 9.7) is very similar in each case to the values noted for the alkali metals, and there is no systematic trend. The value of $\mathfrak{R}$ does not seem very sensitive to the shape of the Fermi surface, but there is no complete calculation to verify this theoretically.

The temperature variation of ρ_L is enshrined in the parameter Θ_R (E & P, § 9.6), which turns out to be very close to the ordinary Debye temperature Θ_D derived from the lattice specific heat (see table 7). This in itself has some significance; it shows that the electrons are not being scattered entirely by longitudinal modes, whose Debye temperature, Θ_l is much larger than Θ_D, but that a great part of the electrical resistance, especially at low temperatures, is associated with scattering of the electrons by the shear waves of the lattice.

We can look at this from two related points of view. At low temperatures we are talking about long-wave phonons, whose interaction with electrons can be represented by a 'deformation potential' (E & P, § 5.6). For reasons of symmetry, this interaction involves only the longitudinal modes if the Fermi surface is a sphere, but a multiply-connected surface should be much more sensitive to shear strains in the lattice, and there should be strong interactions with the transverse phonon modes, especially in the neck regions.

The alternative view-point is based on an analytical theory of the electron–phonon interaction (J. G. Collins, to be published). In the case of free electrons the matrix element for the transition from state $\mathbf{k}$ to state $\mathbf{k}'$ is given by the Bardeen method (E & P, § 5.7);

$$\mathscr{I}(\mathbf{k},\mathbf{k}') = \mathbf{e}_\mathbf{q} \cdot (\mathbf{k}-\mathbf{k}')\mathscr{C}(|\mathbf{k}-\mathbf{k}'|) \quad . \quad . \quad . \quad . \quad (9.1)$$

where $\mathscr{C}(\mathbf{K})$ is approximately $\frac{2}{3}\mathscr{E}_F$ at $K=0$ but falls away rapidly as we go to large values of K. The phonon polarization vector is $\mathbf{e}_\mathbf{q}$, so that if $\mathbf{q}=\mathbf{k}'-\mathbf{k}$ we find a factor $\mathbf{e}_\mathbf{q}\cdot\mathbf{q}$ which selects only the longitudinal lattice modes. To get interaction with the shear modes, we must study the electron–phonon U-processes, where

$$\mathbf{e}_\mathbf{q}\cdot(\mathbf{k}'-\mathbf{k}) = \mathbf{e}_\mathbf{q}\cdot(\mathbf{q}+\mathbf{g}). \quad . \quad . \quad . \quad . \quad . \quad . \quad (9.2)$$

That is, when $\mathbf{k}'-\mathbf{k}$ is too large to lie inside the Debye sphere we add a suitable reciprocal lattice vector, $\mathbf{g}$, to $\mathbf{q}$. Evidently (9.2) need not vanish automatically for transverse modes in which $\mathbf{e}_\mathbf{q}$ is normal to $\mathbf{q}$.

Now if we study the same matrix element for transitions between wave functions like (3.1), we get a more complicated formula; one can easily verify by substituting that this takes the form

$$\mathbf{e}_{\mathbf{q}} \cdot \int \psi_{\mathbf{k}}^* \nabla \mathscr{U} \psi_{\mathbf{k}'} \, d\mathbf{r} = \sum_{\mathbf{g}, \mathbf{g}'} \alpha^*_{\mathbf{k}+\mathbf{g}} \alpha_{\mathbf{k}'+\mathbf{g}'} \mathscr{I}(\mathbf{k}+\mathbf{g}, \mathbf{k}'+\mathbf{g}') \quad . \quad . \quad (9.3)$$

where $\mathscr{I}$ $(\mathbf{k}, \mathbf{k}')$ is much the same as in (9.1) and the coefficients α are the solutions of the secular equations (3.3). It is at once obvious that (9.3) contains terms with polarization factors like $\mathbf{e}_{\mathbf{q}} \cdot (\mathbf{k}'+\mathbf{g}'-\mathbf{k}-\mathbf{g})$, which will give contributions from the transverse modes even when $\mathbf{k}'-\mathbf{k}=\mathbf{q}$. Thus, there is no need to invoke U-processes in order to get interactions with the shear waves of the lattice.

Here it is worth making a short digression on the subject of nomenclature. In the free electron model we can label states by their actual wave vectors, so that we know the absolute values of $\mathbf{k}'$ and $\mathbf{k}$, and can verify that their difference, as in (9.2), is larger than any possible $\mathbf{q}$, and hence requires an Umklapp process for scattering. Much of the discussion of the theory of electrical and thermal resistance is concerned with the different roles played by N-processes and by U-processes—as we have just noted, we make statements such as 'transverse modes take part only in U-processes', etc. But in the repeated zone scheme this distinction is only conventional. We can choose to say that the wave vector of our final state is

$$\mathbf{k}''=\mathbf{k}'-\mathbf{g} \quad . \quad . \quad . \quad . \quad . \quad . \quad . \quad . \quad . \quad (9.4)$$

(as in fig. 21) because electron wave-vectors are arbitrary up to the addition of a reciprocal lattice vector. We then have

$$\mathbf{q}=\mathbf{k}''-\mathbf{k} \quad . \quad . \quad . \quad . \quad . \quad . \quad . \quad . \quad . \quad (9.5)$$

and the transition has the formal properties of an N-process. Of course the polarization factor is still (9.2) (because this depends on the actual wave vector of the free-electron state) but the classification scheme has begun to fail.

When we have a multiply connected Fermi surface, as in fig. 22, the distinction between U and non-U becomes entirely artificial. Suppose that $\mathbf{k}''$ lies on a neck, just across the zone boundary from $\mathbf{k}$. Are we to distinguish the transition to such a state from the transition to $\mathbf{k}_1$ say, which lies on the same neck but just inside the zone boundary. In the repeated zone scheme the energy surfaces are continuous along the necks, and the zone boundary is only a conventional plane for counting unit cells in reciprocal space. It is more natural to describe the transition by the shortest possible vector, from $\mathbf{k}$ to $\mathbf{k}''$, than to add on a reciprocal lattice vector, go to $\mathbf{k}'$, and then have to subtract the same reciprocal lattice vector from $\mathbf{k}'-\mathbf{k}$ in order to find the phonon wave vector $\mathbf{q}$. This seems to be the best convention to use in (9.3) say, trusting to the values of the coefficients $\alpha_{\mathbf{k}}$ etc., to give the right contributions from the various OPW's. One can show, for example, that the matrix

element is a continuous function as the final state vector crosses the zone boundary, so that there is a smooth change-over from 'N-processes' to 'U-processes', without any abrupt alteration in the physical phenomena.

In this formulation, can we understand the anisotropy of $\tau_{\mathbf{k}}$? The problem is very complex, and can only be solved numerically (Ziman, to be published). There are a number of different competing factors, such as the following:

Fig. 21

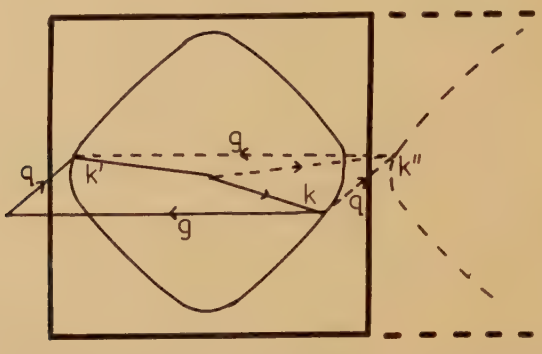

The same transition, —— as U-process, – – – as N-process.

Fig. 22

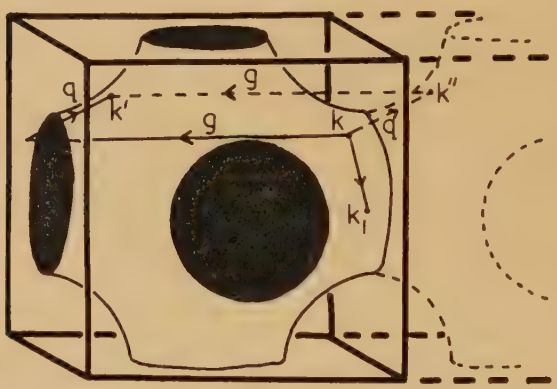

N-processes and U-processes on a multiply-connected Fermi surface.

In the first place, the coefficients $\alpha_{\mathbf{k},\mathbf{g}}$, etc., vary considerably over the Fermi surface; according to (5.5) and (5.6) we have something like a single OPW over the belly regions, but this is modified into a mixed state, with two OPW's of nearly equal amplitude as we go to the zone boundary. If $\mathscr{U}_{111}$ is negative all the terms in (9.3) will be positive, so that there will be an enhancement of the scattering matrix element in the neck regions.

Then we must look at the density-of-states factor in the scattering probability. If the bulk of the scattering is through small distances on the Fermi surface (and there is a tendency for this, especially at low temperatures) a high local density of states, as at a neck, will give a high transition rate, and a small value of $\tau_{\mathbf{k}}$.

A third factor lies in the definition of $\tau_{\mathbf{k}}$ itself. This is by no means a simple question, for we are really studying the solution of a complex integral equation and there is no guarantee that there is a solution even of the form (cf. E & P, §§ 7.7, 9.5)

$$\Phi_{\mathbf{k}} = \tau_{\mathbf{k}} \mathbf{v}_{\mathbf{k}} \cdot \mathbf{E} \quad . \quad . \quad . \quad . \quad . \quad . \quad . \quad . \quad . \quad (9.6)$$

in the electric field $\mathbf{E}$. But if this is so one can argue, as a rough approximation, that

$$\frac{1}{\tau_k} \approx \int \mathcal{Q}_{\mathbf{k}}^{\mathbf{k}'} \{1 - \cos(\mathbf{v}_{\mathbf{k}}, \mathbf{v}_{\mathbf{k}'})\} \mathbf{dk}' \quad . \quad . \quad . \quad . \quad (9.7)$$

where $\mathcal{Q}_{\mathbf{k}}^{\mathbf{k}'} \mathbf{dk}'$ is the probability of a transition from state $\mathbf{k}$ into a state $\mathbf{k}'$ in the range $\mathbf{dk}'$ and $(\mathbf{v}_{\mathbf{k}}, \mathbf{v}_{\mathbf{k}'})$ is the angle between the electron velocities in those two states. Now, if $\mathcal{Q}_{\mathbf{k}}^{\mathbf{k}'}$ has a strong forward lobe, the value of the integral will be larger on the necks than on the belly because the radius of curvature is smaller on the necks, so that $\cos(\mathbf{v}_{\mathbf{k}}, \mathbf{v}_{\mathbf{k}'})$ deviates more quickly from unity as we take $\mathbf{k}'$ away from $\mathbf{k}$, and the weight function has less effect in suppressing the contribution of 'local' scattering to the integral. This argument is equivalent to the statement we make in the free electron model where a U-process, of quite small phonon wave vector, can reverse the direction of the electron, and hence make a large contribution to the electrical resistance. (cf. fig. 21).

Can we also understand why the anisotropy of $\tau_{\mathbf{k}}$ should vary from one scattering mechanism to another? This is a much more uncertain problem, but there are arguments above which make $\tau_{\mathbf{k}}$ depend on the shape of the differential scattering cross section of the impurity or phonon displacement, and we may expect this to vary a lot when we compare the scattering by the screened Coulomb field of a charged impurity (e.g. Blatt 1957) with the effect of a homovalent impurity such as Ag in Au. This effect, also, has been confirmed by a detailed calculation (Ziman, to be published), and the behaviour of $\tau_{\mathbf{k}}$ found to be consistent with the Hall effect in alloys.

How is it then, that the conventional theories of the residual resistance produced by chemical impurities work so well? As shown in E & P (§ 9.2) there is good agreement between the experiments and a theory of free electrons scattered by screened charged impurities. Until we have exact solutions for the scattering matrix elements of the proper wave functions, this is an open question, but it may be simply that the relaxation time of the electrons in the neck is so short that they play little part in the conductivity and the belly states carry the current and are scattered

nearly as if free. The attempt to calculate by the variational method (Ziman 1959 b) may be seriously misleading, for it may greatly overemphasise the contribution of the strong scattering in the contact regions.

Whilst discussing electrical resistance we naturally think of the 'resistance minimum' phenomenon, and the corresponding anomaly in the thermoelectric properties. It now seems (Gold *et al.* 1960) that this effect is always associated with the presence of free Fe, or other magnetic impurities, and is not related directly to the shape of the Fermi surface. An interpretation in terms of breaking away of contact with the zone boundary (Ziman 1959 b), is not supported by the other evidence, and must now be abandoned.

Linde (1958) has observed changes in the apparent slopes of the resistance/temperature curves in Cu and Au when alloyed with certain other metals, and has noted a correlation with the pressure coefficient of the additional resistivity. This is most likely to be due to changes in the Fermi level (on thermal expansion or elastic compression of the lattice), which sweeps through the supposed broad 'resonances' in the scattering cross-section of transition metal impurities (Friedel 1956).

§ 10. Thermal Conductivity

At high temperatures this is given (presumably; has it ever been thoroughly checked?) by the Wiedemann–Franz law, and introduces no new results. The low temperature value is of some interest because there are certain theoretical comparisons that can be made (Klemens 1956). Thus, one can calculate

$$D_3 = 1/\mathfrak{W}_1 = 64T^2 W_L(\infty)/\Theta^2 W_L(T) \quad . \quad . \quad . \quad . \quad (10.1)$$

$$D_4 = 1/\mathfrak{W}_2 = 0{\cdot}129\Theta^2 \rho_L(T)/\mathfrak{L}_0 T^3 W_L(T) \quad . \quad . \quad . \quad (10.2)$$

(for notation see E & P, § 9.10) which are tabulated in table 7. Despite some uncertainty in the proper choice of Θ (we simply follow Klemens) there is obviously a significant difference between the observed values of these parameters for the noble metals and the theoretical Bloch-type free-electron model which would have $D_3 = D_4 = 1$.

Table 7

	Cu	Ag	Au
Θ_D (°K)	310–335	210–225	165–186
Θ_R (°K)	320–333	200–223	170–200
D_3	6·2	5·2	5·8
D_4	5·4	4·2	4·5

We notice at once that the magnitudes of D_3 and D_4 are correlated with the diameters of the necks on the Fermi surfaces. Is this significant? The conventional argument is that these ratios are sensitive to the degree to which U-processes dominate the electron scattering, especially at low temperatures; there is an important difference between electrical and thermal conduction (and between thermal conduction at high and at low temperatures) in that the former is particularly sensitive to scattering through large angles, as in a typical U-process right across the electron sphere, whereas heat conduction at low temperatures is affected chiefly by the loss of energy of an electron when it collides with a phonon, irrespective of the angle of scatter. For a nearly spherical surface one can discuss these ratios in terms of the shape of the electron–phonon interaction (E & P, § 9.10), and it is easy to show that D_3 and D_4 need neither be equal to unity nor to one another (Cohen and Heine discuss the role of different averages of sound velocity in D_3 and D_4, but this is not the whole story by any means). For our more complex surfaces it is difficult to draw any quantitative conclusions from the values in table 7. We can note that we have the equivalent of U-processes in the scattering of electrons across regions of high curvature on the Fermi surface, and these should, according to (9.7), have a larger effect on ρ_L than on W_L, but it does not seem possible as yet to compute D_3 or D_4 directly and to see how they should depend in detail on the shape of the Fermi surface.

Indeed there is a difficulty about (10.1) and (10.2). It is assumed that $T^2/W_L(T)$ is a constant at low temperatures—that the 'ideal' thermal conductivity obeys the theoretical Bloch–Wilson law $\kappa \propto T^{-2}$. In the case of Cu there is strong experimental evidence against this; Powell *et al.* (1959) favour a function like $T^{-2\cdot 8}$, which would make D_3 and D_4 into variables increasing as the temperature falls. But really this should not surprise us. The T^{-2} formula is based upon very special assumptions about the form of the electron–phonon interaction. It can be shown (Ziman 1954) that this formula must be modified when we allow for U-processes, even on a nearly spherical Fermi surface. For a surface with contact, and with a complicated interaction with phonons, we might get considerable deviations from a simple quadratic law. By the same tokens, the T^{-5} law for the electrical conductivity is not sacrosanct; deviations from it have been reported (Powell *et al.* 1959) although the full experimental position is not yet clear.

Another phenomenon showing how far we are from the conventional Bloch theory is the deviation from Matthiessen's rule, for both electrical and thermal resistivity in cold-worked Cu (Powell *et al.* 1959). But this is just what we would expect from our hypothesis that the anisotropy of the relaxation time of the electrons is quite large, and varies from one type of scattering to another. It can easily be shown (E & P, § 7.10) that there must be positive deviations from Matthiessen's law—the resistivity of a system containing several species of scatter must be larger

than the sum of the resistances due to each species separately—if $\tau_{\mathbf{k}}$ is different for the different types of scattering. It is dangerous to combine data from different sources, but it is worth noting that Berlincourt (1958) found the Hall coefficient of cold-worked Cu to depend considerably on the temperature, as if the anisotropy of $\tau_{\mathbf{k}}$ for scattering by dislocations etc. were very different from the anisotropy due to phonon scattering at 200°K. It would be interesting to make a systematic search for deviations from Matthiessen's rule in specimens showing unusual values of the Hall coefficient, and see whether these effects are correlated.

§ 11. Thermoelectric Power : the 'Diffusion' Term

By tradition, the thermoelectric properties of metals and alloys offer important clues to their electron structure. For example, it is well established theoretically that a simple free-electron system should have a negative thermopower—just what we observe at room temperature in all the alkali metals except Li. So, when the thermopower is positive, we feel that the Fermi surface must be complicated, with a preponderance of 'hole' states etc. The fact that Q is positive for the pure noble metals then seems strong qualitative evidence for the sort of multiply-connected surfaces which we are here studying.

But when we look quantitatively at this evidence, it is not so impressive. On the contrary, the theory of the thermopower of the noble metals is as uncertain as many of the experimental results which it sets out to explain!

First the observations: fig. 23 shows the temperature dependence of Q, the absolute thermopower of pure Cu, Ag and Au, at low temperatures (Pearson, private communication) and up to the melting point (Cusack and Kendall 1958). These data are probably the best at present available but they have not the weight of being agreed by a number of independent authorities. The points to notice are (*a*) that Q is positive except at very low temperatures, (*b*) that there is a hump in Q at low temperatures, (*c*) that for Cu it varies linearly with absolute temperature above about 200°K, (*d*) that the line for Ag does not go through the origin and (Gold, private communication) tends to bend over above 1000°K, (*e*) that Au does not show a definite linear portion above room temperature, but rises to a broad maximum and then falls slightly.

The standard theory gives a very simple formula for the electronic contribution; thus (E & P, § 9.11)

$$Qe = \frac{\pi^2}{3}\frac{\boldsymbol{k}}{\boldsymbol{e}}\boldsymbol{k}T\left[\frac{\partial \ln \sigma(\mathscr{E})}{\partial \mathscr{E}}\right]_{\mathscr{E}=\zeta} \quad . \quad . \quad . \quad . \quad . \quad (11.1)$$

where $\sigma(\mathscr{E})$ is 'the electrical conductivity if the Fermi level were at $\mathscr{E}$'. In this formula $\boldsymbol{e}$ is the conventional charge of an electron, that is, a negative quantity. For a simple free-electron system, we write

$$\sigma(\mathscr{E}) \propto \tau(\mathscr{E}) v_{\mathrm{F}}(\mathscr{E}) \mathscr{D}(\mathscr{E}) \quad . \quad . \quad . \quad . \quad . \quad . \quad (11.2)$$

showing how the conductivity depends on the Fermi energy through the relaxation time, the Fermi velocity, and the area of the Fermi surface. It follows very easily that

$$Q_e = \frac{\pi^2}{3}\frac{\boldsymbol{k}}{\boldsymbol{e}}\frac{\boldsymbol{k}T}{\mathscr{E}_F}\left(\frac{3}{2}+\frac{\partial\{\ln\tau(\mathscr{E})\}}{\partial\{\ln\mathscr{E}\}}\right).$$

$$= -\frac{\pi^2}{3}\frac{\boldsymbol{k}}{|\boldsymbol{e}|}\frac{\boldsymbol{k}T}{\mathscr{E}_F}\xi \qquad \ldots\ldots\ldots \quad (11.3)$$

where ξ is a dimensionless constant, which, for phonon scattering at high temperatures should lie between $+2{\cdot}5$ and $+3$.

Fig. 23

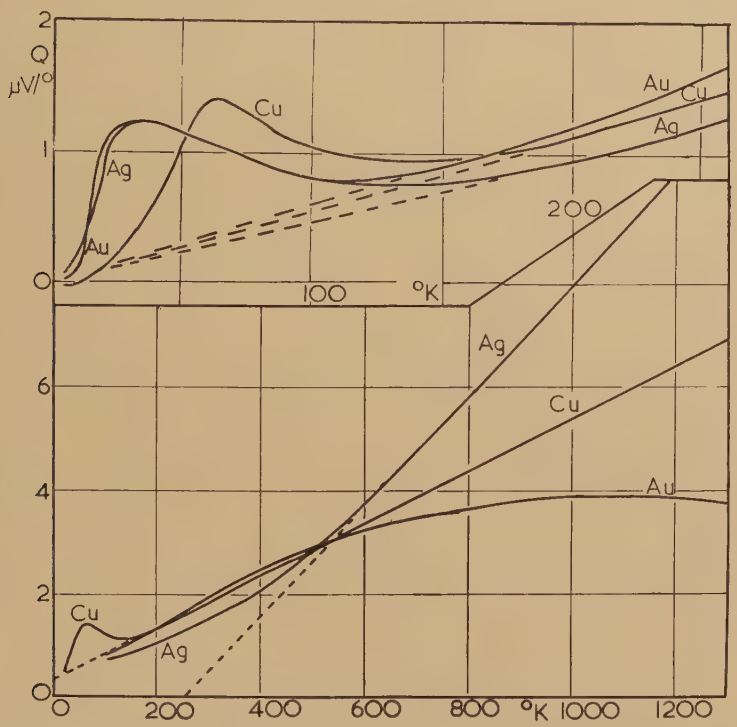

The thermoelectric power of the noble metals (Gold *et al.* 1960, Pearson, private communication, Cusack and Kendall 1958).

This theory tells us that Q_e should be directly proportional to T. If we look at the curves of fig. 23 below 300°K, and assume that the hump is due to phonon drag and has disappeared at about 200°K, we find for ξ the values $-1{\cdot}7$ for Cu, $-1{\cdot}1$ for Ag and $-1{\cdot}5$ for Au. But these linear trends are not continued at high temperatures except for Cu. For Ag the slope above 600°K corresponds to $\xi \sim -2{\cdot}5$, whilst for Au the value of ξ is quite uncertain. Thus, the experimental parameters are not well defined.

Nevertheless, we want to explain these negative values of ξ. Is the funny shape of the Fermi surface a sufficient cause? Let us look at the rate of change with energy of the analogue of v_F i.e.

$$\xi_1 = \mathscr{E}_F \left[\partial \left\{ \ln \int v d\text{S} \right\} \Big/ \partial \mathscr{E} \right]_{\mathscr{E}=\zeta} . \qquad . \quad . \quad . \quad (11.4)$$

This has the value $\frac{3}{2}$ in (11.3). From (6.2), using (4.6) and (4.7) we find a simple formula for ξ_1, for our 8-cone model

$$\xi_1 = \left(\frac{1}{m^*}\right)\left(\frac{2}{3\pi^2}\right)^{1/3} \frac{2(z_2 - z_1) + f'(z_2) - \{\frac{7}{9}z_1^2 + [f'(z_1)]^2\}/\{\frac{7}{9}z_1 + f'(z_1)\}}{\int_{z_1}^{z_2} \{2\epsilon - 2f(z) + [f'(z)]^2\} dz} .$$

$$. \quad . \quad . \quad (11.5)$$

In fig. 24 this quantity (with $m^* = 1$) is plotted against the number of electrons per atom, for several values of u. We see that it falls steeply from about 1·5 as the Fermi surface expands, and there is a change of slope at the contact with the zone boundary. Yet ξ_1, remains obstinately positive until the surface holds 1.1 electrons or more, and certainly does not reach negative values of the order of -1. In other words, if the main part of the diffusion thermopower were simply due to changes in the mean Fermi velocity, and Fermi area, we should expect Q_e to be between $-0{\cdot}5$ and $-1\,\mu$V/°C at room temperature, instead of the observed values which lie between $+1{\cdot}5$ and $+2\,\mu$V/°C.

This argument is not, of course, complete, for it ignores the variation of τ with energy. To allow for this, Bailyn (private communication) has suggested that $\tau(\mathscr{E})$ simply mirrors $\int v d\text{S}$, so that $\xi = 2\xi_1$. This obviously does not fit the observations; the argument for it depends on a crude use of the variational method, which is not really sufficiently accurate for such a delicate calculation. Jones (1955) has pointed out that for phonon scattering one might expect $\tau(\mathscr{E}) \propto \mathscr{E}^2/\mathscr{N}(\mathscr{E})$, putting the emphasis on the probability of scattering being proportional to the density of states into which the electron can go. But if we look at fig. 9 we see that this does not help to make Q change sign. It is true that

$$\frac{\partial \ln \tau(\mathscr{E})}{\partial \ln \mathscr{E}} = 2 - \frac{\partial \ln \mathscr{N}(\mathscr{E})}{\partial \ln \mathscr{E}} \qquad . \quad . \quad . \quad . \quad . \quad (11.6)$$

can become negative as we approach the zone boundary—indeed $\mathscr{N}(\mathscr{E})$ has infinite slope at that point—but beyond the point of contact the density of states falls again, and the contribution of (11.6) to ξ will be firmly positive.

We may try to blame our model of the energy surfaces—to argue, for example, that the proximity of other zone boundaries may already have taken us beyond the point where

$$\frac{\partial v_{\mathbf{k}}}{\partial \mathscr{E}_{\mathbf{k}}} = \frac{1}{\hbar} \frac{\partial^2 \mathscr{E}_{\mathbf{k}}}{\partial k^2} \Big/ \frac{\partial \mathscr{E}_{\mathbf{k}}}{\partial k} \qquad . \quad . \quad . \quad . \quad . \quad . \quad (11.7)$$

has become negative over a large part of the Fermi surface (cf. fig. 8). But remember that the Hall coefficient also contains terms of this sort (M_{zz}^{-1} in (7.5)) and we cannot afford to improve our value of Q at the

expense of R (which should already be smaller, theoretically, than we actually observe). In vulgar parlance, we have already found the Hall effect showing more 'electrons' than 'holes' in the noble metals: now the thermopower suggests that 'holes' predominate over 'electrons'.

Fig. 24

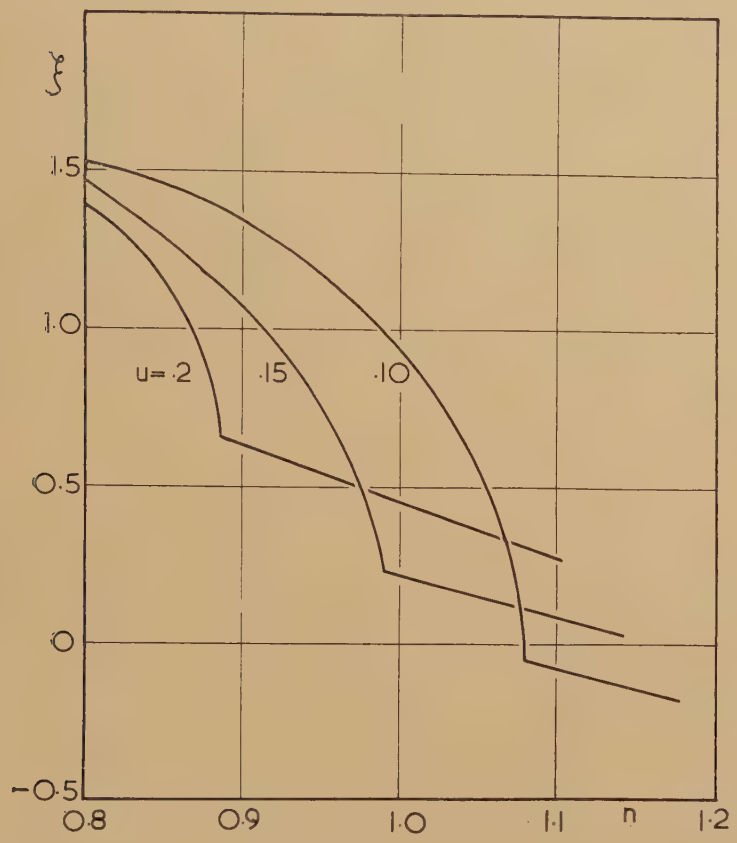

Calculated variation of ξ_1, with electron density, in the neighbourhood of contact.

The only hope lies, again, in a more complete theory of $\tau(\mathscr{E})$. We must write

$$\sigma(\mathscr{E}) \propto \int \tau_{\mathbf{k}} v \, d\mathbb{S} \quad . \quad . \quad . \quad . \quad . \quad . \quad . \quad (11.8)$$

and calculate the derivative of the whole function. There will be effects due to τ as a weight function in expressions like (11.4), but, more particularly, there will be the explicit variation of $\tau_{\mathbf{k}}$ with energy. Going back to § 9, we may expect large contributions from the variation of the coefficients $\alpha_{\mathbf{k}}$, etc., with energy (cf. (5.6)). Our hypothesis that $\tau_{\mathbf{k}}$ is smaller on the necks than on the belly of the surface is consistent

with the need for $\tau(\delta)$ to decrease rapidly as δ increases, i.e. as we approach the zone boundary in general. It is possible that we could find a link between a calculation of this effect and the magnetoresistance coefficients, as in (8.11). But all this waits on a good computation of the 'ideal' resistance of the noble metals sensitive to the details of the electron–phonon interaction.

There is a considerable literature on the thermoelectric properties of alloys of Cu, and a few results for alloys of the other noble metals (e.g. Domenicali and Otter 1954, Domenicali 1958, Friedel 1956). It is generally observed that any element added to Cu reduces the thermopower sharply—presumably because $\partial \ln \tau(\delta)/\partial\delta$ is smaller for scattering by impurity atoms than it is for phonon scattering. But most of the analysis that has been made of these data has been based upon the simple free-electron model with scattering by screened, charges, etc. Now that we know the full complexity of the Fermi surface, it is extremely difficult to accept the results of this analysis, even though some of its qualitative features (e.g. 'resonance' scattering by d-shells of transition metals) may be retained. All that one can hope is that the anisotropy of $\tau_{\mathbf{k}}$ is so great that there is not much contribution from the neck regions, so that the thermoelectric and other effects come mainly from the belly, where the electrons are more or less free anyway.

§ 12. Thermoelectric Power : Phonon Drag

It is now recognized that there may be an important contribution to the thermoelectric power from the heat carried by the lattice waves which are emitted as a current of electrons is drawn through the solid. This effect has been shown to be especially important at low temperatures; in the alkali metals (MacDonald *et al.* 1958, Ziman 1959a) the sign and magnitude of the 'lattice thermopower' may be correlated with the shape of the Fermi surface. We must therefore consider this phenomenon in the case of the noble metals.

The formal theory (E & P, §§ 9.13, 10.9) is complicated; in the end we can use one or other of the following formulae:

$$Q_L = \begin{cases} \dfrac{\boldsymbol{k}}{\boldsymbol{e}} \dfrac{1}{n} \left(\dfrac{C_L}{3\Lambda \boldsymbol{k}} \right) \left(\dfrac{-P_{1L}}{P_{LL}} \right), & \ldots\ldots (12.1) \\ \dfrac{\kappa_L}{\sigma_e T} \dfrac{\boldsymbol{e}}{\boldsymbol{k}} n \left(\dfrac{3N\boldsymbol{k}}{C_L} \right) \left(\dfrac{-P_{1L}}{P_{11}} \right), & \ldots\ldots (12.2) \end{cases}$$

Here C_L is the lattice specific heat, κ_L is the lattice conductivity, and σ_e is the 'ideal' electrical conductivity. These formulae are in principle, equivalent, but the first is more convenient at low temperatures (say $T < 0{\cdot}2\Theta$) and the second at higher temperatures.

For the moment let us ignore the symobols P_{1L}, P_{LL}, P_{11}, and concentrate on the other factors, which fix the general scale and temperature dependence of Q_L. Remembering that $\boldsymbol{k}/\boldsymbol{e} = -86\,\mu\text{v}/^\circ\text{c}$, we see

that Q_L can be quite large. At low temperatures, where (12.1) is appropriate, the T^3 specific heat law holds:

$$\frac{C_L}{3N\boldsymbol{k}} = \frac{4\pi^4}{5}\left(\frac{T}{\Theta}\right)^3. \qquad \ldots\ldots\ldots \quad (12.3)$$

Thus Q_L could be of the order of $1\,\mu$v/°c at $T = \Theta/20$, and should increase rapidly in magnitude above this temperature. But then the lattice conduction begins to be influenced by phonon–phonon interactions, etc.

Fig. 25

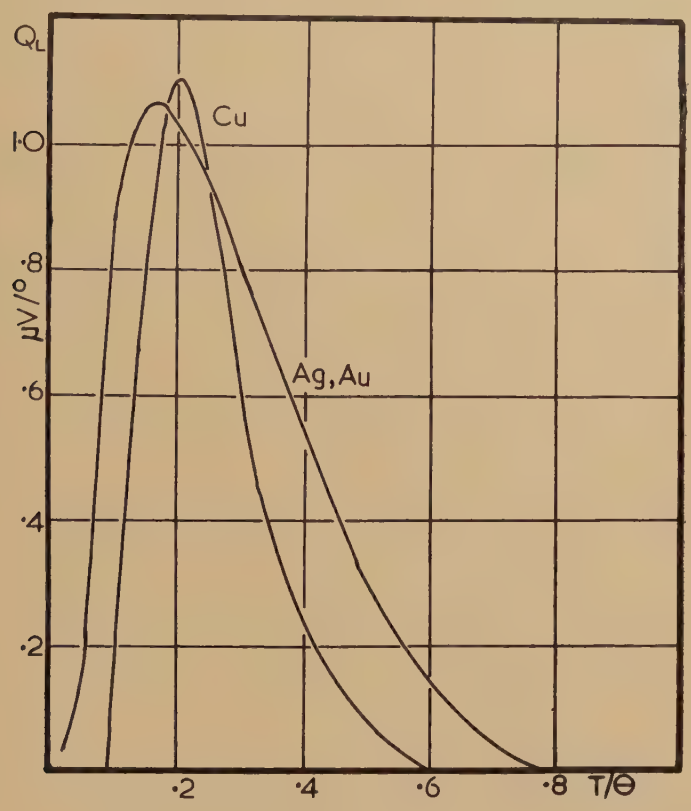

Lattice thermopower, estimated from fig. 23.

(which makes it difficult to estimate P_{LL}) and we go over to (12.2). As shown in E & P, §§ 8.2, 8.9, when we get above the Debye temperature, we can expect to write

$$\frac{\boldsymbol{e}}{\boldsymbol{k}}\left(\frac{\kappa_L}{\sigma_e T}\right) \sim \frac{1}{2{\cdot}5\gamma^2}\left(\frac{\Theta}{T}\right)\frac{\boldsymbol{k}}{\boldsymbol{e}}\frac{1}{n}, \qquad \ldots\ldots \quad (12.4)$$

where γ is the Gruneisen parameter—say $\gamma \sim 2$. This again, if $-P_{1L}/P_{11}$ is not too small, means quite a large thermopower—perhaps $8\,\mu$v/°c at $T = \Theta$; at lower temperatures it would rise exponentially as the U-processes are frozen out, until electron–phonon interaction dominates κ_e.

It is true that in Cu and Ag this would be reduced by isotope scattering of phonons, but a short calculation (E & P, § 8.6) suggests that this would be a negligible effect above room temperature. In fig. 23 we see well-developed humps in the thermopower at low temperatures which Blatt and Kropschot (1960) have shown to be due to phonon drag. If we suppose that Q_L is added on to a linear diffusion thermopower, we get the curves of fig. 25 (which are plotted in terms of T/Θ, to make them comparable). There is no doubt that the phenomenon is much the same in all three metals—Q_L is positive, rising rapidly to a peak of about $1\,\mu V/°C$ near $T = 0{\cdot}15\,\Theta$ and a slower fall to zero at about $T = \Theta$. Cu differs slightly by having a narrower peak shifted to about $0{\cdot}2\,\Theta$, and has, it seems, a small negative part at very low temperatures.

Do our formulae (12.1)–(12.4) explain these phenomena? Having said nothing, so far, about $(-P_{1L}/P_{LL})$ and $(-P_{1L}/P_{11})$, let us treat these as adjustable parameters; we find that we may represent the general shape of the experimental curves by using (12.1) and (12.3), with $(-P_{1L}/P_{LL}) \sim -0{\cdot}14$ below the peak, and using (12.2) and (12.4), with $(-P_{1L}/P_{11}) \sim -0{\cdot}025$ at higher temperatures. The major discrepancy is that the observed value of Q_L seems to fall to zero more rapidly than this model would allow at temperatures above $0{\cdot}5\,\Theta$ (indeed it may become slightly negative, although this is difficult to check against the linear diffusion term).

So we are forced to discuss these variational integrals P_{11}, P_{1L}, P_{LL}. In the theory of E & P these are defined as follows:

$$\left.\begin{aligned} P_{11} &= \frac{1}{\boldsymbol{k}T}\int\int\int (\Phi_{\mathbf{k}} - \Phi_{\mathbf{k}'})^2 \mathscr{P}_{\mathbf{kq}}{}^{\mathbf{k}'}\,\mathbf{dk}\,\mathbf{dq}\,\mathbf{dk}', \\ -P_{1L} &= \frac{1}{\boldsymbol{k}T}\int\int\int (\Phi_{\mathbf{k}} - \Phi_{\mathbf{k}'})\Phi_{\mathbf{q}} \mathscr{P}_{\mathbf{kq}}{}^{\mathbf{k}'}\,\mathbf{dk}\,\mathbf{dq}\,\mathbf{dk}', \\ P_{LL} &= \frac{1}{\boldsymbol{k}T}\int\int\int (\Phi_{\mathbf{q}})^2 \mathscr{P}_{\mathbf{kq}}{}^{\mathbf{k}'}\,\mathbf{dk}\,\mathbf{dq}\,\mathbf{dk}', \end{aligned}\right\} \quad . \quad . \quad (12.5)$$

(strictly speaking P_{LL} should contain further terms corresponding to phonon–phonon interactions, scattering of phonons by impurities, etc., but these are all taken care of by using (12.2) at high temperatures—i.e. in the range where scattering of electrons by phonons is no longer the sole agent governing κ_L).

In E & P we further postulated that

$$\Phi_{\mathbf{k}} = \mathbf{k}\cdot\mathbf{u}; \quad \Phi_{\mathbf{q}} = \mathbf{q}\cdot\mathbf{u} \quad . \quad . \quad . \quad . \quad . \quad . \quad (12.6)$$

whence we find, for electron-phonon N-processes, that $P_{11} = -P_{1L} = P_{LL}$. This would probably be the asymptotic situation at low temperatures for a spherical Fermi surface. But for our more complicated system this assumption is too crude. Fortunately (12.6) is not the essential condition for (12.1), (12.2) and (12.5) to yield an acceptable variational estimate

of Q_L. We can use any trial functions $\Phi_{\mathbf{k}}$ and $\Phi_{\mathbf{q}}$, provided that they are normalized to make

$$\frac{U_L}{TJ_1} = \frac{\int v_{\mathbf{q}} \Phi_{\mathbf{q}} (\partial n_{\mathbf{q}}^0/\partial T)\, \mathbf{dq}}{-\int \mathbf{e} v_{\mathbf{k}} \Phi_{\mathbf{k}} (\partial f_{\mathbf{k}}^0/\partial \mathscr{E}_{\mathbf{k}})\, \mathbf{dk}} = \frac{\mathbf{k}}{\mathbf{e}} \frac{1}{n} \left(\frac{C_L}{3N\boldsymbol{k}} \right). \quad . \quad . \quad . \quad (12.7)$$

Naturally we should like to choose these trial functions so that they conform to the functional behaviour of the electron and phonon distributions that actually satisfy the Boltzmann equation. We can do this by writing

$$\Phi_{\mathbf{k}} = \frac{\tau_{\mathbf{k}}}{\tau_e} \frac{m}{\hbar} \mathbf{v}_{\mathbf{k}} \cdot \mathbf{u}; \quad \Phi_{\mathbf{q}} = \frac{\tau_{\mathbf{q}}}{\tau_L} \mathbf{q} \cdot \mathbf{u} \quad . \quad . \quad . \quad . \quad . \quad (12.8)$$

where $\tau_{\mathbf{k}}$, $\tau_{\mathbf{q}}$ are relaxation times for electrons in state $\mathbf{k}$, phonons in state $\mathbf{q}$, and τ_e, τ_L are average relaxation times for electrons and phonons —i.e. defined so that the kinetic formulae

$$\sigma_e = nN\mathbf{e}^2\tau_e/m; \quad \kappa_L = \tfrac{1}{3} C_L v_L^2 \tau_L \quad . \quad . \quad . \quad . \quad . \quad (12.9)$$

give the actual ideal electrical conductivity and lattice heat conductivity. Of course we do not know $\tau_{\mathbf{k}}$ and $\tau_{\mathbf{q}}$ directly, and can scarcely calculate them but at least we have some intuitive ideas about how they should behave.

When we put (12.8) into (12.5), we get some complicated integrals for P_{11}, P_{1L} and P_{LL} which can be reduced a bit by the use of the methods of E & P, §9.5, but which cannot easily be evaluated. P_{11} and P_{LL} come out as positive definite functions, not necessarily equal. But the sign and strength of Q_L will depend on $-P_{1L}$ about which we can make the following qualitative comments.

At low temperatures, only long-wave phonons, with small values of q, are allowed. All processes in our formulation (cf. fig. 22) are N-processes, so that $\mathbf{k}' = \mathbf{k} + \mathbf{q}$, and we can approximate to the key factor in $-P_{1L}$:

$$\begin{aligned} \frac{m}{\hbar} (\tau_{\mathbf{k}'} \mathbf{v}_{\mathbf{k}'} - \tau_{\mathbf{k}} \mathbf{v}_{\mathbf{k}}) \cdot \tau_{\mathbf{q}} \mathbf{q} &\approx \frac{m}{\hbar} \mathbf{q} \cdot \frac{\partial}{\partial \mathbf{k}} (\tau_{\mathbf{k}} \mathbf{v}_{\mathbf{k}}) \cdot \tau_{\mathbf{q}} \mathbf{q} \\ &= m \tau_{\mathbf{k}} \tau_{\mathbf{q}} (\mathbf{q} \cdot \mathbf{M}^{-1} \cdot \mathbf{q}) + \frac{m}{\hbar} \left(\mathbf{q} \cdot \frac{\partial \tau_{\mathbf{k}}}{\partial \mathbf{k}} \right) (\mathbf{v}_{\mathbf{k}} \cdot \tau_{\mathbf{q}} \mathbf{q}). \quad (12.10) \end{aligned}$$

The second term will tend to be small, because $\mathbf{q}$ will lie nearly in an energy surface, normal to $\mathbf{v}_{\mathbf{k}}$. In other words, we see again the inverse mass tensor. If we suppose, even more crudely, that $\tau_{\mathbf{k}}$ is cancelled, in the integration, by the scattering probability factor, we are led to something like an average value of the components of $\mathbf{M}^{-1}$ tangential to the Fermi surface. To get some idea of how this might behave, we calculate

$$m^* \int \mathsf{M}_{xx}^{-1} + \mathsf{M}_{yy}^{-1} + \mathsf{M}_{zz}^{-1}) \frac{d\mathbb{S}}{v} \Big/ 3 \int \frac{d\mathbb{S}}{v} = \tfrac{2}{3} + \frac{f'(z_2) - f'(z_1)}{3(z_2 - z_1)} \quad (12.11)$$

This is now our (wildly approximate) estimate of the limiting value of

$-P_{1L}/P_{LL}$. Using the numerical data already amassed, one finds a number that is small, and positive, being about $+0{\cdot}1$ for the sort of surface that we assume for Ag, a bit larger for Au, and perhaps $+0{\cdot}2$ for Cu. If one looks closely at fig. 25, at the very low temperature end, one can say that the 'observed' values run from about $-0{\cdot}3$ for Ag, through $-0{\cdot}07$ for Au, to a small positive value for Cu. These are in the right order, but shifted to more negative values. Obviously we cannot expect numerical agreement, but we do see that there is no inconsistency between the thicker necks in Cu and a slightly negative value of Q_L at the lowest temperatures. The simple statement that 'when the surfaces contact the zone boundary U-processes are possible down to the smallest phonon frequencies, and these make Q_L positive' is only roughly correct.

At higher temperatures, when larger values of q are allowed, it becomes impossible to discuss these integrals in terms of the local differential geometry of the Fermi surface. Above the Debye temperature we have transitions between all parts of the surface, weighted by the electron–phonon matrix element, the density of states, etc. In the conventional theory, these transitions will contribute positively to $-P_{1L}P_{11}$ (i.e. negatively to the thermopower) if they are N-processes, but may subtract (i.e. give positive contributions to Q_L) if they are U-processes. In our model, whence U-processes have been banished by law, we need another criterion. From the fact that $-P_{1L}$ contains the factor

$$\mathbf{q} \cdot (\tau_{\mathbf{k}'}\mathbf{v}_{\mathbf{k}'} - \tau_{\mathbf{k}}\mathbf{v}_{\mathbf{k}})$$

this comes down, more or less, to the statement that the contribution to Q_L will be negative or positive according to whether the chord $\mathbf{q}$ between the points $\mathbf{k}$ and $\mathbf{k}'$ passes through occupied or unoccupied regions of the Fermi surface (fig. 26). In fact this criterion is similar to the rule for calculating the sign of the contribution of an 'orbit' to the Hall effect in a strong magnetic field; if the orbit encloses filled states in the zone, then it is an 'electron' orbit; if it encloses empty regions, then it is a 'hole' orbit. Transitions between points on an 'electron' orbit then give negative lattice thermopower; transitions across a "hole" orbit give a contribution corresponding to carriers of positive charge. This argument is not quite exact if the Fermi surface has a very complicated geometry, but it does avoid the language of 'N-processes' and 'U-processes'.

Unfortunately, without a long and complicated calculation, it is impossible to verify the experimental conclusion that $(-P_{1L}/P_{11})$ is small and negative in the three noble metals—although perhaps it goes to zero around $T = \Theta$. No explanation is offered for the extremely similar values of Q ar the maximum in all three metals, although we may note that this peak value is rather less than the maxima in Rb and Cs, which go up to $3\,\mu\text{v}/^{\circ}\text{c}$. (MacDonald *et al* 1958). There is conflicting evidence (Powell *et al.* 1959, Pearson 1955, von Oijen 1957) on the effect of cold

work on the thermopower of Cu. It now seems (Pearson 1960) that these effects are due almost entirely to traces of Fe impurity, but it would be interesting to see whether, by changing the dislocation concentration and also altering the isotropic constitution of the Cu (c.f. Blatt and Kropschot 1960), one could change Q_L through a change in the form of τ_q. Finally, it must be agreed that there is little hope of explaining the anomalous behaviour of the thermopower of Ag and Au at high temperatures (fig. 23) by appeal to phonon drag, which by (12.4) will surely have disappeared above the Debye temperature.

Fig. 26

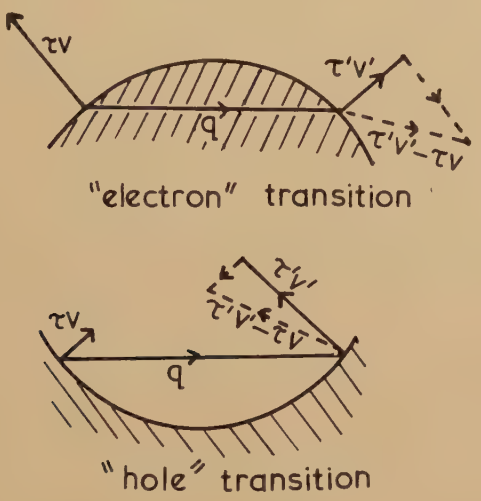

§ 13. Some Undoubted Facts and Uncertain Theories

It is not easy to sum up this complicated subject. The noble metals have suffered so many experimental observations, which have been subjected to so many theoretical explanations, that one can always find some evidence to support any point of view. Many of the observations are inconsistent with one another, and with all the theories. The abnormal sensitivity of many properties to small amounts of impurity leads to conflict of evidence, which only further deliberate experiments can resolve. It is not merely a question of fitting together a jig-saw puzzle; every piece has several spurious versions which must be identified and discarded.

But the overall conclusion is simple; there is no serious inconsistency between the observed transport properties and the assumption that the energy surfaces discovered by the 'topological' techniques remain more or less rigid when the temperature is raised or when the metal is alloyed with other metals. If there is any sphericizing effect of alloying, it does not seem enough to draw the Fermi surface out of contact with the

zone boundary. It is a pity that we cannot, therefore, maintain the well-known and elegant explanation of the Hume-Rothery rules—that the phase boundary in alloy systems comes at a definite electron-atom ratio corresponding to contact of a spherical Fermi surface with the face of the zone—for now we must believe that there is already substantial contact in all the noble metals. Perhaps another geometrical criterion will be found to explain this phenomenon, see Hume-Rothery and Roaf (1961).

More detailed points that have been discussed are as follows:

(i) The band gap at the zone boundary should lie in the range of 5–10 ev to be consistent with the shape of Fermi surface found by the topological techniques.

(ii) The change in the electronic specific heat with alloying cannot be explained by a simple alteration of the shape of the Fermi surface.

(iii) The observed optical mass is consistent with the shape of the Fermi surface and the electronic specific heat.

(iv) The Hall effect cannot be fitted without assuming considerable anisotropy of the relaxation time of the electrons.

(v) The change in the Hall coefficient with alloying is probably due to differences in the anisotropy of the relaxation time for different scattering mechanisms.

(vi) The low-field magnetoresistance depends very much on the anisotropy of τ, and cannot be used for estimating the shape of the Fermi surface.

(vii) Deviations from the simple Bloch–Wilson theory of electrical and thermal conductivity are qualitatively explicable, but cannot yet be interpreted quantitatively, although there is good experimental and theoretical evidence for fairly strong interaction between the electrons and transversely polorized phonons.

(viii) Substantial anisotropy of the relaxation time can be explained from the anisotropy of the Fermi surface and variation of the electron wave functions in the matrix element of the electron–phonon interaction.

(ix) The positive thermoelectric power at high temperatures is not due to changes in Fermi velocity or Fermi area, but to a rapid decrease of $\tau(\mathscr{E})$ as we approach the zone boundary.

(x) Phonon drag is the cause of the low-temperature hump in the thermopower, but this does not provide much quantitative information about the shape of the Fermi surface.

Acknowledgments

I am grateful for the comments, criticism and advice of my colleagues in the Cavendish Laboratory—in particular Dr. Shoenberg, Professor Pippard, Dr. Heine, Mr. J. G. Collins, Mr. L. Falicov, Mr. M. G. Priestley,

Mr. D. Roaf and Mr. W. G. Chambers. The temporary presence of Dr. J. C. Phillips in Cambridge has been extremely valuable. I have been helped in the discussion of the thermoelectric power by correspondence with Dr. A. V. Gold, thus maintaining contact with the N.R.C. group in Ottawa.

Note added in proof.—This paper was written shortly before the Conference on the *Fermi Surface of Metals*, held at Cooperstown, N.Y., U.S.A., August 22–24, 1960. The *Proceedings* of this conference (to be published by Wiley) contain many comments, which are relevant to this review but which I have not tried to incorporate in the text.

References

Alekseevski, N. E., and Gaidukov, Y. P., 1959, *J. exp. theor. Phys., Moscow*, **37,** 672.
Andrewartha, G. G., and Evans, E. J., 1941, *Phil. Mag.*, **31,** 265.
Berlincourt, T. G., 1958, *Phys. Rev.*, **112,** 381.
Biondi, M. A., and Rayne, J. A., 1959, *Phys. Rev.*, **115,** 1522.
Blatt, F. J., 1957, *Phys. Rev.*, **108,** 285.
Blatt, F. J., and Kropschot, R. H., 1960, *Phys. Rev.*, **118,** 480.
Blue, M. D., 1959, *J. Phys. Chem. Solids*, **11,** 31.
Chambers, R. G., 1956, *Proc. roy. Soc.* A, **238,** 344.
Cohen, M. H., 1958, *Phil. Mag.*, **3,** 762.
Cohen, M. H., and Heine, V., 1958, *Advanc. Phys.*, **7,** 395.
Coles, B. R., 1956, *Phys. Rev.*, **101,** 1254.
Cooper, J. R. A., and Raimes, S., 1959, *Phil. Mag.*, **4,** 145.
Corak, W. S., Garfunkel, M. P., Satterthwaite, C. B., and Wexler, A., 1955, *Phys. Rev.*, **98,** 1699.
Cusack, N., and Kendall, P., 1958, *Proc. phys. Soc. Lond.*, **72,** 898.
de Launay, J., Dolecek, R. L., and Webber, R. T., 1959, *J. Phys. Chem. Solids*, **11,** 37.
Domenicali, C. A., 1958, *Phys. Rev.*, **112,** 1863.
Domenicali, C. A., and Otter, F. A., 1954, *Phys. Rev.*, **95,** 1134.
Dorfman, Y. G., and Zhukova, P. N., 1939, *J. exp. theor. Phys., Moscow*, **9,** 51.
Flanagan, W. F., and Averbach, B. L., 1956, *Phys. Rev.*, **101,** 1441.
Frank, V. K., 1955, *Math.-fys. Medd.*, **30,** No. 4.
Frank, V. K., 1957, *Appl. sci. Res.* B, **6,** 379.
Friedel, J., 1954, *Advanc. Phys.*, **3,** 446; 1956, *Canad. J. Phys.*, **34,** 1190.
Fukuroi, T., and Ikeda, T., 1956, *Sci. Rep. res. Inst. Tôhôku Univ.* A, **8,** 205.
García-Moliner, F., 1958 a, *Proc. phys. Soc. Lond.*, **72,** 996; 1958 b, *Phil. Mag.*, **3,** 207.
Gavenda, J. D., and Morse, R. W., 1959, *Bull. Amer. phys. Soc.*, **4,** 463.
Gold, A. V., Macdonald, D. K. C., Pearson, W. B., and Templeton, I. M., 1960, *Phil. Mag.*, **5,** 765.
Guthrie, G., 1959, *Phys. Rev.*, **113,** 793.
Harrison, W. A., 1959, *Phys. Rev.*, **116,** 555.
Hume-Rothery, W., and Roaf, D., 1961, *Phil. Mag.*, **6,** 55.
Jones, H., 1955, *Proc. phys. Soc. Lond.*, A, **68,** 1191; 1957, *Proc. roy. Soc.* A, **240,** 321.
Klemens, P. G., 1956, *Handb. Phys.*, **14,** 198.
Langenberg, D. N., and Moore, T. W., 1959, *Phys. Rev. Letters*, **3,** 328.
Linde, J. O., 1958, *Physica*, **24,** 109.

Love, W. F., 1959, *J. Phys. Chem. Solids*, **9,** 281.
Macdonald, D. K. C., Pearson, W. B., and Templeton, I. M., 1958, *Proc. roy. Soc.* A, **248,** 107.
Olsen, R., and Rodriguez, S., 1957, *Phys. Rev.*, **108,** 1212.
Onnes, K., and Beckman, B., 1912, *Proc. Acad. Sci. Amst.*, **15,** 307, 319, 664, 988.
Pearson, W. B., 1955, *Phys. Rev.*, **97,** 666.
Pearson, W. B., 1960, *Canad. J. Phys.*, **38,** 1048.
Phillips, J. C., and Kleinman, L., 1959, *Phys. Rev.*, **116,** 287.
Pines, D., 1955, *Solid State Physics*, **1,** 367.
Pippard, A. B., 1957, *Phil. Trans.* A, **250,** 325.
Powell, R. L., Roder, H. M., and Hall, W. J., 1959, *Phys. Rev.*, **115,** 314.
Priestley, M. G., 1960, *Phil. Mag.*, **5,** 11.
Rayne, J. A., 1956, *Aust. J. Phys.*, **9,** 189; 1957 a, *Phys. Rev.*, **108,** 22; 1957 b, *Ibid.*, **108,** 649; 1958, **110,** *Ibid.*, 606; 1959, *Phys. Rev. Letters*, **3,** 512.
Schindler, A. I., and Pugh, E. M., 1953, *Phys. Rev.*, **89,** 295.
Schulz, L. G., 1957, *Advance. Phys.*, **6,** 102.
Shoenberg, D., 1960, *Phil. Mag.*, **5,** 105.
Slater, J. C., and Koster, G. F., 1954, *Phys. Rev.*, **94,** 1498.
Suffczynski, M., 1960, *Phys. Rev.*, **117,** 663.
van Oijen, D. J., 1957, Thesis, Delft.
Wortman, J., 1933, *Ann. Phys., Lpz.*, **18,** 233.
Ziman, J. M., 1954, *Proc. roy. Soc.*, A, **226,** 436; 1959 a, *Phil. Mag.*, **4,** 371; 1959 b, *Proc. roy. Soc.* A, **252,** 63; 1960, *Electrons and Phonons* (Oxford: Clarendon Press).

The Many-body Theory of Electrons in Metal or Has a Metal Really Got a Fermi Surface?

By L. M. Falicov† and V. Heine
Royal Society Mond Laboratory, Cambridge

CONTENTS

§ 1. The Nearly Independent Quasi-particle Model.
1.1. Introduction.
1.2. The Model Described.
1.3. The Consequences of Interactions.
1.3.1. Auger transitions and the lifetime $T(\mathbf{k})$.
1.3.2. Inter-particle collisions.
1.3.3. Breakdown of the exclusion principle.
1.3.4. Energy corrections to transport phemomena.
1.3.5. Current interactions.

§ 2. Theoretical Foundations.
2.1. Theory of the Electron Gas.
2.2. The Ground State.
2.3. The Single Quasi-particle States.
2.4. The Effective Quasi-particle Interaction.
2.5. The Effect of the Periodic Potential.
2.6. Derived Properties.

§ 3. Velocity, Charge and Acceleration.
3.1. The Velocity.
3.2. Current and Effective Charge.
3.3. Acceleration in Applied Fields.

§ 4. 'Transport' Phenomena.
4.1. Electronic Specific Heat.
4.2. Paramagnetic Spin Susceptibility.
4.3. Anomalous Skin Effect.
4.4. Electrical Resistivity.
4.5. Cyclotron Resonance.
4.6. De Haas–van Alphen Effect.
4.7. Ultrasonic Attenuation.

§ 5. Summary, Discussion and Comparison with Experiment.
Appendix.

† Now at the Institute for the Study of Metals, University of Chicago, Chicago 37, Ill.

§ 1. The Nearly Independent Quasi-particle Model

The usual electron theory of metals developed since the 1930's has been built up on the independent-electron model, i.e. on the assumption that the electrons can be treated as if they did not interact with each other at all. However the coulomb repulsion between the electrons is a very strong force, and the purpose of this paper is to discuss the electron theory of metals taking the coulomb force into account from the beginning. We shall not discuss many-electron effects such as plasma oscillations, but limit ourselves to transport phenomena. For the purposes of this paper, the term 'transport phenomena' will be taken to cover all genuine transport properties such as electrical and thermal conductivities, as well as other properties like the electronic specific heat and the magnetic spin susceptibility that depend only on the electrons at or near the Fermi level. The thesis we shall develop is that such properties can be understood in terms of quasi-particle excitations at the Fermi level, which to a first approximation are independent so that one can still use the language and framework of the independent-electron model: but the short-range screened coulomb interaction existing between the excitations leads to some important corrections and modifications of various types which we shall describe in detail. Indeed, this paper explores how far it is or is not possible to cast the exact theory of the electron gas into the preconceived mould of an independent-electron model or at least a nearly-independent quasi-particle model; for the independent electron model has served solid-state physics so well for so long and will probably continue to be used for a long time in analysing and correlating the various electronic properties of metals.

1.1. *Introduction*

In the independent-electron approach, each electron is in a Bloch state $\psi_{\mathbf{k}}(\mathbf{r})$ with energy $\epsilon(\mathbf{k})$, and all states with energy $\epsilon(\mathbf{k})$ less than the Fermi energy ϵ_F are occupied by electrons. (We shall use ϵ for the energy of single particles and reserve E for the energy of the whole system of electrons.) The ground state of the electron gas is a single determinant of all the $\psi_{\mathbf{k}}(\mathbf{r})$ with $\epsilon(\mathbf{k}) \leqslant \epsilon_F$, corresponding to the assumption that each electron moves completely independently of all the other electrons. The Fermi surface defined by $\epsilon(\mathbf{k}) = \epsilon_F$ is an immediate natural concept, dividing the occupied and unoccupied regions in $\mathbf{k}$-space. The excited states of the system are still single determinants, but now with some of the Bloch functions $\psi_{\mathbf{k}}$ with $\mathbf{k} = \mathbf{k}_\alpha, \mathbf{k}_\beta \ldots\ldots$ from below the Fermi surface omitted, and an equal number with $\mathbf{k} = \mathbf{k}_i, \mathbf{k}_j, \ldots$ from above the Fermi surface included. As is often done, we shall describe such a state by ignoring the unchanged part of the Fermi distribution and simply saying that we have some excited electrons with $\mathbf{k} = \mathbf{k}_i, \mathbf{k}_j \ldots\ldots$ and some holes with $\mathbf{k} = \mathbf{k}_\alpha, \mathbf{k}_\beta \ldots$. (We shall continue to distinguish electrons and holes by Roman and Greek letter subscripts.) Such states can be excited

thermally and by electromagnetic fields, and it is on this independent-electron model that all the usual electron theory of metals found in the standard texts is based (Mott and Jones 1936, Seitz 1940, Wilson 1953).

As is universally known, the independent-electron theory has served solid-state physics extraordinarily well, and it is still the basis of almost all discussions of transport phenomena; see for instance Ziman (1960). At first sight this is rather surprising, because the electrons in a metal cannot be moving independently of one another, and the coulomb repulsion between them is in fact a very strong force. For instance, in sodium the electrostatic energy of two electrons at the interatomic distance apart is 4 ev while the Fermi band width is only 3 ev. Thus the electrons accelerate and decelerate one another, and even in the ground state there is ample energy available to excite some electrons temporarily into high-momentum states. The wave function for the ground state of the system is very complicated, and if we expand it as a sum of determinants of Bloch functions, it will certainly contain some $\psi_{\mathbf{k}}$ with energies well above the Fermi level. Thus we might expect the Fermi surface and all simple properties associated with it to be more or less completely washed out.

While this is true in the simple sense of the independent-electron model, there are strong experimental and theoretical reasons for believing that a sharp Fermi surface in some more sophisticated sense does exist and that much of the independent-electron model can be salvaged provided it is interpreted in a modified way. As one piece of experimental evidence, consider for example the de Haas–van Alphen effect (Shoenberg 1957), which indicates the existence of very small pieces of Fermi surface enclosing in some metals less than 10^{-5} electrons per atom, forming pockets perhaps at corners of the Brillouin zone. The radius of the pockets is about 2% of the radius of the Fermi surface, and the maximum variation of $\epsilon(\mathbf{k})$ within the pockets about 0·04 ev. Also most de Haas–van Alphen oscillations are unobservably weak due to thermal excitation at already a few degrees absolute where $kT \approx 10^{-3}$ ev. As Mott (1956) has emphasized, such results reveal some very fine detail in the electron distribution, and would be quite inexplicable if everything were smoothed out by 1 ev or more and no sharp Fermi surface existed in some sense. Another argument is due to Skinner (1940) who observed sharp emission and absorption edges corresponding to the Fermi level in the soft x-ray spectra of metals. From the discussion of the last paragraph, one might expect a broadened edge due to the electrons temporarily in high-momentum states. However the point to note is that the soft x-ray spectrum corresponds to the energy levels of the whole system, the one-electron fluctuations inherent in the ground state being irrelevant. Consider a state of the system in which one electron has been given some extra energy ϵ above the ground state. It will rapidly collide with other electrons, exciting them and sharing its energy with them. Since the extra energy any one electron can get varies between 0 and ϵ, we would expect that the number of different configurations that the original state can decay into would be at least proportional

to ϵ. Thus as we consider a state with excess energy tending to zero, we would expect the lifetime τ of the excitation to tend to infinity because there are no states for it to decay into. This would imply that the states of the whole system with infinitesimal excitation energy have zero energy broadening $\Delta\epsilon \approx \hbar/\tau$, leading to a sharp edge in the soft x-ray spectra in agreement with experiment. It also implies that the excitation can move a long distance through the lattice, and experimentally mean free paths of the order of 1 mm have been reported for very pure specimens of tin and other metals at low temperatures. One can define a wave vector $\mathbf{k}$ for the excited state in the usual way:

$$\Psi(\mathbf{r}_1 + \mathbf{R}_n, \mathbf{r}_2 + \mathbf{R}_n, \ldots) = \exp(i\mathbf{k} \cdot \mathbf{R}_n)\, \Psi(\mathbf{r}_1, \mathbf{r}_2, \ldots) \quad . \quad . \quad (1.1)$$

where Ψ is the complete wave function for the state and $\mathbf{R}_n$ any lattice displacement. The existence of a sharp energy in the limit of infinite lifetime, coupled with a $\mathbf{k}$ vector, again suggests a sharp Fermi surface outside which $\mathbf{k}$ for the excitation has to lie. Finally we may consider a semiconductor like germanium where the mean electron–electron electrostatic energy (several ev) is larger than the band gap (about 1 ev) and at first sight quite able to excite electrons across it. Indeed the ground state of the system will contain high momentum fluctuations as before, but we know experimentally that these cannot carry a current and contribute to transport phenomena, because with high purity material at low temperatures free carrier concentrations of 10^{-10} per atom can be achieved. However, if we put an extra electron into the crystal, it can move about, having strong electrostatic interactions with all the valence electrons, locally exciting them and temporarily being excited by them which will involve high-momentum components in the wave function. We can now picture the whole mess of electron plus the local disturbance it causes moving together through the lattice with well-defined energy and wave vector and a long free path leading again to a one-electron-like band structure $\epsilon(\mathbf{k})$.

This is about as far as the experimental evidence itself can take us—not at all conclusive but nevertheless suggestive of the existence of a Fermi surface, sharp in some sense at least to about 10^{-4} ev, with low-energy one-electron-like excitations having well-defined wave vector and energy and a relatively long lifetime.

On the theoretical side, much sophisticated work has been done recently, and this is reviewed in § 2. Although a complete and rigorous solution to the problem is not yet possible, nevertheless a fairly clear picture does emerge from the theory to date. This picture, which we shall now describe, is in complete accord with what has already been conjectured from the experimental side and indeed puts it on a much more detailed footing. Indeed Landau (1956) realized early on that a picture of this sort must apply, and analysed some properties of the electron gas in terms of it. A very readable comment on the whole situation has been given by Herring (1960).

1.2. *The Model Described*

Let the ground state of a gas of N electrons be denoted by Ψ_{GN} or $|GN\rangle$ in the Dirac notation or $|G\rangle$ for short, and its energy by E_G. Ψ_{GN} is a very complicated wave function, embodying all the correlations beween the movements of the electrons and their accelerations and decelerations. We can always define a total $\mathbf{k}$ vector for a many-electron state using (1.1), and we assume that N has been adjusted to the symmetry of the system so that the ground state is non-degenerate with total $\mathbf{k}=0$, e.g. N has to be even.

Now there is a minimum energy ϵ_F, the electron affinity of the system, required to add one extra electron to the system. If we add the electron with an energy ϵ greater than ϵ_F, we can produce certain one-excited-electron-like states $|\mathbf{k}_i\rangle$ of the $N+1$ particle system, which Hugenholtz (1958) has shown can be expressed in the form

$$|\mathbf{k}_i\rangle = O_{\mathbf{k}i}^*|G\rangle, \quad . \quad . \quad . \quad . \quad . \quad . \quad . \quad . \quad . \quad (1.2)$$

where the creation operator, $O_{\mathbf{k}i}^*$ is a definite operator defined by eqn. (2.31) below. Since the electron interacts with all the other electrons, we cannot ascribe to it an individual Bloch function and wave vector, but it follows from general principles of group theory (see for example Heine 1960) that the lattice symmetry of the crystal and (1.1) can be used to define a total $\mathbf{k}$-vector $\mathbf{k}_i$ for the state as a whole. We shall in what follows take the symbol $\mathbf{k}_i$ to include also a specification of the spin direction. The expectation value of the energy for the state (which in general is not an eigenstate, see below) we shall write as

$$E = E_G + \epsilon(\mathbf{k}_i) \quad . \quad . \quad . \quad . \quad . \quad . \quad . \quad . \quad . \quad (1.3)$$

and we shall describe $\epsilon(\mathbf{k}_i)$ as the energy of the electron-like excitation which we have put into the system. For large values of $\epsilon(\mathbf{k})-\epsilon_F$ our whole description breaks down, but for energies less than an ev or so the wave vector $\mathbf{k}_i$ always lies outside a precise surface defined by

$$\epsilon(\mathbf{k}) = \epsilon_F. \quad . \quad . \quad . \quad . \quad . \quad . \quad . \quad . \quad . \quad . \quad (1.4)$$

This, the Fermi surface, has the same size as in the independent-electron model, i.e. it contains exactly one electron per atom or whatever the valency of the metal is. (For a proof of these and other statements, see the references reviewed in § 2.)

The minimum energy required to remove an electron from $|G,N\rangle$ is also ϵ_F. This is one of the characteristics of a metal, for it is equal to the energy that has to be added in going back from $|G,N-1\rangle$ to $|G,N\rangle$ and this is the same as in going from $|G,N\rangle$ to $|G,N+1\rangle$ by continuity. Only in an insulator or semi-conductor with a band gap at the Fermi level is there a discontinuity at N electrons when the valence band is completely full and the next electron has to go into the conduction band. Now by extracting an electron from below the Fermi level, we can create certain excited states $|\mathbf{k}_\alpha\rangle$ of the $N-1$ particle system

$$|\mathbf{k}_\alpha\rangle = O_{\mathbf{k}\alpha}|G\rangle \quad . \quad . \quad . \quad . \quad . \quad . \quad . \quad . \quad . \quad (1.5)$$

where the annihilation operator $O_{\mathbf{k}\alpha}$ is the Hermitian conjugate of the $O_{\mathbf{k}}^*$ defined by (2.31). The expectation value of the energy of the state is

$$E = E_G - \epsilon(\mathbf{k}_\alpha), \quad . \quad . \quad . \quad . \quad . \quad . \quad . \quad . \quad (1.6)$$

and we say the system contains one hole-like excitation of energy $-\epsilon(\mathbf{k}_\alpha)$. The function $\epsilon(\mathbf{k}_\alpha)$ is continuous with $\epsilon(\mathbf{k}_i)$ at the Fermi level ϵ_F, and $\mathbf{k}_\alpha$ has to lie inside the Fermi surface for the state (1.5) to exist.

Now the states defined by (1.2) and (1.5) are not in fact eigenstates of the system, and they decay with a lifetime $T(\mathbf{k})$ into more complicated states (see § 1.3.1 and § 2.3). However $T(\mathbf{k})$ is proportional to $[\epsilon(\mathbf{k}) - \epsilon_F]^{-2}$ so that the lifetime tends to infinity at the Fermi level. In particular the excitations produced thermally and by electromagnetic fields have a sufficiently low energy, that their lifetime $T(\mathbf{k})$ is much longer than their relaxation time due to collisions with lattice vibrations and impurities.

Fig. 1

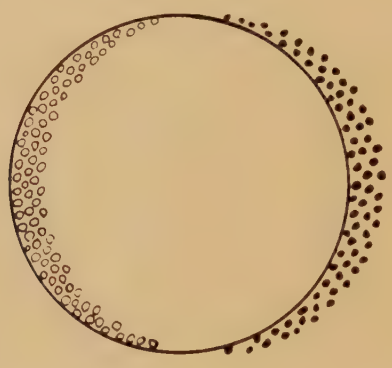

Multiple excitation corresponding to a uniform current. ●—electron-like excitations ; ○—hole-like excitations.

Thus we shall describe the excited states of the N-electron gas in terms of multiple excitations.

$$|\mathbf{k}_i, \mathbf{k}_j, \ldots; \mathbf{k}_\alpha, \mathbf{k}_\beta, \ldots\rangle = O_{\mathbf{k}i}^* O_{\mathbf{k}j}^* \ldots O_{\mathbf{k}\alpha} O_{\mathbf{k}\beta} \ldots |G\rangle \quad . \quad . \quad . \quad (1.7)$$

with equal numbers of electron-like excitations (wave vectors $\mathbf{k}_i, \mathbf{k}_j, \ldots$) and hole-like excitations ($\mathbf{k}_\alpha, \mathbf{k}_\beta, \ldots$). It does not matter that these states are not eigenstates, although they actually tend to eigenstates as all $\mathbf{k}_i, \mathbf{k}_\alpha$ tend to the Fermi surface and the life time becomes infinite. For finite energy of excitation, the proper eigenstates are very complicated combinations of all states of type (1.7) with the same total energy and same total $\mathbf{k} = \sum \mathbf{k}_i - \sum \mathbf{k}_\alpha$, and they do not seem to correspond to anything of physical significance. We can describe all normal excitations of the system in terms of the states (1.7). For example, a uniform electric field

produces electron-like excitations on one side of the Fermi surface and hole-like excitations on the other (fig. 1), equivalent to the usual uniform displacement of the whole Fermi distribution in the independent-electron model.

Thus an excited state of the system can be represented as a low density gas of quasi-particles, namely electron-like and hole-like excitations. Although the density of electrons is of order one per atom, the density of quasi-particles is much less, e.g. of order $kT/(\epsilon_F - \epsilon_0) \sim 10^{-2}$ per atom at room temperature where $\epsilon_F - \epsilon_0$ is the band width, corresponding to the number of excited electrons in the independent-electron model. From the way in which the quasi-particles have been defined from (1.2) and (1.5), we expect them to be closely related to electrons and holes. Indeed the operator O_k^* and the properties of the quasi-particles are derived using perturbation theory from the corresponding independent-electron states by mathematically 'switching on' the coulomb-repulsion. However a quasi-particle differs from an actual electron (or hole) in several respects. For instance, it is not a point particle because it includes all the local disturbance in the electron gas which screens the charge. The screening results in the interaction between two quasi-particles being modified from a pure coulomb repulsion to a short-range 'screened coulomb' force. For present purposes we shall take it to have the form

$$(e^2/r) \exp(-Qr) \quad . \quad . \quad . \quad . \quad . \quad . \quad . \quad (1.8)$$

where the screening distance $1/Q$ is of the order of the interatomic spacing: a discussion of its precise shape is given in § 2.4. Finally, if we form a wave-packet out of our excitations, the charge e^* transported by the packet is not exactly that of one electron. The whole question of the velocity, charge and current carried by the excitations is discussed in § 3.

1.3. *The Consequences of Interactions*

So far we have reviewed the individual properties of the quasi-particles, treating them as independent. We must now take account of the screened-coulomb interaction between them, and also discuss their lifetime $T(\mathbf{k})$ which is a related effect.

1.3.1. *Auger transitions and the lifetime* $T(\mathbf{k})$

Consider a state with a single excitation with wave vector $\mathbf{k}_1$ and energy $\epsilon_1 \equiv \epsilon(\mathbf{k}_1)$. As already mentioned this is not an eigenstate of the system because it can make Auger transitions to other states with the same total energy and total $\mathbf{k}$, the only two quantities that are proper constants of the motion (Skinner 1904, Landsberg 1949, Hugenholtz 1957, Quinn and Ferrell 1958). In particular because of the coulomb force, the excitation can "collide with an electron at $\mathbf{k}_4$ below the Fermi surface", be scattered to $\mathbf{k}_2$ loosing energy $\epsilon_1 - \epsilon_2$, and 'eject' an 'electron' into the excited state $\mathbf{k}_3$ leaving a hole at $\mathbf{k}_4$ (fig. 2). A better description would perhaps be to say that the original excitation has interacted with the Fermi sea

and decayed into another excitation at $\mathbf{k}_2$ plus an electron-hole-like pair at $\mathbf{k}_3$, $\mathbf{k}_4$. We must have

$$\mathbf{k}_1 = \mathbf{k}_2 + \mathbf{k}_3 - \mathbf{k}_4 \text{ and } \epsilon_1 = \epsilon_2 + \epsilon_3 - \epsilon_4. \quad . \quad . \quad (1.9\,a, b)$$

It is easy to do an approximate calculation. The lifetime $T(\mathbf{k})$ is given by

$$\frac{1}{T} = \frac{2\pi}{\hbar} M^2 \mathcal{N}(E) \quad . \quad . \quad . \quad . \quad . \quad . \quad (1.10)$$

Fig. 2

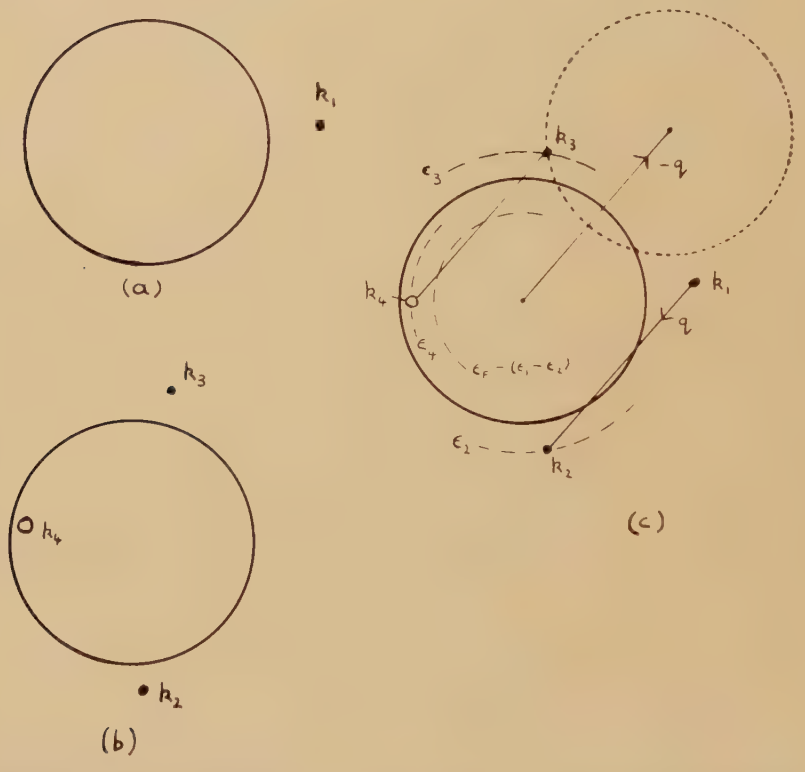

(*a*) Initial and (*b*) final states for Auger transition. (*c*) Construction for density of states.

where $\mathcal{N}(E)$ is the density of states for the whole system and M the matrix element of the Hamiltonian connecting the two states. We approximate to M using independent-electron wave functions with plane waves and the interaction (1.8):

$$M = \int \frac{\exp(-i\mathbf{k}_2 \cdot \mathbf{r}_1)}{\Omega^{1/2}} \frac{\exp(-i\mathbf{k}_3 \cdot \mathbf{r}_2)}{\Omega^{1/2}} \frac{e^2}{r_{12}} \exp(-Qr_{12}) \times \frac{\exp(i\mathbf{k}_i \cdot \mathbf{r}_1)}{\Omega^{1/2}} \frac{\exp(i\mathbf{k}_4 \cdot \mathbf{r}_2)}{\Omega^{1/2}} d\mathbf{r}_1 d\mathbf{r}_2$$

$$= \frac{4\pi e^2}{q^2 + Q^2} \frac{1}{\Omega} \delta(\mathbf{k}_1, \mathbf{k}_2 + \mathbf{k}_3 - \mathbf{k}_4). \quad . \quad . \quad . \quad . \quad . \quad . \quad . \quad (1.11)$$

where $\mathbf{q}=\mathbf{k}_2-\mathbf{k}_1=\mathbf{k}_4-\mathbf{k}_3$. To calculate $\mathcal{N}(E)$, we note that $\mathbf{k}_3$ can lie anywhere in the shell between energy ϵ_1 and ϵ_F, i.e. can range over a volume $4\pi k_F{}^2\Delta$ in $\mathbf{k}$-space where Δ is the distance of $\mathbf{k}_1$ from the Fermi surface. Having fixed ϵ_2 and $\mathbf{k}_2$, we next fix ϵ_4 which can have any energy between ϵ_F and $\epsilon_F-(\epsilon_1-\epsilon_2)$, i.e. the surface $\epsilon=\epsilon_4$ can cut a radius of the Fermi sphere anywhere along a section of length about $\frac{1}{2}\Delta$ in $\mathbf{k}$-space if we assume on the average that half of the energy is given to the electron-hole pair. $\mathbf{k}_3$ must now lie on the energy surface $\epsilon_3=\epsilon_4+(\epsilon_1-\epsilon_2)$. In order to satisfy (1.9*a*), we redraw the surface $\epsilon(\mathbf{k})=\epsilon_4$ displaced by wave vector $-\mathbf{q}$ (shown dotted in fig. 2). $\mathbf{k}_3$ can then lie on the circle of intersection of this surface with $\epsilon(\mathbf{k})=\epsilon_3$, i.e. along a line of length $2\pi(\frac{1}{2}k_F)$ say, which then fixes $\mathbf{k}_4$ at $\mathbf{k}_3+\mathbf{q}$. In order to get the density of states per unit energy, we allow $\mathbf{k}_3$ to range from energy ϵ_3 to energy ϵ_3+dE, giving a strip of width $dE/(\partial\epsilon/\partial k)$. Multiplying by the density $\Omega(2\pi)^{-3}$ of points in $\mathbf{k}$-space, we obtain

$$\mathcal{N}(E)\approx\Omega^2(2\pi)^{-6}(4\pi k_F{}^2\Delta)\tfrac{1}{2}\Delta\pi k_F(\partial\epsilon/\partial k)^{-1}.$$

Putting $\Delta=(\epsilon-\epsilon_F)/(\partial\epsilon/\partial k)$, $q\sim Q\sim k_F=1{\cdot}9/r_s$, $\partial\epsilon/\partial k\sim 2\epsilon_F/k_F$, substituting in (1.10) and dropping all numerical factors, we obtain finally

$$\frac{\hbar}{T(\mathbf{k})}\sim\left(\frac{e^2}{r_s}\right)^2\frac{1}{\epsilon_F}\left(\frac{\epsilon}{\epsilon_F}-1\right)^2 \quad . \quad . \quad . \quad . \quad . \quad (1.12)$$

where r_s is the radius of the sphere containing one electron. As stated in § 1.2, $\hbar/T$ varies as $(\epsilon-\epsilon_F)^2$ giving a very long life for excitations near the Fermi level: e.g. for $\epsilon-\epsilon_F=kT=3\times10^{-2}$ ev at room temperature, we obtain a mean free path of $\sim10^{-3}$ cm which is much longer than that for phonon collision and therefore negligible. However (1.12) also shows that for energies of more than a few ev, the lifetime broadening is sufficiently large for the concept of a band structure with single identifiable excitations to be no longer very meaningful.

1.3.2. *Inter-particle collisions*

The Auger process discussed above represents the decay of a single excitation by itself. At a finite temperature when there are many quasi-particles, there are also collisions between them. We can calculate the mean free path approximately as follows. For static obstacles of concentration c, a quasi-particle has to travel through $1/c$ atomic cells before striking an impurity and we have $L\sim r_s/c$. In our case the concentration of scatterers, namely other quasi-particles, is of order kT/ϵ_F. Also the momentum transferred to the struck quasi-particle has to be such that the latter can conserve energy, i.e. the available $\mathbf{k}$-space into which it can be scattered is only a fraction kT/ϵ_F of the whole space available, which reduces the scattering by this factor:

$$L\sim r_s(kT/\epsilon_F)^{-2}.$$

This formula is very similar to (1.12). Indeed the two processes are very similar, collision with an unexcited electron just below the Fermi

level in the one case and with an excited electron or hole in the other, and they are usually treated together in making proper calculations. Such calculations are described by Abrahams (1954) and by Ziman (1960), who also reviews the relevant experimental data. The results briefly are these. In a free electron gas, electron–electron scattering cannot affect the electrical resistivity because the total $\mathbf{k}$ and hence the total current are conserved in each collision. However, with a lattice potential and complicated Fermi surface, it contributes a term AT^2 to the electrical resistance both by Umklapp scattering and by scattering from a part of the Fermi surface with high velocity to one with low velocity. Electron–electron scattering also contributes to the thermal resistance even for a free electron gas, because a state in which 'hot' quasi-particles are flowing against a counter stream of 'cold' ones can clearly be spoilt by collisions between them. Numerically the effects seem to be just a little too small to be clearly detectable except for a T^2 term in the electrical resistance of transition metals (Ziman 1960, Baber 1937, Mendelssohn 1956).

In conclusion, the interaction effects of § 1.3.1 and this section just give another scattering mechanism, whose contributions to the thermal and electrical resistances can be calculated by the usual independent-electron transport theory and anyway are in almost all cases small. Thus they do not give any new effect of an essentially *non*-independent particle nature, and we shall not consider them further.

1.3.3. *Breakdown of the exclusion principle*

Although the operators $O_{\mathbf{k}}^*$ of (1.2), (1.5) are too complicated for making explicit calculations with as yet, we shall assume that the exclusion principle applies exactly at the Fermi level and the operators $O_{\mathbf{k}}^*$ satisfy the usual Fermi commutation rules exactly there, since at the Fermi level single excitations represent eigenstates of the system. Thus one can only have one excitation of a particular $\mathbf{k}$, and a state $O_{\mathbf{k}}^* O_{\mathbf{k}}^* |G\rangle$ is identically zero. This however may not apply at higher energies where the excitations are not eigenstates, and our whole mode of labelling and counting states begins to break down. For example, if we start with one electron gas at a low temperature and another at a high temperature and accelerate the electrons with electric fields in the same way, the resulting currents may not be exactly equal. Any deviations would presumbaly be proportional to $(\epsilon - \epsilon_F)^2$, giving a contribution in T^2 to the electrical resistance. We shall assume that the effects are at most comparable with those of electron electron scattering discussed in the previous section, and not consider them further.

1.3.4. *Energy corrections to transport phenomena*

The interaction between quasi-particles gives corrections to the energy which in principle are important for all transport properties. If we consider as state of the system with two quasi-particle excitations $\mathbf{k}_1$ and

$\mathbf{k}_2$, then the energy E of the system is not just the sum of their individual energies but includes a term $\eta(\mathbf{k}_1, \mathbf{k}_2)$ due to their interaction:

$$E(\mathbf{k}_1, \mathbf{k}_2) = \pm \epsilon(\mathbf{k}_1) \pm \epsilon(\mathbf{k}_2) + \eta(\mathbf{k}_1, \mathbf{k}_2). \quad . \quad . \quad . \quad (1.13)$$

(Here as elsewhere the minus signs have to be used for holes; compare (1.3) and (1.6).) Following (1.12) we write it in the form

$$\eta(\mathbf{k}_1, \mathbf{k}_2) = A(\mathbf{k}_1, \mathbf{k}_2) \frac{1}{N} \frac{e^2}{r_s}, \quad . \quad . \quad . \quad . \quad . \quad . \quad (1.14)$$

where the last factor is a few ev and the first a numerical factor whose value we might expect to depend roughly as follows on spin and on whether we have electron-like or hole-like excitations:

both holes or both electrons	parallel spin	$A \sim -0{\cdot}2$
one hole and one electron	parallel spin	$A \sim +0{\cdot}2$
both holes or both electrons	antiparallel spin	$A \sim -0{\cdot}05$
one hole and one electron	antiparallel spin	$A \sim +0{\cdot}05$

These are just rough values for ordinary metallic densities calculated from the theory of Bohm and Pines (Pines 1955, eqns. (6.4), (6.23)): in detail A of course varies with $\mathbf{k}_1$, $\mathbf{k}_2$ through $\epsilon(\mathbf{k})$ and the electron density.

In an ordinary transport process, multiple excitations with n quasi-particles are excited where n is of order N but a very small fraction of it: $n/N \sim kT/v_F$ or v_D/v_F, where v_D is the drift velocity $e\mathscr{E}/m\tau$ and v_F the Fermi velocity. The total energy is

$$\begin{aligned} E &= E_1 + E_2 \\ &= [\textstyle\sum \epsilon(\mathbf{k}_i) - \sum \epsilon(\mathbf{k}_\chi)] + \frac{1}{2} \sum\sum \eta(\mathbf{k}, \mathbf{k}'). \quad . \quad . \quad . \quad . \quad . \quad (1.15) \end{aligned}$$

The two-particle interaction energy E_2 includes the double summation over all pairs of quasi-particles, and is therefore of order n^2/N. As regards the one-particle energy E_1, if the excitations were all by a finite amount $\Delta\epsilon$ about the Fermi level, then E_1 would be of order n and the interaction energy negligible by comparison with it. But the multiple excitations one always has in transport phenomena are really distortions of the Fermi surface, the change in energy being quadratic of order n^2/N, so that the interaction energy is comparable with the one-particle contribution E_1. As regards order of magnitude, E_2 can of course be larger than E_1 in metals like nickel or cobalt with small $\partial\epsilon/\partial k$, where it leads to ferromagnetism. In ordinary metals it is perhaps 40% of E_1 if a change of spin and hence the exchange energy are involved, as evidenced by the corrections to the Pauli spin susceptibility (Pines 1955). When spin changes are not involved, corrections of the order of 10% might be expected. This is probably a maximum estimate actually, because with a simple band structure one has a sum of an equal number of positive and negative terms on account of the equal numbers of electrons and holes. We take up the topic of the size of the corrections again in § 5, and shall see that the above figures based on the Bohm and Pines theory are seriously overestimated. The actual effective electron–electron interaction is both weaker and more smoothly varying with $\mathbf{k}$ than the interaction of Bohm and Pines, resulting

in substantially smaller corrections. Incidentally the fact that the density of excitations is always so small, allows us to neglect three-body and higher interaction terms in (1.15).

Although it is clear that the interaction energy affects quantities like the spin susceptibility which depend essentially on an energy balance, it is not immediately obvious whether it comes into genuine transport phenomena like the d.c. conductivity. Here the normal mode of calculation determines the amount of momentum given to the electrons by the electric field and hence the current carried, without explicit mention of the energy. But fundamentally electrical resistance is concerned with the *energy* fed into the electron gas and its rate of dissipation into heat, and we have to develop a slightly unorthodox method of calculating resistivity to bring this out.

Every transport phenomenon is characterized by the type of multiple excitation it produces: in the case of d.c. conduction there are electron-like excitations on one side of the Fermi surface and hole-like ones on the other (fig. 1). The whole is equivalent to a distortion of the Fermi surface measured by some parameter Δ; in the present case $\Delta = \delta k / k_F$ where δk is the side-ways shift of the surface. The total energy of the excitations is

$$E = \alpha \Delta^2, \quad . \quad . \quad . \quad . \quad . \quad . \quad . \quad . \quad . \quad (1.16)$$

where the constant α contains significant contributions from the interaction energy since like E_1 it varies as Δ^2, as already discussed. The electric current carried by the system is discussed in § 3: in any case it is proportional to Δ:

$$J = \beta \Delta. \quad . \quad . \quad . \quad . \quad . \quad . \quad . \quad . \quad (1.17)$$

The electrons are scattered by impurities and phonons, so that without an electric field to maintain it the current would decay with relaxation time τ:

$$dJ/dt = -J/\tau. \quad . \quad . \quad . \quad . \quad . \quad . \quad . \quad . \quad (1.18)$$

Thus from (1.17) we can write the energy as

$$E = (\alpha/\beta^2) J^2. \quad . \quad . \quad . \quad . \quad . \quad . \quad . \quad . \quad (1.19)$$

and its rate of dissipation as

$$-\frac{dE}{dt} = -2(\alpha/\beta^2) J \frac{dJ}{dt}$$

$$= \frac{2\alpha}{\beta^2 \tau} J^2.$$

But the rate of dissipation of energy is RJ^2 where R is the resistivity, and we have

$$R = 2\alpha/\beta^2 \tau, \quad . \quad . \quad . \quad . \quad . \quad . \quad . \quad . \quad (1.20)$$

which shows explicitly how the interaction energy contributes to R through the value of α.

In § 4 we shall apply such arguments to some particular transport processes.

1.3.5. *Current interactions*

It is in principle possible that the interaction between quasi-particles leads to corrections, analogous to η in (1.13), to the current carried by them. We can regard the $n-1$ other excitations as constituting a modification of the background medium in which a particular quasi-particle moves, producing a change of order $v_{\mathbf{k}}n/N$ in its velocity $v_{\mathbf{k}}$. Now the total current carried is of order nv_{F}, i.e. linear in n (unlike the one-particle energy E_1 of eqn. (1.15)). In comparison with this, the total interaction corrections to the current are of order $v_{\mathrm{F}}n^2/N$ and can therefore be neglected.

§ 2. Theoretical Foundations

In this section we review the most important contributions to the theory of the electron gas made in the last five years. We emphasize those works which, directly or indirectly, point to the existence of a sharp Fermi surface. In particular we shall be interested in the existence and properties of the low-energy excited states, defined in terms of quasi-particles. In § 2.1 we discuss the various methods of calculation and the difficulties that arise in evaluating the resulting expressions. In § 2.2 we review the theory of the ground state in the free electron approximation while § 2.3 deals with the excited states and the quasi-particles. In § 2.4 the screened interaction between quasi-particles is discussed. In § 2.5 we summarize briefly what has been done to include the periodic potential of the lattice, and in 2.6 the work on the derived properties of the electron gas such as specific heat etc.

2.1. *The Theory of the Electron Gas*

We first define our notation. The many-body hamiltonian for our N-particle system is

$$\mathscr{H} = \mathscr{H}_0 + \mathscr{H}_1 \qquad . \; . \; . \; . \; . \; . \; . \; . \quad (2.1)$$

where

$$\mathscr{H}_0 = \tfrac{1}{2}\sum_{\mathbf{k}} \mathbf{k}^2 a_{\mathbf{k}}^* a_{\mathbf{k}} + \sum\sum_{\mathbf{G}\neq 0} U(\mathbf{G}) a_{\mathbf{k}}^* a_{\mathbf{k}+\mathbf{G}} \qquad . \; . \; . \quad (2.2)$$

gives the kinetic energy and the lattice potential energy of the electrons, and

$$\mathscr{H}_1 = \tfrac{1}{2}\sum_{1234} v_{1234} a_{\mathbf{k}1}^* a_{\mathbf{k}2}^* a_{\mathbf{k}3} a_{\mathbf{k}4} \qquad . \; . \; . \; . \; . \quad (2.3)$$

expresses the electron–electron interaction energy.

In this formulation $a_{\mathbf{k}}^*$ and $a_{\mathbf{k}}$ are respectively the creation and annihilation operators of electrons of momentum $\mathbf{k}$ and spin σ; $\mathbf{G}$ is a reciprocal lattice vector and

$$U(\mathbf{G}) = \frac{\delta(\sigma,\sigma')}{\Omega}\int U(\mathbf{r}) \exp(i\mathbf{G}\cdot\mathbf{r})\, d^3\mathbf{r} \qquad . \; . \; . \; . \quad (2.4)$$

is a Fourier coefficient of the lattice potential. The matrix element v_{1234} is defined by

$$v_{1234} = \frac{1}{\Omega} v(\mathbf{k}_1 - \mathbf{k}_4)\delta(\sigma_1, \sigma_4)\delta(\sigma_2, \sigma_3)\delta(\mathbf{k}_1 + \mathbf{k}_2, \mathbf{k}_3 + \mathbf{k}_4), \quad . \quad (2.5)$$

and

$$v(\mathbf{k}) = \begin{cases} 4\pi/\mathbf{k}^2 & \mathbf{k} \neq 0 \\ 0 & \mathbf{k} = 0 \end{cases} \quad . \quad . \quad . \quad . \quad . \quad . \quad . \quad (2.6)$$

is the Fourier transform of the coulomb interaction. We have chosen for simplicity atomic units, i.e.

$$\hbar = e = m = 1,$$

and Ω is the volume of the system (assumed to be indefinitely large).

The eigenvectors of (2.1) must satisfy the condition†

$$\sum_{\mathbf{k}} a_{\mathbf{k}}^* a_{\mathbf{k}} |\Psi'\rangle = N|\Psi'\rangle \quad . \quad . \quad . \quad . \quad . \quad . \quad (2.7)$$

expressing the constancy of the number N of electrons where the density of electrons $\rho_0 = N/\Omega$ remains finite as $\Omega \to \infty$. The interelectronic spacing is defined by the parameter

$$r_s = \left(\frac{3}{4\pi\rho_0}\right)^{1/3} . \quad . \quad . \quad . \quad . \quad . \quad . \quad . \quad (2.8)$$

The solution of the problem consists now of finding the eigenvectors and eigenvalues of (2.1) which satisfy (2.7). In most cases the free electron approximation has been used; i.e. the potential due to the crystal lattice is replaced by a uniform background of positive charge, and in (2.2) we put

$$U(\mathbf{G}) = 0. \quad . \quad . \quad . \quad . \quad . \quad . \quad . \quad . \quad (2.9)$$

This drastic approximation greatly simplifies the calculation, and it is not definitely clear yet whether the results obtained for the free electron gas can be directly generalized for the lattice case. It is in general assumed that qualitatively this generalization is possible, although some important corrections might be perhaps necessary (see below).

To solve the Schroedinger equation

$$\mathscr{H}|\Psi'\rangle = E|\Psi'\rangle$$

use of perturbation theory has almost invariably been made, the interaction $\mathscr{H}_1$ being considered the perturbation term. A comprehensive discussion on the perturbation series by Brueckner (1958) shows that due to the large volume of the system ($\Omega \to \infty$)

(*a*) the Brillouin–Wigner perturbation method gives an essentially non-convergent series and cannot be used to solve the problem of a many-body system;

(*b*) the Rayleigh Schroedinger perturbation theory, although it seems to give a divergent series, can be used to perform the calculation because it can be shown explicitly that the divergent terms, through an exact

† We shall always use angular bras and kets for perturbed states, and round ones for unperturbed.

cancellation of their contributions, give no net contribution to the final result of the energy value. All the perturbation methods used to solve the many-body problem are modifications, in one way or another, of the Rayleigh–Schroedinger series.

Let us firstly study the unperturbed hamiltonian $\mathscr{H}_0$. Its eigenstates which satisfy (2.7) are vectors $|\Psi)$ such that N different $\mathbf{k}$-states are occupied by electrons, the others being empty; these vectors $|\Psi)$ are equivalent to the Slater determinants of the real space representation. The unperturbed ground state $|G)$ consists of N electrons occupying the states

$$k \equiv |\mathbf{k}| \leqslant k_{\mathrm{F}},$$

where k_{F} is defined by

$$k_{\mathrm{F}} = (3\pi^2\rho_0)^{1/3} = \left(\frac{9\pi}{4}\right)^{1/3} r_{\mathrm{s}}^{-1} = 1{\cdot}919 r_{\mathrm{s}}^{-1} \quad . \quad . \quad . \quad (2.10)$$

and its unperturbed energy is

$$W_{\mathrm{G}} = \tfrac{3}{10} N k_{\mathrm{F}}^2 \quad . \quad . \quad . \quad . \quad . \quad . \quad . \quad . \quad . \quad (2.11)$$

in atomic units. The occupation function $f(k)$ is a constant equal to 1 for $k \leqslant k_{\mathrm{F}}$ and zero for $k > k_{\mathrm{F}}$; it has thus a discontinuity $\Delta f = 1$ at $k = k_{\mathrm{F}}$. The low-energy excited states of the unperturbed system can be defined as the ground state, plus n electrons in given states $\mathbf{k}_i (k_i > k_{\mathrm{F}})$ and n empty states or holes $\mathbf{k}_\alpha (k_\alpha < k_{\mathrm{F}})$. These excited states will be denoted by

$$|\mathbf{k}_i, \mathbf{k}_j, \ldots ; \mathbf{k}_\alpha, \mathbf{k}_\beta, \ldots) \quad . \quad . \quad . \quad . \quad . \quad . \quad . \quad (2.12)$$

and their energy is

$$W(\mathbf{k}_i, \mathbf{k}_j \ldots ; \mathbf{k}_\alpha, \mathbf{k}_\beta, \ldots) = W_G + \tfrac{1}{2} \sum_i k_i^2 - \tfrac{1}{2} \sum_\alpha k_\alpha^2 . \quad . \quad . \quad (2.13)$$

In this way it is possible to redefine the unperturbed system in terms of unperturbed quasi-particles. In this new picture the ground state is considered the vacuum, and each excited state (2.12) consists of n electron-like quasi-particles of momentum $\mathbf{k}_i$, spin σ_i and energy $\frac{1}{2}k_i^2$, together with n hole-like quasi-particles of momentum $(-\mathbf{k}_\alpha)$, spin $(-\sigma_\alpha)$ and energy $(-\frac{1}{2}k_\alpha^2)$.

To study the perturbation we use the time-dependent adiabatic formulation. This method has been employed by Goldstone (1957) and Hubbard (1957, 1948 a). The other methods used by other investigators are slightly different. We do not attempt to describe them but shall give their results expressed systematically in terms of the present adiabatic formulation as far as possible.

We must mention separately the works by Kohn and Luttinger (1960) and Luttinger and Ward (1960), where using a thermodynamic approach, they have tested the validity of the adiabatic approximation. In fact they have shown that Goldstone's method of calculation is valid for the free electron case, but it is in error for the non-spherical Fermi surface due to the contribution of some terms which the adiabatic approximation necessarily neglects. However, as we shall restrict ourselves mostly to the free electron case, the adiabatic approach is still a sound method of calculation in what follows.

We assume that the electron–electron interaction, expressed in the interaction representation, is exponentially switched on between $t=-\infty$ and $t=0$, i.e. is represented by

$$\mathscr{H}_\alpha(t)=\exp(i\mathscr{H}_0 t)\mathscr{H}_1 \exp(-i\mathscr{H}_0 t)\exp(\alpha t) \quad . \quad . \quad . \quad (2.14)$$

where the parameter α governs the rate of switching on the perturbation. The adiabatic theorem (Gell-Mann and Low 1951) establishes that if $|\chi_\alpha(t))$ satisfies the Schroedinger equation

$$i\frac{d}{dt}|\chi_\alpha(t))=\mathscr{H}_\alpha(t)|\chi_\alpha(t)) \quad . \quad . \quad . \quad . \quad . \quad (2.15)$$

and initially ($t=-\infty$) is an eigenstate of $\mathscr{H}_0$, i.e.

$$|\chi_\alpha(-\infty))=|\Psi),$$

and if in addition the limit

$$\Delta E=\lim_{\alpha\to 0}\frac{(\Psi|\mathscr{H}_1|\chi_\alpha(0))}{(\Psi|\chi_\alpha(0))} \quad . \quad . \quad . \quad . \quad . \quad (2.16)$$

exists and is real, then the state-vector

$$|\Psi\rangle=\lim_{\alpha\to 0}\frac{|\chi_\alpha(0))}{(\Psi|\chi_\alpha(0))} \quad . \quad . \quad . \quad . \quad . \quad . \quad (2.17)$$

is an eigenstate of the total hamiltonian $\mathscr{H}$ with an energy eigenvalue

$$E=W+\Delta E,$$

where W is the unperturbed energy given by (2.13). This means that when the interaction is switched on infinitely slowly, an eigenvector of the unperturbed system is transformed into an eigenvector of the total hamiltonian.

Assuming the existence of the limit (2.16), if the unperturbed state $|\Psi)$ is non-degenerate, ΔE is always real and the hypotheses of the theorem are satisfied; this is the case of the ground state $|G)$. If, on the other hand we apply (2.16), (2.17) to a state $|\Psi')$ which is degenerate, then ΔE turns out in general to have an imaginary part, its physical meaning being that the perturbation transforms the original eigenstate $|\Psi')$ into a decaying state $|\Psi'\rangle$ of the total system with a mean life given by

$$T=[\mathrm{Im}\,\Delta E]^{-1}. \quad . \quad . \quad . \quad . \quad . \quad . \quad . \quad (2.18)$$

After a time of the order T, the system decays into other states due to electron–electron collisions. It is theoretically possible to find linear combinations of degenerate states $|\Psi')$ such that the imaginary part of ΔE vanishes for each of them: these are the true excited eigenstates of the total hamiltonian. However, due to the formidable degeneracy of the electron gas and the enormous difficulties in exactly evaluating the matrix elements (2.16), the problem of finding the exact excited eigenstates has never been solved. Even if we could calculate them explicitly, these would probably be of very little use for studying the transport properties of the system; the complicated linear combinations of different $|\Psi')$ would mix the states in such a disordered way that no one-to-one correspondence between the eigenstates of the independent particle model and the true hamiltonian would be possible.

However, as discussed in § 2.3, it is possible to find some unperturbed excited states which give rise to decaying functions $|\Psi\rangle$ with a very long mean life, i.e. with a very small imaginary part of ΔE. If one such state is excited by an external agent and its mean life is longer than the relaxation time of the whole process (due to impurities or the motion of the lattice), it can be considered for all purposes of transport theory an eigenstate with energy

$$E = W = \mathrm{Re}\,\Delta E.$$

The imaginary part of E can thus be taken into account as a small correction to the relaxation time.

To compute the energy shift (2.16), the operator $S_\alpha(t)$ (similar to the S-matrix of quantum field theory) is introduced in such a way that

$$S_\alpha(t)|\Psi) = |\chi_\alpha(t)). \quad . \quad . \quad . \quad . \quad . \quad . \quad . \quad (2.19)$$

It satisfies the Schroedinger equation

$$i\frac{d}{dt}S_\alpha(t) = \mathscr{H}_\alpha(t)S_\alpha(t) \quad . \quad . \quad . \quad . \quad . \quad . \quad (2.20)$$

with the initial condition

$$S_\alpha(-\infty) = 1.$$

Solving (2.20) by iteration under the assumption that the perturbation series converges, the final formula for $S_\alpha(0) = S_\alpha$ is obtained:

$$S_\alpha = 1 + \sum_{n=1}^{\infty} (-i)^n \frac{1}{n!}\int_{-\infty}^{0} dt_1 \int_{-\infty}^{0} dt_2 \ldots \int_{-\infty}^{0} dt_n \times P[\mathscr{H}_\alpha(t_1)\mathscr{H}_\alpha(t_2)\ldots\mathscr{H}_\alpha(t_n)] \quad . \quad . \quad . \quad . \quad . \quad . \quad . \quad (2.21)$$

where the operator P places the hamiltonians in chronological order such that the times never decrease going from left to right.

Inserting (2.19) in (2.16) and (2.17), we write the perturbed energy and state vector as

$$\Delta E = \lim_{\alpha\to 0} \frac{(\Psi|\mathscr{H}_1 S_\alpha|\Psi)}{(\Psi|S_\alpha|\Psi)} \quad . \quad . \quad . \quad . \quad . \quad (2.22)$$

and

$$|\Psi\rangle = \lim_{\alpha\to 0} \frac{S_\alpha|\Psi)}{(\Psi|S_\alpha|\Psi)}. \quad . \quad . \quad . \quad . \quad . \quad . \quad (2.23)$$

Finally substituting (2.21) for S_α gives perturbation series for ΔE and $|\Psi\rangle$. Each term of these series can be represented by a diagram similar to those introduced by Feynman (1949) in quantum field theory. For the sake of definiteness, we give explicitly the prescription for building up one of the graphs contributing to the numerator of (2.22), and the rules for calculating from it the corresponding contribution to the energy:

(i) Mark $n+1$ pairs of points on the diagram; both points of each pair must be at the same time (considered to increase from bottom to top of the diagram), but different pairs are at different times;

(ii) Label each pair with times $t_0, t_1, \ldots t_n$ beginning with the uppermost pair and proceeding downwards;

(iii) Join both points of each pair with an interaction (dashed) line;

(iv) Draw particle (full) lines joining different points, or going from one point to the upper or lower end of the diagram, or going vertically across the graph without touching any point; put arrows on them such that at each point there are two and only two particle lines, one with incoming and the other with outgoing arrows, and at both ends of the diagram there are as many lines pointing upwards as electron-like quasi-particles exists in $|\Psi'\rangle$ and as many lines with arrows pointing downwards as hole-like quasi-particles exist in $|\Psi'\rangle$.

(v) Label each external line (line going to one or both ends of the diagram) with indices $\mathbf{k}_i$ or $\mathbf{k}_\chi$ corresponding respectively to the electron-like (upwards arrows) or hole-like (downward arrows) quasi-particles of $|\Psi'\rangle$.

(vi) Label each internal line (line joining two points of the diagram) with indices $\mathbf{k}, \mathbf{k}', \mathbf{k}''$, etc.

To evaluate the contribution of each diagram to the series for the numerator of (2.22):

(A) Write for each interaction line the factor

$$\tfrac{1}{2}v_{1234}\exp[\tfrac{1}{2}i(k_1^2+k_2^2-k_3^2-k_4^2)]t_m\exp(\alpha t_m)$$

where $\mathbf{k}_1$ and $\mathbf{k}_4$ are respectively the labels of the outgoing and incoming particles at one point of the pair t_m, and $\mathbf{k}_2$ and $\mathbf{k}_3$ the labels of the outgoing and incoming particles at the second point of the pair;

(B) Write a factor

$$D(t_l-t_m)=Y(t_l-t_m)-Y(k-k_F)$$

for each internal line $\mathbf{k}$ going from a point t_m to a point t_l; the function $Y(x)$ is defined by

$$Y(x)=1 \quad x>0,$$
$$=0 \quad x\leqslant 0;$$

(C) Put $t_0=0$ and integrate over all other time variables between $-\infty$ and 0;

(D) Multiply the integral by a factor

$$(-i)^n(n!)^{-1}(-1)^\nu$$

where n is the number of interaction lines minus one and ν the number of closed particle loops of the diagram;

(E) Sum over all $\mathbf{k}$, $\mathbf{k}'$, $\mathbf{k}''$ ..., the labels of the internal particle lines;

(F) Evaluate the limit $\alpha\to 0$.

Similar prescriptions can be given for all the other relevant matrix elements. The results which follow in the next subsections have been obtained by systematic use of this or other very similar techniques.

2.2. *The Ground State*

In evaluating

$$\Delta E'_G=\lim_{\alpha\to 0}\frac{(G|\mathscr{H}_1 S_\alpha|G)}{(G|S_\alpha|G)} \quad \ldots\ldots \quad (2.24)$$

Goldstone (1957) has proved that disconnected diagrams such as that

shown in fig. 3, i.e. diagrams with two or more different parts not connected to each other by lines, give contributions only to the normalization of the wave function. Although the integrals arising from these disconnected diagrams diverge, their contribution is exactly cancelled by the denominator of (2.24); they can be completely disregarded and the series is then reduced to only connected diagrams. This is called the linked-cluster expansion. The linked-cluster perturbation formula was also proved by Goldstone to be a continuous function of α and therefore the limit can be taken by putting $\alpha = 0$. The final formula for the energy is expressed by

$$\Delta E_G = \sum_L (G|\mathscr{H}_1 \left(\frac{1}{W_0 - \mathscr{H}_0} \mathscr{H}_1 \right)^n |G) \quad . \quad . \quad . \quad (2.25)$$

where $\sum_L$ means summation over connected graphs only. The same result was obtained by Hugenholtz (1957, 1958) by a somewhat different method. To evaluate (2.25) explicitly it was necessary to overcome a crucial difficulty: the divergence of the summation over the intermediate states **k**, **k'**, ... due to the piling up of factors $1/k^2$. The first-order term of the series is

Fig. 3

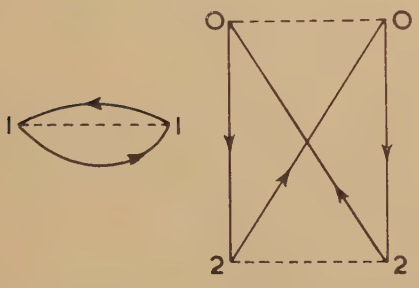

Fig. 4

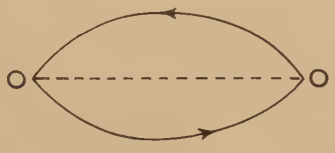

shown in fig. 4 and its calculation is straightforward; it gives the exchange energy in the Hartree–Fock approximation. The second-order diagrams are shown in fig. 5; the first one is the direct term and diverges logarithmically, while the second represents the exchange term and is finite. Gell-Mann and Brueckner (1957) have proved that the divergence of the direct term is cancelled by similar divergences in high-order terms such as those shown in fig. 6. By summing the contribution of these diagrams up to infinite order before performing the summation over the divergent internal line they were able to get an expression for the energy of the ground state in terms of the interelectronic spacing:

$$E_G = N[2{\cdot}21 r_s^{-2} - 0{\cdot}916 r_s^{-1} + 0{\cdot}0622 \ln r_s - 0{\cdot}096 + 0(r_s)]ry. \quad . \quad (2.26)$$

This expression is only valid in the high density limit, $r_s < 1$ as has been shown by Nozières and Pines (1958), and is therefore not useful for metallic densities $2 \leqslant r_s \leqslant 5{\cdot}5$.

Hubbard (1958a) using the effective interaction method developed by him (Hubbard 1957) was able to repeat Gell-Mann and Brueckner's calculation (to second order in the perturbation expansion). He also made

an approximate evaluation of the third-order diagrams, obtaining results which may be valid even in the region of metallic densities. These are shown in table 1, where values of the formula derived by Bohm and Pines (Pines 1955) using the collective description are also displaced. The latter is given by

$$E_G = N[2{\cdot}21 r_s^{-2} - 0{\cdot}916 r_s^{-1} + 0{\cdot}031 \ln r_s - 0{\cdot}115]ry \quad . \quad . \quad (2.27)$$

and can be considered a suitable interpolation formula for metallic densities (Nozières and Pines 1958), where the last two terms give the correlation energy within an accuracy of about 15%.

Fig. 5

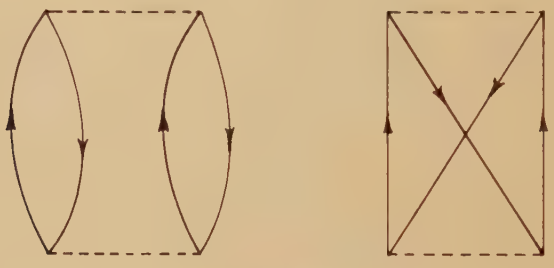

Fig. 6

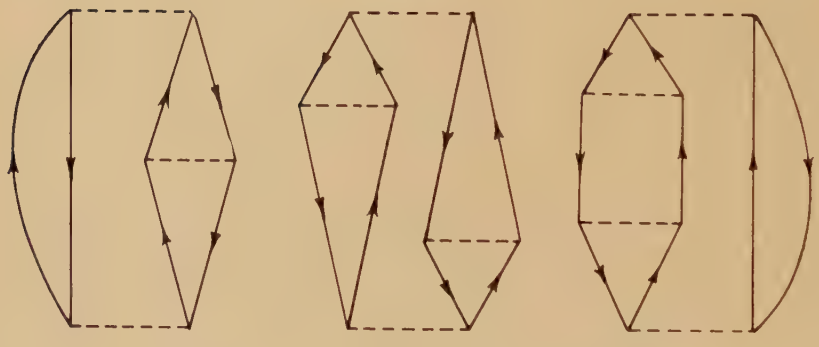

Table 1. The energy of the ground state

r_s	E_c	
	Hubbard's value	Bohm and Pines's value
2·0	−0·099	−0·093
3·0	−0.086	−0·081
4·0	−0·074	−0·072
5·0	−0·067	−0·066

Note : E_c is usually called the correlation energy and is defined by

$$E_G = N[2{\cdot}21\ r_s^{-2} - 0{\cdot}916\ r_s^{-2} + E_c]ry.$$

Concerning the structure of the ground state, i.e. the explicit form of the eigenvector $|G\rangle$, the results obtained are very few and only related to some particular details. The reason for this partial failure of the method lies in the fact that the series (2.23) for the state vector, due to the divergence of the normalization terms, is essentially non-convergent; the cancellation of terms that give rise to the linked-cluster expansion for the energy is not valid here and up till now every perturbation method has failed in giving even an approximate solution for $|G\rangle$ (see, for instance, Brueckner 1958). However, Migdal (1957) and Luttinger (1960) have proved that the average occupation probability $f(k)$ in the ground state $|G\rangle$, although different from the simple step function characteristic of the unperturbed $|G\rangle$, still exhibits a discontinuity $\Delta f < 1$ at some values of $\mathbf{k}$, in terms of which the Fermi surface can be clearly defined (fig. 7). Luttinger (1960)

Fig. 7

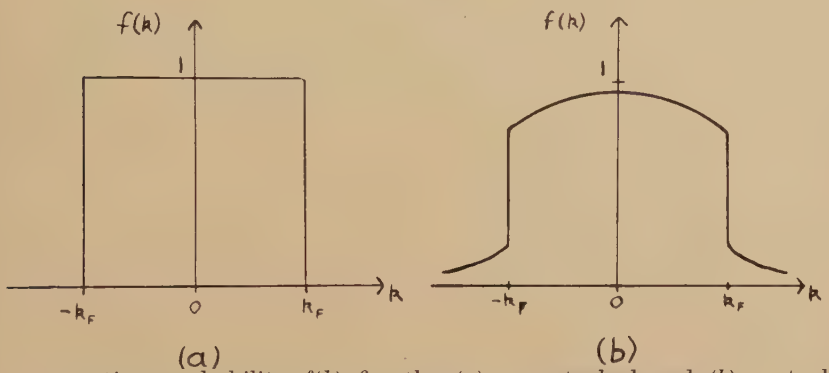

The occupation probability $f(k)$ for the (a) unperturbed and (b) perturbed ground state, showing discontinuity at the Fermi level.

has also proved that the volume in $\mathbf{k}$-space enclosed by the Fermi surface defined in this way is equal to the volume of the Fermi distribution of the corresponding non-interacting system, i.e. contains exactly 1 or 2 or ... electrons per atom.

2.3. *The Single Quasi-particle States*

Suppose that in (2.22), (2.23) we put $|\Psi'\rangle = |\mathbf{k}_i)$, i.e. a single unperturbed electron-like quasi-particle in an $N+1$ particle system (or a hole-like quasi-particle in an $N-1$ particle system). Due to the degeneracy of unperturbed states having this total $\mathbf{k}$ and total energy, the energy (2.16) turns out in general to have an imaginary part as already mentioned and the adiabatic theorem that (2.23) is an eigenstate collapses. Nevertheless we can still use (2.23) to define the perturbed state $|\mathbf{k}_i\rangle$ corresponding to $|\mathbf{k}_i)$

$$|\mathbf{k}_i\rangle = \lim_{\alpha \to 0} \frac{S_\alpha |\mathbf{k}_i)}{(\mathbf{k}_i|S_\alpha|\mathbf{k}_i)} \quad . \quad . \quad . \quad . \quad . \quad . \quad (2.28)$$

and investigate its properties.

Consider first the case $k_i = k_F$ with the quasi-particle just at the Fermi level. The degeneracy of the unperturbed state tends to zero, and Hugenholtz (1957, 1958) has proved that the adiabatic theorem holds and we obtain an eigenstate with a real energy

$$E(\mathbf{k}) = E_{G,N} \pm \epsilon(\mathbf{k}) \quad . \quad . \quad . \quad . \quad . \quad . \quad . \quad (2.29)$$

where the plus or minus refers to electron-like or hole-like quasi-particles. He has also shown that the state $|\mathbf{k}_i\rangle$ defined by (2.28) can be written in the form of an excitation of the ground state,

$$|\mathbf{k}_i, N+1\rangle = O_{\mathbf{k}i}{}^*|G, N\rangle \quad . \quad . \quad . \quad . \quad . \quad (2.30\,a)$$

where

$$O_{\mathbf{k}}{}^* = N_{\mathbf{k}} \sum_c \sum_\nu \{a_\nu\}^* [\nu| \left(\frac{-1}{\mathscr{H}_0 - E_G - \epsilon_{\mathbf{k}}} \right)^n |\mathbf{k}_i]. \quad . \quad . \quad (2.31)$$

Here $\{a_\nu\}^*$ is the product of creation and annihilation operators of the 'bare' electrons that transforms $|G, N\rangle$ into an arbitrary unperturbed state $|\nu)$, and $\sum_c$ means that the sum over n must be performed taking account only of connected diagrams whose intermediate states are all different from $|k_i)$. The energies in the denominator are the perturbed energies. Similarly for holes

$$|\mathbf{k}_\alpha, N-1\rangle = O_{\mathbf{k}\alpha}|G, N\rangle \quad . \quad . \quad . \quad . \quad . \quad (2.30\,b)$$

where $O_{\mathbf{k}\alpha}$ is the hermitian conjugate of $O_{\mathbf{k}}{}^*$.

For $k_i > k_F$ (or $k_\alpha < k_F$), we can use either (2.28) or (2.30) formally to define the perturbed states. Incidentally it has only been proved that the two states so defined are identical at k_F: away from k_F there may be slight differences in the imaginary parts increasing with $k_i - k_F$, but for practical purposes near the Fermi level we shall treat them as identical. We shall use (2.30) formally to define our states as in § 1.2. but revert to the series for (2.22), (2.28) for quantitative calculations. The energy $\epsilon(\mathbf{k})$, still defined by (2.29), varies as follows (Hugenholtz and van Hove 1958):

$$\left.\begin{aligned} &\mathrm{Re}\,\epsilon(\mathbf{k}) - \epsilon_F \propto k - k_F, \\ &\mathrm{Im}\,\epsilon(\mathbf{k}) \quad\quad \propto (k-k_F)^2 \end{aligned}\right\} \quad . \quad . \quad . \quad (2.32)$$

where we define ϵ_F as the Fermi energy. Hugenholtz (1957, 1958) showed that in evaluating $\epsilon(\mathbf{k})$ only connected diagrams need be taken into account: the disconnected diagrams contribute only to $E_{G,N}$ and to the normalization of the state vector.

The Fermi energy ϵ_F has the property

$$E_{G,N+1} - \epsilon_F = E_{G,N} = E_{G,N-1} + \epsilon_F$$

showing that ϵ_F can be defined as the separation energy of one electron. In fact this equation as it stands is not very meaningful because $E_{G,N}$ is of order N and $N \to \infty$. It can be rewritten in the form

$$\epsilon_F = \frac{d}{d\rho}\left(\frac{E_G}{\Omega}\right)$$

which has a well-defined meaning for an infinitely large system. As usual

the Fermi surface is defined by $\epsilon(\mathbf{k}) = \epsilon_F$ and the whole calculation, particularly (2.32), shows that its radius k_F is still given by (2.10) the same as in the Sommerfeld model. This shows it is also the same as the Fermi surface defined in § 2.2 by the discontinuity in the occupation function so that no ambiguity can arise.

The operators $O_{\mathbf{k}}^*$, $O_{\mathbf{k}}$ are creation and annihilation operators for 'dressed' quasi-particles. Thus as described in § 1.2, we can set up a whole system of excited states of the electron gas in terms of multiple excitations of the ground state. From their mode of derivation, they must at the Fermi level satisfy the usual anticommutation relations for fermion operators, although their structure is too complicated to verify this explicitly. It is not clear whether the same property holds when the definition (2.31) is extended away from the Fermi surface, although it is probable that this is not so, with the consequences discussed in § 1.3.3.

Quinn and Ferrell (1958) have computed $\epsilon(\mathbf{k})$ to second order of perturbation theory using the effective electron–electron interaction given by Lindhard (1954) and eliminating the divergences by subtracting the contribution of the vacuum. Although the calculation is only valid for very high densities, it shows some important features of $\epsilon(\mathbf{k})$ and the lifetime of the quasi-particles. As far as we know, no good calculation of $\epsilon(\mathbf{k})$ for metallic densities has been completed up till now. In fact all the available formulae are only rather crude approximations. In this paper we shall take for performing explicit calculations, the Bohm and Pines formula (Pines 1955) obtained through a quite different approach, i.e. the collective coordinates model. For quasi-particles near the Fermi surface

$$\epsilon(\mathbf{k}) = \left[k^2 - \frac{0{\cdot}611}{r_s} \left\{ 1 - 2\beta + \frac{3k^2 + (\beta^2 - 1)k_F^2}{2kk_F} + \frac{k_F^2 - k^2}{kk_F} \ln \frac{k_F + k}{\beta k_F} \right\} \right] ry \,, \quad . \quad . \quad . \quad (2.33)$$

where β is a parameter that governs the cut-off of the effective interaction (see § 2.4). According to Pines (1955)

$$\beta = 0{\cdot}353 r_s^{1/2} \quad . \quad . \quad . \quad . \quad . \quad . \quad . \quad . \quad . \quad (2.34)$$

and Fletcher and Larson (1958) give

$$\beta = 0{\cdot}4 r_s^{1/2}$$

as a better value that brings the theoretical values to a better agreement with experimental results.

A more accurate calculation of $\epsilon(\mathbf{k})$ would be desirable and even necessary to apply theoretical results to the real metals; but the discouraging mathematical difficulties of the problem have restricted the application of well elaborated methods, such as Hubbard's perturbation techniques, to numerical evaluation of the ground state energy only.

2.4. *The Effective Quasi-particle Interaction*

From the work of Bohm and Pines (Pines 1955) it is well known that the collective properties of the electron gas result in an effective screening

of the coulomb interaction. It has been shown that the long-range part of the interaction results in some collective oscillations of the system as a whole; these collective oscillations have a very high frequency and are excited only in very energetic processes. The remaining short-range part constitutes the effective quasi-particle interaction. Bohm and Pines, in a somewhat arbitrary way, eliminate the long-range effects by changing the Fourier transform of the coulomb potential

$$v(\mathbf{k}) = 4\pi/k^2$$

into an interaction

$$V_{\mathrm{BP}}(\mathbf{k}) \begin{cases} = 0, & k < \beta k_{\mathrm{F}} \\ = 4\pi/k^2, & k > \beta k_{\mathrm{F}} \end{cases} \quad . \ . \ . \ . \quad (2.36)$$

that shows a cut-off on the small $\mathbf{k}$-vector side. The cut-off parameter β was chosen by a variational argument, but many doubts have arisen concerning what is the most suitable magnitude to minimize; the selection of the best β is not yet quite clear (see for instance Fletcher and Larson 1958). In a way it is a rather academic question anyway since the form of the interaction is too unrealistic for most quantitative calculations (see below and § 5).

Fig. 8

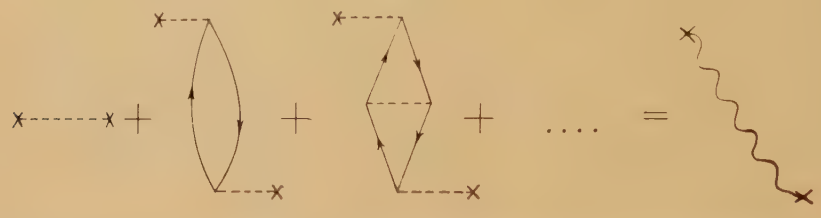

The screened character for the effective interaction and the existence of collective motions of the system have been also obtained by means of the many-body approach. Hubbard (1957) has shown that some parts of the diagrams in the perturbation series can be summed up to give a modified interaction, which is time-dependent and short ranged.

The portions of the diagrams to be summed are the so-called polarization parts and consist of those sections of any diagram connected to the rest only through two interaction lines. The summation, that is schematically shown in fig. 8, means that all polarization parts of the diagrams can be suppressed if the interaction $v(\mathbf{k})$ is replaced by an effective potential V. But now, since the interaction lines join points at different times, V must necessarily be time dependent, representing a retarded interaction. The Fourier transform (t to ω) of the effective potential can be expressed as†

$$V(\mathbf{k}, \omega) = \frac{v(\mathbf{k})}{\epsilon(\mathbf{k}, \omega)} \quad . \ . \ . \ . \ . \ . \ . \quad (2.36)$$

where $\epsilon(\mathbf{k}, \omega)$ can be interpreted as a dielectric constant, energy and

† The double use of ϵ for one-particle energy $\epsilon(\mathbf{k})$ and for dielectric constant $\epsilon(\mathbf{k}\omega)$ in this section only, should lead to no confusion.

momentum dependent, due to the electron gas. Hubbard (1958 a) has computed $\epsilon(\mathbf{k}, \omega)$ up to second order (in first order $\epsilon = 1$) and his result agrees with the formula given by Lindhard (1954) and used by Quinn and Ferrell (1958) to compute single-quasi-particle energies. This second-order dielectric constant is a good approximation for the high-density limit, but not suitable for real electron gases in metals. None the less it clearly shows the screened character of the interaction. Putting

$$\epsilon(\mathbf{k}, \omega) = 1 - F(\mathbf{k}, \omega) \quad . \quad . \quad . \quad . \quad . \quad . \quad (2.37)$$

the second-order computation gives

$$F_2(\mathbf{k}, \omega) = \frac{k_F}{\pi k^2} \left\{ \frac{k_F \left(\frac{\omega}{k k_F} - \frac{k}{2k_F} \right)^2 - k_F}{k} \ln \frac{\omega - k k_F - \frac{1}{2}k^2}{\omega + k k_F - \frac{1}{2}k^2} \right.$$
$$\left. + \frac{k_F \left(\frac{\omega}{k k_F} + \frac{k}{2k_F} \right)^2 - k_F}{k} \ln \frac{\omega + k k_F + \frac{1}{2}k^2}{\omega - k k_F + \frac{1}{2}k^2} - 2 \right\} .$$
$$. \quad . \quad . \quad . \quad (2.38)$$

This, for $\omega = 0$ and k very small, reduces approximately to

$$F_2'(\mathbf{k}, 0) \approx -4k_F/\pi k^2 \quad . \quad . \quad . \quad . \quad . \quad (2.39\,a)$$

which is equivalent to an interaction $V(\mathbf{k})$ equal to a Yukawa type of potential (1.8) with effective screening length

$$1/Q = (\pi/4k_F)^{1/2}. \quad (2.39\,b)$$

The approximate expression (2.39) has been used by Quinn and Ferrell (1959) to study some properties of an idealized metal at high density and a similar expression has been used in § 1.3 as prototype of an effective screened interaction.

We must also note that for small k and large ω, (2.38) reduces to

$$F_2(\mathbf{k}, \omega) \approx 4k_F^3/3\pi\omega^2$$

showing the possibility of collective oscillations of the system with the classical plasma frequency

$$\omega_p = (4k_F^2/3\pi)^{1/2}$$

for which the dielectric constant vanishes.

For metallic densities, it is necessary to evaluate $\epsilon(\mathbf{k}, \omega)$ at least up to third order of perturbation theory. Hubbard (1958 a) has evaluated approximately the contribution of the third polarization sub-diagram shown in fig. 8 and a series of related diagrams, with the result

$$F_3(\mathbf{k}, \omega) = \frac{F_2(\mathbf{k}, \omega)}{1 + \frac{k^2}{2(k^2 + k_F^2)} F_2(\mathbf{k}, \omega)} \quad . \quad . \quad . \quad (2.40\,a)$$

A better formula is probably (Hubbard, private communication)

$$F(\mathbf{k}, \omega) = \frac{F_2(\mathbf{k}, \omega)}{1 + \frac{1}{2}k^2 F_2(\mathbf{k}, \omega)/(k^2 + k_F{}^2 + Q^2)} \quad . \quad . \quad (2.40\,b)$$

where Q is given by (2.39 b), though neither of these has quite the correct form for small k (see fig. 9) where (2.38) is more correct. The different results are plotted in fig. 9, where we also include our fudged best estimate based on (2.39) and (2.40 b). All of these calculations neglect certain effects which must be of some importance at actual metallic densities, so that one cannot say how reliable the results are.

Fig. 9

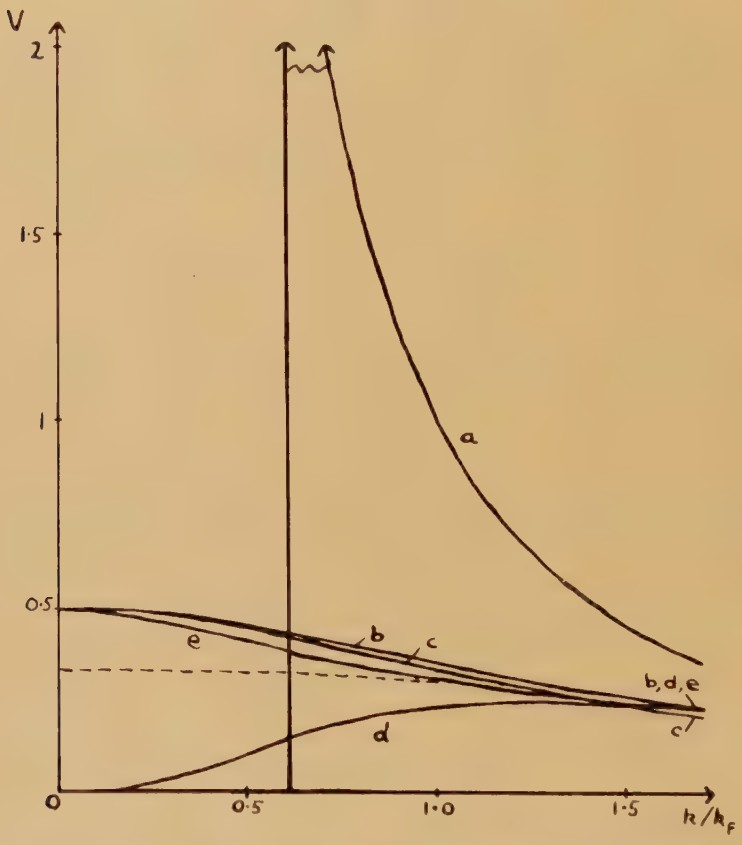

Various approximations for $V(k, 0)$ for $r_s = 3$ using : (a) Bohm and Pines' cut-off function (2.35), (2.34) : (b) Lindhard's second-order calculation (2.38) ; (c) Yukawa interaction (1.8), (2.39) : (d) Hubbard's original calculation (2.40 a). The fact that the curve tends very nearly to zero at $k = 0$ is not a general feature but is associated with the particular value $r_s = 3$; (e) our best estimate (after Hubbard, private communication). Within the limit of the effects being considered here, this should tend to Lindhard's value at $k = 0$. For $k \gtrsim 1$ we have used (2.40 b) (shown dotted for small k). The ordinates are in units of $4\pi k_F{}^2$.

The introduction of the quasi-particle formalism and the effective interaction, allows us to make a change of representation of our hamiltonian, which now becomes

$$\mathscr{H}_{\text{eff}} = \mathscr{H}_{\text{eff}}^{0} + \mathscr{H}_{\text{eff}}^{1}, \quad . \quad . \quad . \quad . \quad . \quad . \quad . \quad (2.41)$$

where

$$\mathscr{H}_{\text{eff}}^{0} = E_G + \sum_{\mathbf{k}i} \epsilon(\mathbf{k}_i) O_{\mathbf{k}i}{}^{*} O_{\mathbf{k}i} + \sum_{\mathbf{k}\alpha} \epsilon(\mathbf{k}_\alpha) O_{\mathbf{k}\alpha} O_{\mathbf{k}\alpha}{}^{*} \quad . \quad . \quad (2.42)$$

gives the single quasi-particle energies, and

$$\mathscr{H}_{\text{eff}}^{1} = \tfrac{1}{2} \sum_{1,2,3,4} V_{1234} \{ O_{\mathbf{k}1}{}^{*} O_{\mathbf{k}2} O_{\mathbf{k}3}{}^{*} O_{\mathbf{k}4} \} \quad . \quad . \quad . \quad (2.43)$$

gives the quasi-particle interaction term. Here

$$V_{1234} = (1/\Omega) V(\mathbf{k}_1 - \mathbf{k}_4, \epsilon_1 - \epsilon_4) \delta(\sigma_1, \sigma_4) \delta(\sigma_2, \sigma_3) \delta(\mathbf{k}_1 + \mathbf{k}_2, \mathbf{k}_3 + \mathbf{k}_4) \quad (2.44)$$

Fig. 10

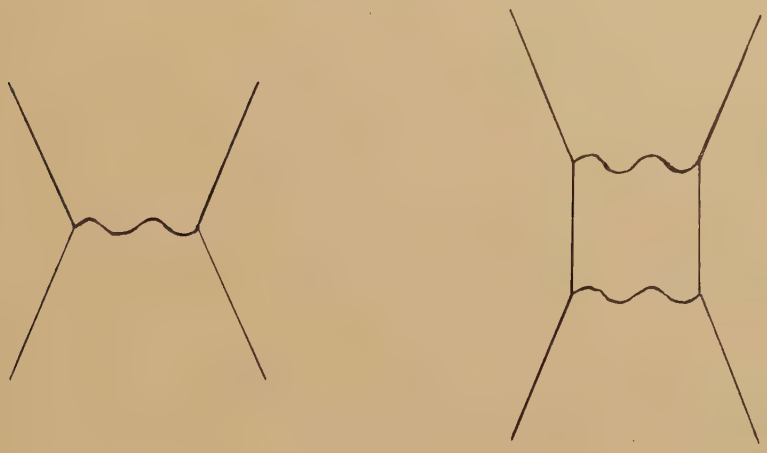

and $\sum^{*}$ means that in calculating the evolution of the system, diagrams with interactions not connecting different quasi-particles as well as those containing polarization parts, must be disregarded. The bracket means that in ordering the O operators, the pair $O_{\mathbf{k}\alpha}{}^{*} O_{\mathbf{k}\alpha}$ for holes must be replaced by $-O_{\mathbf{k}\alpha} O_{\mathbf{k}\alpha}{}^{*}$, because the contribution coming from the term 1 in the commutation relation is already taken into account in the ground state energy E_G.

Since we are only dealing with quasi-particles near the Fermi level, we can put $\epsilon_1 - \epsilon_4 = 0$ and consider only the so-called static effective interaction $V(\mathbf{k}, 0)$. Figure 9 shows various approximations for $V(\mathbf{k}, 0)$ for a typical metallic density of $r_s = 3$. We note that our best estimate (curve e) is much smoother and considerably smaller in average magnitude than the Bohm and Pines interaction. We shall return to this in § 5

when discussing numerical estimates of the correction terms due to the interaction.

Consider now a state containing two quasi-particles, The interaction $\mathscr{H}_{\text{eff}}{}^{1}$ (2.43) contributes in first order of approximation an interaction energy

$$\eta_1(\mathbf{k}_1, \mathbf{k}_2) = (V_{1221} + V_{1212})$$

which amounts to $\mp (1/\Omega) V(\mathbf{k}_1 - \mathbf{k}_2, 0)$ for particles of parallel spin and zero for antiparallel spin. The minus refers to two electron-like quasi-particles or two holes, the plus to an electron interacting with a hole. We can now apply $\mathscr{H}_{\text{eff}}{}^{1}$ in higher order of perturbation, represented by diagrams of the sort shown in fig. 10, and the second order ones give small contributions η_2 both for parallel and antiparallel spin. The total interaction energy $\eta(\mathbf{k}_1, \mathbf{k}_2)$ of (1.13) is taken to include the effect of all orders of perturbation in this way.

2.5. *The Effect of the Periodic Potential*

To find the eigenfunctions and eigenvalues of (2.1) when

$$U(\mathbf{G}) \neq 0$$

implies the solution of an extremely cumbersome problem that has never been solved up to the present, even for simplified or trivial models of lattice potentials. However, the existence of the Fermi surface, defined as the points in $\mathbf{k}$-space where occupation density $f(\mathbf{k})$ is discontinuous, has been proved very generally by Luttinger (1960) and this, as well as the generality of many conclusions drawn from the free electron case, seem to indicate the existence of quasi-particles of long mean life near the Fermi surface.

Of course, the existence of interband transitions in the metallic band case can bring important quantitative correction to the properties of the quasi-particles and their interactions. However it is reasonable to assume that their mean life decreases quadratically as they approach the Fermi level while their energy varies linearly, which is all that is necessary for the quasi-particle picture to hold. It is also very probable that the effective interaction, although it must exhibit some angular dependence, is not too different from the free electron value in the sense that it is very unlikely to exhibit strong oscillations or sharp differences, because it really is an integrated effect involving all the electrons. Of course in metals with incomplete d shells the effects of correlation can become very large and even lead to a Heitler–London localized type of wave function.

All these assumptions must be confirmed or corrected when definite and complete calculations are available. Up till now only methods of calculation have been proposed, but as far as we know none of these has yet been carried through explicitly. Hubbard (1958 b) has developed a modification of his free electron treatment to study the ground state. The method involves a formidable amount of numerical computation to solve, firstly, the Hartree equations for the electrons in a lattice, and secondly the

effective interaction, expressed as an integral equation, when the screening is modified by the ionic field. The method has been extended by Pratt (1960) to obtain a Schroedinger-like equation for the quasi-particle energies $\epsilon(\mathbf{k})$.

The formal difficulties noted by Kohn and Luttinger (1960) and Luttinger and Ward (1960) about the applicability of the Goldstone formula have already been mentioned in § 2.1.

2.6. *Derived Properties*

Quinn and Ferrell (1958, 1959) have studied various physical properties of an idealized metal, using a quasi-particle approach similar to that used in the present work. Their results are qualitative and applicable to the high density limit only.

Wolff (1959) has studied the effect of the electron correlation on some optical properties of metals. He has used the diagrammatic analysis of Hubbard and has obtained a formal expression for the current when the electron gas is excited by an external electromagnetic field. In the free electron case, no contribution from the electron–electron interaction appears in the current as expected. However, for non-spherical Fermi surfaces the contribution can be important and Wolff discusses the metallic gas in the extreme and idealized case of two isotropic bands of electrons and holes respectively.

The thermodynamical properties of the electron gas have been the subject of several contributions. In particular Gell-Mann (1957) has calculated the specific heat of the free electron gas in the high-density limit by a method similar to the one which led to the elimination of the divergences in the ground state energy due to the coulomb interaction. The determination of the thermodynamical functions of the interacting electron gas by means of diagrammatic analysis has been published by Lee and Yang (1960), Montroll and Ward (1958) and Bloch and de Dominicis (1958). The technique used by the latter has been employed by Luttinger (1960), Kohn and Luttinger (1960), and Luttinger and Ward (1960) to test the validity of Goldstone expansion in an arbitrary non-free electron case, as well as to calculate the specific heat and other properties. Brueckner and Sawada (1958) have calculated the paramagnetic spin susceptibility in the high-density limit. The specific heat has also been calculated by Chen and Chow (1958).

§ 3. Velocity, Charge and Acceleration

When we ask what is the current carried by a quasi-particle an apparent paradox immediately appears. One answer would seem to be

$$\mathbf{j}(\mathbf{k}) = e\mathbf{v}(\mathbf{k}) \quad . \quad . \quad . \quad . \quad . \quad . \quad . \quad . \quad . \quad (3.1)$$

where

$$\mathbf{v}(\mathbf{k}) = \frac{1}{\hbar}\frac{\partial \epsilon(\mathbf{k})}{\partial \mathbf{k}} \quad . \quad . \quad . \quad . \quad . \quad . \quad . \quad . \quad (3.2)$$

is the usual group velocity of the quasi-particle and e the electronic

charge. On the other hand, from fundamental quantum mechanical arguments

$$\mathbf{j} = \left\langle \frac{e\mathbf{P}}{m} \right\rangle , \quad . \quad . \quad . \quad . \quad . \quad . \quad . \quad . \quad . \quad (3.3)$$

which relates the current to the expectation value of the total momentum $\mathbf{P}$. In the case of a single electron, free or in a periodic potential, it is easy to prove that both answers are the same (Wilson 1953, eqn. (2.8.3.)). However, we can see that (3.1) and (3.3) are not equivalent in a many-particle system when the mutual interaction is taken into account. The discrepancy is evident even in the simple Hartree–Fock aproximation for the free electron gas. In this case the momentum of a single particle is $\hbar\mathbf{k}$, but

$$\epsilon(\mathbf{k}) \neq \hbar^2 k^2/2m$$

due to the contribution of the exchange term, and therefore

$$e\mathbf{v} \neq e\hbar\mathbf{k}/m.$$

We shall resolve this apparent paradox in § 3.2 through a calculation of the effective charge e^* carried by a quasi-particle.

3.1. *The Velocity*

The usual argument of the group velocity of a wave leads to the well-known formula (3.2) for the velocity of a single quasi-particle. However, since the definition of effective charge (§ 3.2) rests mainly on this concept, it is worth giving a detailed argument.

We shall need the single quasi-particle states $|\mathbf{k}_i\rangle$ of the $N+1$ electron system defined in § 2.3, and their development in time

$$|\mathbf{k}_i, t\rangle = |\mathbf{k}_i\rangle \exp[-i(E_G + \epsilon_{\mathbf{k}i})t/\hbar] \quad . \quad . \quad . \quad . \quad . \quad (3.4)$$

where we have assumed that t is sufficiently long to be of physical interest but short compared with the natural lifetime T of the state so that we can treat $|\mathbf{k}_i\rangle$ effectively as an eigenstate of the hamiltonian.

To study the evolution of the system in real space, we introduce the density-of-particles operator

$$\rho^{\mathrm{op}}(\mathbf{r}) = (1/\Omega) \sum_{\mathbf{k},\,\mathbf{q}} a_{\mathbf{k}}{}^* a_{\mathbf{k}+\mathbf{q}} \exp i\,\mathbf{q}\cdot\mathbf{r}. \quad . \quad . \quad . \quad . \quad (3.5)$$

The mean value of this operator for a state $|\Psi(t)\rangle$

$$\rho(\mathbf{r}, t) = \langle \Psi(t)|\rho^{\mathrm{op}}(\mathbf{r})|\Psi(t)\rangle$$

gives the density of particles at $\mathbf{r}$ at time t. We observe that in (3.5) each term only connects states with total momenta differing by an amount $\mathbf{q}$. Therefore, the terms contributing to $\langle \mathbf{k}_i|\rho^{\mathrm{op}}(\mathbf{r})|\mathbf{k}_i\rangle$ are only those with $\mathbf{q}=0$, and the particle density for the state $|\mathbf{k}_i\rangle$

$$\rho(\mathbf{r}, t) = (1/\Omega)\langle \mathbf{k}_i| \sum_{\kappa} a_{\kappa}{}^* a_{\kappa} |\mathbf{k}_i\rangle = (N+1)/\Omega$$

is uniform. This is, of course, a trivial result since the electrons must necessarily be uniformly distributed when the total momentum is a good quantum number.

In order to get a localization of particles in real space, we form a wave packet of quasi-particles

$$|\mathbf{k}_0, \alpha\rangle = \sum_i \alpha(\mathbf{k}_i)|\mathbf{k}_i\rangle \quad . \quad . \quad . \quad . \quad . \quad . \quad . \quad . \quad (3.6)$$

where $\alpha(\mathbf{k}_i) \neq 0$ only in a small region of $\mathbf{k}$-space around $\mathbf{k}_0$ and

$$\sum |\alpha(\mathbf{k}_i)|^2 = 1 \quad . \quad . \quad . \quad . \quad . \quad . \quad . \quad . \quad . \quad (3.7)$$

so that the packet is normalized.

We can always choose the coefficients $\alpha(\mathbf{k}_i)$ in order to obtain a high density of electrons concentrated in a small region about $\mathbf{r}_0$ at a given time t_0. The density of electrons for this wave packet is

$$\rho(\mathbf{r}, t) = \langle \mathbf{k}_0, \alpha, t|\rho^{\mathrm{op}}(\mathbf{r})|\mathbf{k}_0, \alpha, t\rangle = \sum_{i,j} \alpha^*(\mathbf{k}_i)\alpha(\mathbf{k}_j)\rho_{\mathbf{k}i,\,\mathbf{k}j}(\mathbf{r}, t) \quad . \quad (3.8)$$

$$\rho_{\mathbf{k}i,\,\mathbf{k}j}(\mathbf{r}, t) = \langle \mathbf{k}_i, t|\rho^{\mathrm{op}}(\mathbf{r})|\mathbf{k}_j, t\rangle . \quad . \quad . \quad . \quad . \quad . \quad (3.9)$$

These matrix elements can be written in the form,

$$\rho_{\mathbf{k}i,\,\mathbf{k}i} = (N+1)/\Omega, \quad . \quad . \quad . \quad . \quad . \quad . \quad . \quad . \quad (3.10)$$

$$\rho_{\mathbf{k}i,\,\mathbf{k}i\,-\,\mathbf{q}} = B(\mathbf{k}_i, \mathbf{k}_i+\mathbf{q})\exp[i\mathbf{q}\cdot\mathbf{r} - i\{\epsilon(\mathbf{k}_i+\mathbf{q}) - \epsilon(\mathbf{k}_i)\}t/\hbar, \quad \mathbf{q} \neq 0, \quad (3.11)$$

$$B(\mathbf{k}_i, \mathbf{k}_i+\mathbf{q}) = (1/\Omega)\sum_{\varkappa} \langle \mathbf{k}_i|a_{\varkappa}{}^* a_{\varkappa+\mathbf{q}}|\mathbf{k}_i+\mathbf{q}\rangle . \quad . \quad . \quad . \quad (3.12)$$

Inserting (3.10) and (3.11) into (3.8) we obtain

$$\rho(\mathbf{r}, t) = \frac{N+1}{\Omega} + \sum_{\mathbf{k}i,\,\mathbf{q}\neq 0} \alpha^*(\mathbf{k}_i)\alpha(\mathbf{k}_i+\mathbf{q})B(\mathbf{k}_i, \mathbf{k}_i+\mathbf{q}) \times \exp\left[i\mathbf{q}\cdot\left\{ \mathbf{r} - \frac{1}{\hbar}\left(\frac{\partial\epsilon}{\partial\mathbf{k}}\right)_{\mathbf{k}0} \right\} t \right], \quad . \quad (3.13)$$

where, using the fact that $\alpha(\mathbf{k}_i)$ is different from zero only around $\mathbf{k}_i = \mathbf{k}_0$, we have made the approximation

$$\epsilon(\mathbf{k}_i) = \epsilon(\mathbf{k}_0) + (\mathbf{k}_i - \mathbf{k}_0)\cdot\left(\frac{\partial\epsilon}{\partial\mathbf{k}}\right)_{\mathbf{k}0} .$$

(3.13) shows clearly that the high concentration of electrons, which at $t = t_0$ was centred at $\mathbf{r} = \mathbf{r}_0$, at a later time $t = t_0 + \Delta t$ is centred at

$$\mathbf{r} = \mathbf{r}_0 + \Delta\mathbf{r} = \mathbf{r}_0 + \frac{1}{\hbar}\left(\frac{\partial\epsilon}{\partial\mathbf{k}}\right)_{\mathbf{k}0}\Delta t$$

and consequently is travelling with a velocity

$$\mathbf{v}(\mathbf{k}_0) = \frac{\Delta\mathbf{r}}{\Delta t} = \frac{1}{\hbar}\left(\frac{\partial\epsilon}{\partial\mathbf{k}}\right)_{\mathbf{k}0}$$

as we wanted to prove.

When we take account of the lattice potential we label our state $|\mathbf{k}_i, s\rangle$ by the reduced wave vector $\mathbf{k}_i$ and band index s. Each term of the particle density operator (3.5) now connects states whose $\mathbf{k}$-vectors differ by $\mathbf{q}$, where

$$\mathbf{k}' - \mathbf{k} = \mathbf{q} + \mathbf{G}_s$$

and G_s is any reciprocal vector of the lattice. Forming as before the wave packet

$$|\mathbf{k}_0, s, \alpha\rangle = \sum \alpha(\mathbf{k}_i)|\mathbf{k}_i, s\rangle$$

the mean value of the density of electrons for this packet is still defined by (3.8) and (3.9), but the matrix elements are now

$$\rho_{\mathbf{k}i,\,\mathbf{k}i} = M(\mathbf{k}_i,\,\mathbf{k}\,;\,\mathbf{r}), \qquad (3.14)$$

$$\rho_{\mathbf{k}i,\,\mathbf{k}i+\mathbf{q}} = M(\mathbf{k}_i,\,\mathbf{k}_i+\mathbf{q}\,;\,\mathbf{r})\exp[i\mathbf{q}\,.\,\mathbf{r} - i\{\epsilon(\mathbf{k}_i+\mathbf{q}) - \epsilon(\mathbf{k}_i)\}t/\hbar], \qquad (3.15)$$

where the functions M are periodic functions of $\mathbf{r}$ with the periodicity of the lattice. For phenomena involving many cells of the crystal (and this is the case we consider throughout this paper), the spatial modulation can be ignored by replacing $M(\mathbf{r})$ by its mean value $\bar{M}$. It follows, then, that

$$\bar{M}(\mathbf{k}_i,\,\mathbf{k}_i) = (N+1)/\Omega, \qquad (3.16)$$

$$\bar{M}(\mathbf{k}_i,\,\mathbf{k}_i+\mathbf{q}) = (1/\Omega)\textstyle\sum_{\varkappa}\langle \mathbf{k}_i,\,s|a_{\varkappa}{}^{*}a_{\varkappa\,.\,\mathbf{q}}|\mathbf{k}_i+\mathbf{q},\,s\rangle, \qquad (3.17)$$

and the argument given above for the free electron case can be applied directly.

3.2. *Current and Effective Charge*

From fundamental quantum mechanical theory, we know that the current carried by a system of many particles is given by the expectation value of the operator

$$\sum_i \frac{e_i \mathbf{p}_i}{m_i}$$

which in the case of the electron gas is

$$\mathbf{J} = \left\langle \frac{e\mathbf{P}}{m} \right\rangle$$

where $\mathbf{P}$ is the total momentum operator. Thus in the case of a single quasi-particle the current is defined by

$$\mathbf{j}(\mathbf{k}) = \left\langle \mathbf{k} \left| \frac{e\mathbf{P}}{m} \right| \mathbf{k} \right\rangle. \qquad (3.18)$$

As already mentioned, we cannot expect $\mathbf{j}(\mathbf{k})$ and $e\mathbf{v}(\mathbf{k})$ to be equal. It is therefore convenient to introduce an effective charge $e^{*}(\mathbf{k})$ for the quasi-particle defined by

$$e^{*}(\mathbf{k}) = \frac{\mathbf{j}(\mathbf{k})}{\mathbf{v}(\mathbf{k})}, \qquad (3.19)$$

so that the charge e^{*} travelling with velocity $\mathbf{v}$ gives the correct current $\mathbf{j}$. We shall prove in the appendix, inter alia, that $\mathbf{v}$ and $\mathbf{j}$ are always parallel so that e^{*} is a scalar. The concept of an effective charge has also recently been developed by Stern (1960).

We shall now give a physical interpretation of e^{*} and show that if we form a wave packet, the actual number of electrons carried along by it is in fact e^{*}/e. Suppose we have a packet of δN electrons localized in space at a particular instant of time, say $t=0$. The particle density $\rho(\mathbf{r})$ is then as shown in fig. 11 (a). If we express the particle density as a Fourier series

$$\rho(\mathbf{r}) = \textstyle\sum_{\mathbf{q}} A(\mathbf{q})\,\exp(i\mathbf{q}\cdot\mathbf{r}),$$

then $A(\mathbf{q})$ is a continuous function of $\mathbf{q}$ at $\mathbf{q}=0$ and the number of electrons δN is given by

$$\delta N = \Omega A(0) = \lim_{\mathbf{q}\to 0} \Omega A(\mathbf{q}). \quad . \quad . \quad . \quad . \quad . \quad (3.20)$$

Suppose now we add a constant uniform electron density $(N+1-\delta N)/\Omega$. Then $\rho(\mathbf{r})$ becomes (fig. 11 *b*)

$$\rho(\mathbf{r}) = \frac{N+1-\delta N}{\Omega} + \sum_{\mathbf{q}} A(\mathbf{q}) \exp(i\mathbf{q}\cdot\mathbf{r}) \quad . \quad . \quad . \quad (3.21)$$

$$= \frac{N+1}{\Omega} + \sum_{\mathbf{q}}{}' A(\mathbf{q}) \exp(i\mathbf{q}\cdot\mathbf{r}), \quad . \quad . \quad . \quad . \quad (3.22)$$

Fig. 11

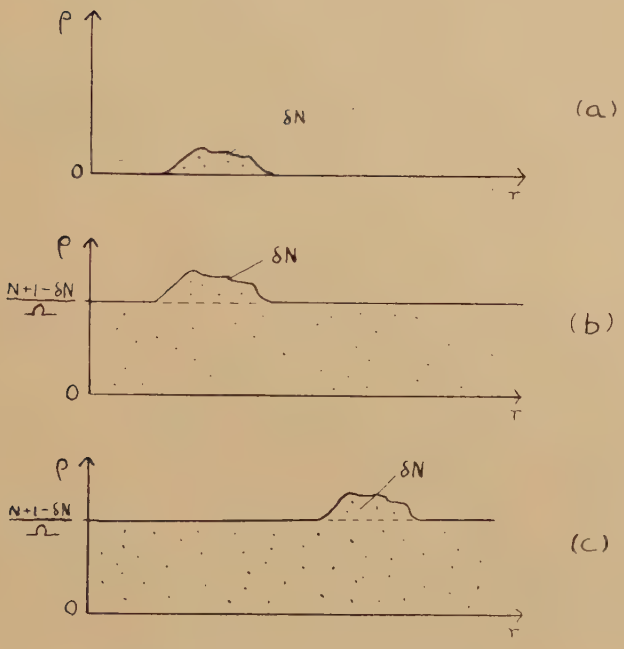

Particle density in a wave packet.

where $\sum'$ excludes the term $\mathbf{q}=0$. It is now clear what we must do to calculate the number of electrons δN transported by a quasi-particle. We already have in (3.13) the charge density for a one-quasi-particle wave packet, expressed (at any particular instant) in the form (3.22). In order to calculate the number of electrons δN localized in the bump of fig. 11 (*b*), we have to work back to the form (3.21) for $\rho(\mathbf{r})$, and thus we obtain

$$\delta N = \lim_{\mathbf{q}\to 0} \Omega \sum_{\mathbf{k}_i} \alpha^*(\mathbf{k}_i)\alpha(\mathbf{k}_i+\mathbf{q}) B(\mathbf{k}_i, \mathbf{k}_i+\mathbf{q}). \quad . \quad . \quad . \quad (3.23)$$

In the Apprendix this expression is evaluated and it is shown that it gives

$$\delta N = e^*(\mathbf{k}_i)/e$$

where e^* is defined by (3.19). Now as the wave packet travels with time (fig. 11 *c*), the charge transported is $e\,\delta N = e^*$ and the current is $j = e\,\delta N \mathbf{v} = e^*\mathbf{v}$ which is our interpretation of (3.19). In order to complete this interpretation of (3.19), we have to show in addition that the uniform background $\rho(\mathbf{r}) = (N + 1 - \delta N)/\Omega$ is in fact stationary and does not contribute to the current; this is also done in the Appendix.

In the free electron case, the perturbed state $|\mathbf{k}\rangle$ is still an eigenstate of the total momentum $\mathbf{P}$ since $\mathbf{P}$ commutes with the coulomb interaction, and the current from (3.18) is

$$\mathbf{j}(\mathbf{k}) = e\hbar\mathbf{k}/m. \quad . \quad . \quad . \quad . \quad . \quad . \quad . \quad . \quad (3.24)$$

The effective charge is therefore given by

$$e^*(\mathbf{k})/e = \frac{\hbar k}{mv} = \frac{\hbar^2 k}{m}\left(\frac{\partial \epsilon}{\partial k}\right)^{-1} . \quad . \quad . \quad . \quad . \quad . \quad . \quad (3.25)$$

Table 2 gives some values of $e^*(k_F)/e$ in the Bohm and Pines approximation, and we note they are considerably less than one. We expect a more realistic interaction to give values much nearer unity as discussed in § 5.

Table 2. The effective charge of quasi-particles at the Fermi level

r_s	$e^*(k_F)/e$	
0·2	0·98 (a)	
0·5	0·98 (a)	
2·0	0·87 (b)	0·90 (c)
3·0	0·88 (b)	0·92 (c)
4·0	0·90 (b)	0·95 (c)
5·0	0·93 (b)	0·96 (c)

(a) High-density limit.
(b) Bohm and Pines's approximation with $\beta = 0{\cdot}353 r_s^{1/2}$.
(c) Bohm and Pines's approximation with $\beta = 0{\cdot}4 r_s^{1/2}$.

3.3. *Acceleration in Applied Fields*

A single quasi-particle, which we may picture in terms of a wave packet, moving in an electric field $\mathscr{E}$ picks up an amount of energy

$$d\epsilon = e^*\mathscr{E}\cdot d\mathbf{r} = \mathscr{E}\cdot\mathbf{j}\,dt$$

where $\mathbf{j}$ is the current carried by it. Thus the acceleration in $\mathbf{k}$-space is given by

$$\dot{\mathbf{k}} = \frac{d\epsilon}{dt}\Big/\frac{\partial \epsilon}{\partial \mathbf{k}} = \frac{e^*\mathscr{E}\cdot\mathbf{v}}{\hbar v} = \frac{e^*\mathscr{E}}{\hbar} \quad . \quad . \quad . \quad . \quad . \quad (3.26)$$

In practice of course one always has multiple excitations, and it is much more difficult to calculate the acceleration then because some of the energy picked up by one quasi-particle goes into the interaction energy with the others. It is for this reason that we avoid any such attempt to calculate

the total acceleration in our derivation of transport coefficients, and use the method of § 1.3.4. We may use (3.26) as an aid to the imagination in guessing the *type* of multiple excitation relevant to a conduction process (not its *magnitude*) and this may be somewhat in error, but our method (1.20) of evaluating the resistivity from it is very closely related to the variational principle of transport theory as discussed in § 5, so that the errors in the answers are expected to be quite small.

By analogy with (3.26), we assume that the acceleration in a magnetic field is given by

$$\hbar\dot{\mathbf{k}} = (1/c)e^*\mathbf{v}\wedge\mathbf{H}. \quad . \quad . \quad . \quad . \quad . \quad . \quad . \quad . \quad (3.27)$$

Since the derivation of (3.26) was based on the conservation of energy, the same technique cannot be applied to the magnetic case. However, the e^* seems to be demanded in (3.27) by the macroscopic law of force $\mathbf{j}\wedge\mathbf{H}/c$. Also by the relativistic connection between electric and magnetic fields, we expect the same factor in (3.26) and (3.27) ; at least it would be difficult to justify the use of e instead of e^* in (3.27). We have set down these rather obvious remarks, because there is considerable uncertainty about the magnetic effects (§§ 4.6 and 5).

§ 4. 'Transport' Phenomena

We can now discuss those properties of a metal which depend only on excitations at the Fermi level. These include the electronic specific heat, paramagnetic spin susceptibility and de Haas–van Alphen effect, as well as most genuine transport processes. As already pointed out in § 1.3.4 the latter must be treated by the method of energy dissipation. Now most transport phenomena involve in an essential way the collision processes suffered by the electrons, and the general uncertainty about these is so large that it completely overshadows the kind of few per cent corrections which we are now discussing. Thus we shall restrict ourselves mostly to those effects which are directly related to the shape of the Fermi surface and the Fermi velocity, independent of the realxation time τ.

4.1. *Electronic Specific Heat*

Calculating the electronic specific heat is fundamentally a problem in statistical mechanics, for which we have to enumerate all the low-lying states of the system with their total energy, so that we have in principle to consider the energy corrections of § 1.3.4. Now at a temperature T we have of the order of $N\mathfrak{k}T/\epsilon_F$ excitations, i.e. a number of order N. In an overwhelming porportion of states, these excitations are more or less uniformly distributed round the Fermi surface with fluctuations of order $\sqrt{N}$. The total interaction energy (see eqn. (1.15))

$$E_2 = \sum\sum\eta(k_1, k_2)$$

is then zero because for every $\eta(k_1, k_2)$ between two electrons or two holes

there will be an η of opposite sign from an electron and a hole with practically the same k_1, k_2. Only the individual particle energy

$$E_1 = \sum \epsilon(\mathbf{k}_i) - \sum \epsilon(\mathbf{k}_\alpha)$$

contributes, and the electronic specific heat is the same as that given by the independent electron model, namely

$$C_{el} = \gamma T = \tfrac{1}{3}\pi^2 k^2 T \mathcal{N}(\epsilon_F). \quad . \quad . \quad . \quad . \quad . \quad . \quad (4.1)$$

Here

$$\mathcal{N}(\epsilon_F) = \frac{1}{4\pi^3}\int \frac{dS}{\partial\epsilon/\partial k_n} = \frac{1}{4\pi^3}\int \frac{dS}{\hbar v(\mathbf{k})} \quad . \quad . \quad . \quad . \quad (4.2)$$

is the usual density of single-excitation states at the Fermi level. The integrals are over the Fermi surface. This result was first pointed out by Landau (1956), and its validity has been verified by the more fundamental calculations mentioned in § 2.6. Although in our nomenclature there are no interaction corrections to the specific heat, it should be noted that (4.1) is not equal to the specific heat in the Sommerfeld model because the band structure $\epsilon(\mathbf{k})$ contains exchange and correlation terms which affect the value of (4.2). What we mean is that the result (4.1) is given correctly by applying independent-electron formulae to the quasi-particle band structure $\epsilon(\mathbf{k})$: we treat this band structure as the fundamental thing and the Sommerfeld model as a (convenient!) fiction of the mathematician's imagination, so that we are only incidentally interested in the deviations from the Sommerfeld values.

4.2. *Paramagnetic Spin Susceptibility*

By this we mean the susceptibility due to turning some electron spins over, independent of spin–orbit or orbital contributions. Because we are altering the number of electrons with given spin, the total exchange energy is altered and this affects the spin susceptibility, as has been pointed out for a long time (Sampson and Seitz 1940, Pines 1955). Here we analyse the effect systematically in terms of our picture of excitations at the Fermi level. We consider the multiple excitation of fig. 12 with n electron-like excitations with up spin just about the Fermi level, and the same number of holes with down spin† just below ϵ_F.

The electrons (holes) take up all states within an energy $\delta\epsilon$ of the Fermi level, where

$$\delta\epsilon = \frac{n}{\frac{1}{2}\mathcal{N}(\epsilon_F)\Omega}.$$

The one-particle contribution E_1 of (1.15) to the total energy is

$$E_1 = n\delta\epsilon = 2n^2/\mathcal{N}(\epsilon_F)\Omega.$$

† We define a down-spin hole-like excitation as one in which a down-spin electron has been removed, i.e. the system is left with a net up spin.

The interaction energy E_2 we write as

$$\begin{aligned} E_2 &= \tfrac{1}{2}\sum\sum\eta(\mathbf{k}_i\uparrow, \mathbf{k}_j\uparrow) + \tfrac{1}{2}\sum\sum\eta(\mathbf{k}_\alpha\downarrow, k_\beta\downarrow) \\ &\quad + \sum\sum\eta(\mathbf{k}_i\uparrow, \mathbf{k}_\alpha\downarrow) \\ &= -\nu E_1, \end{aligned}$$

where using (1.14) ν can be cast in the form

$$-\nu = \frac{2}{\mathscr{N}(\epsilon_F)}\frac{\Omega}{N}\frac{e^2}{r_s}\frac{1}{(2\pi)^6} \times \int\int \frac{dS}{\partial\epsilon/\partial k_n}\frac{dS'}{\partial\epsilon/\partial k_{n'}}[A(\mathbf{k}\uparrow, \mathbf{k}'\uparrow) + A(\mathbf{k}\uparrow, \mathbf{k}'\downarrow)]. \quad (4.3)$$

E_2 is negative, because $A(\uparrow\uparrow)$, consisting mostly of exchange energy, is negative and numerically larger than $A(\uparrow, \downarrow)$. Thus the total energy, including magnetic, is

$$E = \frac{2n^2(1-\nu)}{\mathscr{N}(\epsilon_F)\Omega} - 2n\mu_B H$$

where μ_B is the Bohr magneton. By minimizing E with respect to n at constant H, we calculate the susceptibility χ per unit volume as

$$\chi = n_{\min}/\Omega H = \mathscr{N}(\epsilon_F)\mu_B{}^2(1-\nu)^{-1}. \quad (4.4)$$

Fig. 12

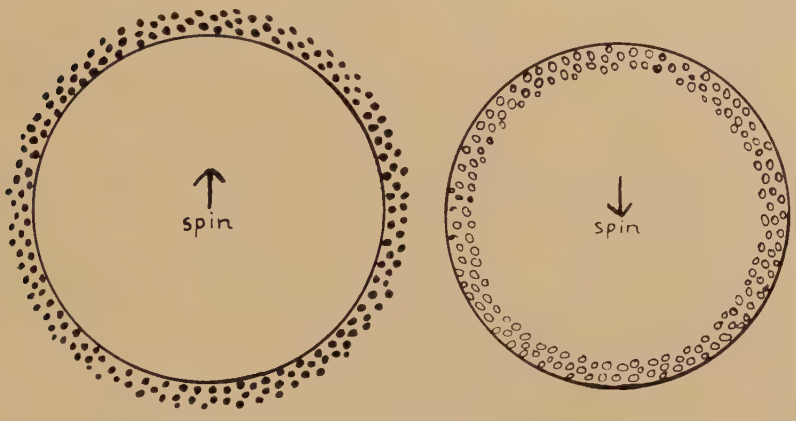

Multiple excitation produced by magnetic field.

The correction factor $(1-\nu)^{-1}$ is greater than unity because a negative E_2 makes it easier to turn spins over. Using the Bohm and Pines interaction for A, the factor is typically 1·2 to 1·5 (Pines 1955), but a more realistic interaction term would probably give values more like 1·1 to 1·2 as discussed in § 5.

Incidentally it should be noted that we give each excitation a magnetic moment of μ_B, not $(e^*/e)\mu_B$. The quasi-particle excitations were obtained in §1.2 by adding (subtracting) one electron to the system: it is irrelevant that only a fraction e^*/e of this gets localized if one forms a wave

packet, the rest being uniformly distributed over the system, because the susceptibility is a bulk property and both the localizable and non-localizable parts contribute to the total magnetic moment.

4.3. *Anomalous Skin Effect*

The surface impedance of a metal in the extreme anomalous limit is governed by the limiting value as $q \to \infty$ of the conductivity $\sigma(q)$ in a spatially varying electric field (Pippard 1960, eqns. (39) and (42))

$$\mathscr{E}_x(z) = \mathscr{E}_{0x} \exp(-iqz).$$

More precisely we consider wavelengths $1/q$ small compared with the mean free path l, but large compared with the interatomic spacing so that the electric field does not see just the bare electron but the whole quasi-particle including all the correlation and exchange hole.

Fig. 13

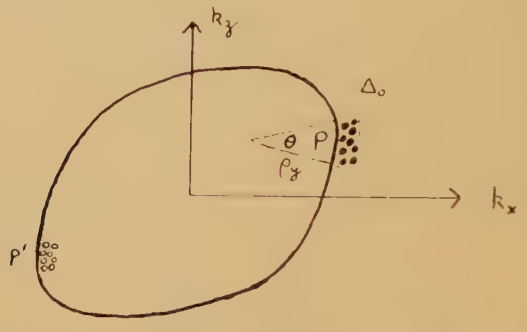

Excitation of Fermi surface in anomalous skin effect.

The displacement of the Fermi surface at any point on the surface is (Pippard 1960, eqn. (15))

$$\Delta(\mathbf{k}) = \frac{(1/\hbar)\tau e^*(\mathbf{k})\mathscr{E}_x}{1 - iq\tau v_z(\mathbf{k})}. \qquad (4.5)$$

For large ql (4.5) is large only over an angular range of order θ,

$$\frac{v_z}{v} \sim \theta = \frac{1}{ql},$$

around the positions P, P′, where $v_z(\mathbf{k}) = 0$. Physically, only those electrons moving nearly parallel to the surface contribute much to the current, and this defines an effective zone PP′ (fig. 13) round the Fermi surface.

We proceed to calculate the constants α and β in (1.20). Consider the total energy (1.15), and let us for a moment idealize (4.5) slightly as (fig. 13)

$$\Delta(\mathbf{k}) = \Delta_0, \quad |v_z/v| < \theta,$$
$$= 0, \quad |v_z/v| > \theta.$$

The one-particle energy is approximately

$$E_1 \approx (1/4\pi^3)\int \tfrac{1}{2}[\epsilon(\mathbf{k})_{\max} - \epsilon_F]\Delta_0\rho_y 2\theta\, dk_y$$
$$= (1/4\pi^3)\int (\partial\epsilon/\partial k_x)\rho_y(\Delta_0{}^2/ql)dk_y$$
$$= O(ql)^{-1}$$

The interaction energy is

$$E_2 \approx (1/16\pi^6)\int\int \eta(\mathbf{k}, \mathbf{k}')(\Delta_0\rho_y 2\theta\, dk_y)(\Delta_0{}'\rho_y{}' 2\theta\, dk_y{}')$$
$$= O(ql)^{-2}.$$

Thus in the limit $ql \to \infty$, E_2 is negligible compared with E_1, and it can easily be verified that this applies also with the correct displacement (3.5). We could now continue to evaluate (1.20). However, since the interaction energy E_2 is negligible, the correct answer must be given by the usual independent-particle analysis provided we give the quasi-particles the correct charge $e^*(\mathbf{k})$. The argument of Pippard can easily be modified in this way, and we obtain the surface impedance Z_∞ for diffuse surface reflection (Pippard 1960, eqns. (16) and (42))

$$\left.\begin{aligned} Z_\infty &= \frac{\sqrt{3}\pi\omega}{s}(1+\sqrt{3}i), \\ s^3 &= \frac{\omega}{\pi\hbar}\int [e^*(\mathbf{k})]^2|\rho_y|\, dk_y, \end{aligned}\right\} \quad . \quad . \quad (4.6)$$

where ρ_y is the radius of curvature at the effective point P in the section $k_y = \text{const}$ (fig. 13). Alternatively we can derive the same result using (1.20).

4.4. *Electrical Resistivity*

We have already derived in principle a formula for the d.c. resistivity R in § 1.3.4 and it only remains to express the energy factor α and the current factor β in (1.20) as integrals over the Fermi surface. As in § 4.3, the acceleration of a quasi-particle is proportional to $e_{\mathbf{k}}{}^*$, and the multiple excitation corresponds to a sideways shift of $(e_{\mathbf{k}}{}^*/e)\Delta$ at each point of the Fermi surface in the direction of the electric field where Δ is now a constant. The total energy and current are then expressed as integrals over the Fermi surface. We shall not write down the explicit results, since the methods have already been illustrated in §§ 4.2 and 4.3 and the assumption of a constant relaxation time is so crude as to rob the results of any valid application. In § 5 we shall discuss taking an arbitrary collision integral into account.

However, it is interesting to analyse the case of free electrons further. By 'free electrons' we mean electrons with coulomb interaction but without an external periodic potential. In this case the total force on the electron

gas in a field $\mathscr{E}$ is $Ne\mathscr{E}$. the acceleration of the centre of mass $Ne\mathscr{E}/Nm$, and the rate of increase of current

$$\left(\frac{dJ}{dt}\right)_{\text{accel}} = \frac{Ne\mathscr{E}}{Nm} Ne$$

At equilibrium this has to equal

$$-\left(\frac{dJ}{dt}\right)_{\text{collisions}} = \frac{J}{\tau}$$

and we obtain for the resistivity R

$$R = \frac{\mathscr{E}}{J} = \frac{m}{Ne^2\tau}. \qquad \ldots\ldots\ldots \quad (4.7)$$

This formula is therefore valid in the presence of coulomb interactions and does not depend on the kind of kinetic arguments found in most books. We shall now verify that it follows from (1.20) in our formalism. The electric field exerts the same force $e\mathscr{E}$ on each electron so that the whole system is accelerated without altering the *relative* motion of the electrons. Now the total energy E can be written, in quantum as in classical mechanics. $E = E$ (motion of centre of mass) $+ E$ (motion relative to centre of mass). We therefore have

$$E = P^2/2Nm + E_G, \qquad (4.8)$$

where E_G is the ground-state energy and P the total momentum. Also (§ 3.2)

$$J = (e/m)P, \qquad \ldots\ldots\ldots \quad (4.9)$$

and from (1.16), (1.17), (1.20) we recover (4.7).

Since (4.7) is also the result for the Sommerfeld model, does this mean the resistivity involves no interaction corrections? No it does not. By 'corrections' in the context of this paper we mean corrections to the results obtained by applying the independent electron calculations to the band structure $\epsilon(\mathbf{k})$ of the quasi-particles. This is the band structure which for instance is relevant to the electronic specific heat as shown in § 4.1 and includes exchange and correlation energy $\epsilon_{ec}(\mathbf{k})$; in our case

$$\epsilon(\mathbf{k}) = \hbar^2k^2/2m + \epsilon_{ec}(\mathbf{k}). \qquad \ldots\ldots \quad (4.10)$$

Now in calculating the energy of the current carrying state, it is essential to include the interaction energy E_2 of (1.15) because it exactly cancels off the contribution of $\epsilon_{ec}(\mathbf{k})$ to the one particle energy E_1, as can easily be shown in a general way. We obtain

$$\begin{aligned} E &= E_1 + E_2 \\ &= (\hbar^2/2m)[\textstyle\sum k_i^2 - \sum k_\alpha^2] \end{aligned}$$

which is equivalent to (4.8). Similarly in calculating the current, we have $v(\mathbf{k}) \neq \hbar k/m$ and $e^*(k) \neq e$ because of $\epsilon_{ec}(\mathbf{k})$, but taking the product $e^*(\mathbf{k})v(\mathbf{k})$ restores the simple result (4.9) as discussed in § 3.2.

With more complicated band structures, similar cancellations will occur so that it might well be sensible to analyse data in terms of the independent electron model using a bogus band structure $\epsilon'(\mathbf{k})$ which has the correct Fermi surface but has $\partial\epsilon'/\partial\mathbf{k}$ adjusted in a way that corresponds to dropping ϵ_{ec} from (4.10).

4.5. *Cyclotron Resonance*

In a metal, cyclotron resonance is usually observed with the magnetic field H parallel to the surface and the skin depth very small compared with the orbit radius (Pippard 1960). The quasi-particles are accelerated each time they come within the skin depth, and the resonant frequency is determined by the time taken to complete one revolution. The acceleration in **k**-space is

$$\dot{\mathbf{k}} = \frac{e^*(\mathbf{k})}{\hbar c}\,\mathbf{v}(\mathbf{k})\wedge\mathbf{H}. \qquad (4.11)$$

Our reasons for including e^* in this are given in § 3.3. The motion of the representative point **k** is perpendicular to $\mathbf{v}(\mathbf{k})$ and to **H**, i.e. along an energy contour in a plane perpendicular to H. The time taken to traverse an element $d\mathbf{k}$ is $\hbar c d\mathbf{k}/e^* v_\perp H$ where $v_\perp$ is the component of **v** perpendicular to H, and the periodic time of the orbit

$$\frac{\hbar c}{H}\oint\frac{dk}{e^* v_\perp}.$$

The cyclotron frequency is therefore

$$\omega_c = \frac{2\pi H}{\hbar c}\left[\oint\frac{d\mathbf{k}}{e^*(\mathbf{k})v_\perp(\mathbf{k})}\right]^{-1} \qquad (4.12)$$

where the integral is taken round a section of the Fermi surface perpendicular to **H**. There are no interaction energy corrections to this, because the acceleration in the field is determined by the current $j = e^* v$ and there are no interaction corrections to the current as shown in § 1.3.5. As it stands expressed in terms of the band structure, (4.12) involves e^* rather than e, but for free electrons (with coulomb interactions) it reduces to the Sommerfeld value $\omega_c = eH/mc$ on account of (3.25) as we might have deduced also by general arguments similar to those in § 4.4.

4.6. *De Haas–van Alphen Effect*

In a magnetic field, various properties including the diamagnetic susceptibility oscillate with constant period in $1/H$. In the usual independent-electron model, the quantized electron orbits are given by (Pippard 1960, eqns. (11) and (25))

$$\mathscr{A} = (n+\phi)2\pi eH/\hbar, \qquad (4.13)$$

and the period of the oscillations by

$$\Delta(1/H) = \frac{2\pi e}{\hbar\mathscr{A}_0}. \qquad (4.14)$$

Here $\mathscr{A}$ is the area of the orbit in k-space, $\mathscr{A}_0$ the extreme cross section of

the Fermi surface perpendicular to H, n and integer, and ϕ a phase factor. Unfortunately there appears to be no plausible way of modifying this analysis to take account of an effective charge: even assuming e^* is a constant, we cannot with any conviction simply replace e by e^* in (4.13), (4.14).

Let us therefore consider a different approach. The first question is: is the de Haas–van Alphen effect essentially a property of the whole ground state, or can we hope to discuss it by quantizing the excitations at the Fermi level? Although at first sight it would appear to be a ground-state property, two reasons suggest it may be correct to analyse it in terms of our excitations. Firstly in the independent electron model all the electrons are quantized according to (4.13), but for electrons well inside the Fermi surface this only amounts to a unitary transformation which does not affect the whole wave function, and just the quantization at the Fermi level is significant. Secondly, if we think of the temperature variation of the de Haas–van Alphen effect or the specific heat rather than the de Haas-van Alphen effect itself, it seems clear that the period is governed by the availability of quantized states for the thermally excited quasi-particles at the Fermi surface.

We must therefore quantize the orbits of the quasi-particles. We have already derived in (4.12) the cyclotron frequency ω_c of revolution. Now from the correspondence principle, we expect the semi-classical absorption of energy in cyclotron resonance described in § 4.5 to be equivalent to the jumping of quasi-particles to higher levels: i.e. we expect $\hbar\omega_c$ to equal the difference in energy between successive quantized levels, as is indeed the case in the independent electron theory (Pippard 1960, p. 193). This immediately implies that there should be some e^* correction to the de Haas–van Alphen period, for if we quantize the orbits according to (4.13), the energy difference between successive levels as measured by $\epsilon(\mathbf{k})$ is *not* $\hbar\omega_c$ (4.12). We therefore look for a generalization of (4.13) which does give $\hbar\omega_c$ (4.12) for the difference between levels. If we assume $e^*(\mathbf{k})$ to be independent of energy $\epsilon(\mathbf{k})$ at each point on the Fermi surface but varying over the Fermi surface, we easily find

$$\frac{1}{2}\oint \frac{\mathbf{k}\wedge d\mathbf{k}}{e^*(\mathbf{k})} = (n+\phi)2\pi H/\hbar \quad . \quad . \quad . \quad . \quad . \quad (4.15)$$

which gives for the period

$$\Delta(1/H) = \frac{2\pi}{\hbar}\left[\frac{1}{2}\oint \frac{\mathbf{k}\wedge d\mathbf{k}}{e^*}\right]^{-1}_{\text{ext}} \quad . \quad . \quad . \quad . \quad . \quad (4.16)$$

However, in general e^* does vary with ϵ, and there does not seem to be a general formula for the quantized orbits which when differentiated with respect to ϵ gives (4.12); for such a formula would have to contain e^* to get e^* into (4.12) and thus would at the same time give terms in $\partial e^*/\partial e$. We can only state that the period should involve some e^*/e correction.

Clearly the chain of reasoning is somewhat tenuous, and we must report that Luttinger (1960) profoundly disagrees with our result. His results

on the oscillations in the specific heat and the work of Idrimura and Tanaka (private communication) on the de Haas–van Alphen effect, indicate that the period is correctly given by (4.14) without any e^* correction. It is not easy to see how this squares with the correspondence principle, as already discussed.

4.7. *Ultrasonic Attenuation*

The ultrasonic attenuation shows oscillations in a magnetic field when successive wave fronts of the ultrasonics measure the size of the quasi-particle orbits like a pair of calipers (Pippard 1960). In the case of constant e^*, the sections of the Fermi surface have the same shape as the orbits in real space, but are larger by a factor $e^*H/\hbar$ and rotated through $\pi/2$, so that the ultrasonic oscillations enable the shape of the Fermi surface to be studied, but a factor e^*/e is involved in the absolute size. If e^* varies over the Fermi surface, the relation between the orbits in $\mathbf{k}$-space and real space breaks down and no general relation seems possible.

The 'fork', 'tilt' or "surf riding" effect (Reneker 1959, Spector 1960) on the other hand measures the Fermi velocity directly

$$v_s = v(Q)\cos\phi$$

were v_s is the ultrasonic velocity, ϕ the critical angle between its direction of propagation and H, and $v(Q)$ is the Fermi velocity at the point Q on the Fermi surface where the velocity is parallel to $\mathbf{H}$.

§ 5. Summary, Discussion and Comparison with Experiment

In §§ 1 and 2 we have described the low-energy excited states of an electron gas in terms of electron-like and hole-like excitations, where these quasi-particles have a well-defined band structure $\epsilon(\mathbf{k})$ near a sharp Fermi surface given by $\epsilon(\mathbf{k}) = \epsilon_F$. For a free electron gas this model seems to be on a sound basis. In the presence of a periodic potential the existence of such excitations has not been proved yet, but it is difficult to believe that the same general picture does not apply because of the experimental evidence (§ 1.1) as well as physical reasonableness. An important property of the quasi-particles is that they carry a charge $e^*(\mathbf{k})$ which is not equal to the bare electronic charge e (§ 3). They also have a long lifetime which tends to infinity at the Fermi surface. Thus in discussing transport phenomena, we assume that a given transport process produces a multiple excitation of the system which can be represented by a certain distribution of quasi-particles, as shown for instance in fig. 1 for a uniform electric field. It has not been proved that the electric field acting on the whole system really produces a state like this. However, such states form semi-stationary states of the system with a long lifetime, so that if something different were produced by the electric field it would rapidly decay into the semi-stationary states. In any case, a multiple excitation of the form of fig. 1 would appear to be demanded by the way the quasi-particles are accelerated in the field, though it is a little obscure how the electric field

creates the elementary excitations in the first place. In fact the validity of our whole model needs verifying by more fundamental and rigorous calculations of particular properties.

We have therefore a description of the electron system in terms of a gas of quasi-particles. Under almost all conditions the density of quasi-particles is low, of order $kT/\epsilon \sim 10^{-2}$ times the electron density. For this reason they can be treated to a first approximation as independent. However, there is a screened coulomb repulsion energy between them, and the consequent interaction energy makes a significant contribution to any process involving energy balance or transfer, e.g. the rate of Joule heating in d.c. conduction (§ 1.3.4). The interaction also leads to a certain amount of scattering which can contribute to the electrical and thermal resistivities (§ 1.3.2).

In order to focus attention on the role of the energy, electrical resistances are calculated from the rate of dissipation of energy as Joule heat. The method of § 1.3.4 is limited by the assumption of a constant relaxation time τ. It is also physically oversimplified in that the primary mechanism destroying the current is usually elastic collisions which themselves do not dissipate the energy. The correct thing is to calculate the rate of entropy production by the primary collisions: in the steady state this entropy is passed around among the electrons before it finally appears in the lattice as heat. With this modification, our method becomes identical with the method of general transport theory based on a variational principle (Ziman 1960, p. 283). We see now that in order to take a general collision process into account, we only need a formula for the entropy of a given multiple-excitation including interaction energy to replace eqns. (7.8.4) to (7.8.6) of Ziman (1960).

Something must be said now about the size of effects described. Unfortunately experimental data are meagre and detailed calculations have only been made for the Bohm and Pines interaction (2.35). Consider first e^*/e. The values calculated for a free electron gas with the Bohm and Pines interaction have already been given in table 2, and we note for example for $r_s = 3$ (corresponding approximately to copper) that $e^*/e = 0{\cdot}88$. However, we expect that the Bohm and Pines interaction overestimates the effect considerably, and that the smoother (and more realistic) interactions shown in fig. 9 will give values of e^*/e much nearer unity. The difference between $\hbar k_{\mathrm{F}}/m$ and v_{F} comes from the rate of change of the exchange energy in $\epsilon(\mathbf{k})$ with k: an interaction which is a constant in $\mathbf{k}$-space would give $e^*/e = 1$. To obtain a rough estimate of the effect, let us write for the mean value and the fluctuation of the interaction

$$\left.\begin{aligned} V_{\mathrm{BP}} &= 0{\cdot}6 \pm 0{\cdot}4, \\ V_{\text{best estimate}}(k) &= 0{\cdot}3 \pm 0{\cdot}1 \end{aligned}\right\}, \qquad \ldots \quad (5.1)$$

where the units and V(best estimate) are those of fig. 9. Since e^*/e depends on the fluctuation of $V(k)$, we expect $V_{\mathrm{BP}}(k)$ to overestimate $(e^*/e) - 1$ by a factor of say 4, and a more realistic estimate is $e^*/e \approx 0{\cdot}97$

As regards the sign of $(e^*/e)-1$, ordinarily we expect the exchange energy to decrease as one goes to higher energy away from the Fermi surface, which gives $e^*/e<1$. However, in real metals with complicated band structure effects, the possibility of $e^*/e>1$ may not be completely ruled out. Experimentally the only measurements at present which allow us to determine e^* appear to be those on the anomalous skin effect in copper and silver. The measurements (Pippard 1957, Morton 1960) were analysed using (4.6) with e^* put equal to e. The apparent Fermi surface obtained in this way should therefore have a volume containing $(e^*/e)^3$ instead of one electron per atom, if as a first approximation we assume e^* is constant over the Fermi surface. Experimentally the volumes of the apparent Fermi surfaces were $1{\cdot}00\pm12\%$ (copper) and $0{\cdot}95\pm9\%$ (silver) electrons per atom. The results are therefore:

$$\text{For copper} \quad e^*/e=1{\cdot}00\pm0{\cdot}04,$$

$$\text{For silver} \quad e^*/e=0{\cdot}98\pm0{\cdot}03.$$

Thus the data are consistent with $e^*/e\approx0{\cdot}97$ but do not give any proof that $e^*/e\neq1$.

A comparison of (4.1) and (4.4) shows that a value for the correction factor $(1-\nu)^{-1}$ may be obtained directly from measurements of the electronic specific heat and spin susceptibility:

$$\frac{\chi}{\gamma}=\frac{{\mu_B}^2}{\frac{1}{3}\pi^2\hbar^2}(1-\nu)^{-1}.$$

We use the data on sodium from Schumacher and Slichter (1956) for χ and two recent measurements of γ by Gaumer and Heer (1969) and Lien and Phillips (1960), giving

$$(1-\nu)^{-1}=1{\cdot}20 \quad \text{(using Gaumer and Heer)},$$

$$=1{\cdot}10 \quad \text{(using Lien and Phillips)}.$$

The difference between these may be taken as an indication of the probable error, largely due perhaps to the partial phase transformation at low temperatures. The value given by the Bohm and Pines theory is 1·48: because of the double integration over the Fermi surface in (4.3), the value is more sensitive to the mean strength of the interaction than to its variation with k and we conclude from (5.1) that V_{BP} overestimates the effect by a factor of say 2, giving a more realistic estimate of $(1-\nu)^{-1}\approx1{\cdot}24$ which is more nearly in agreement with experiment.

Finally we turn to what is probably the greatest gap in the theory at present. Although the acceleration of the quasi-particles in an electric field appears to be correctly given—the theory is certainly self-consistent—uncertainties remain about the motion in a magnetic field, particularly as regards the de Haas–van Alphen effect. We have not been able to resolve theoretically whether or not the de Haas–van Alphen period should contain a correction factor involving e^*/e. The experimental data are analysed using (4.14). Assuming (4.16) to be correct, this would give an apparent Fermi surface containing $(e^*/e)^{-3/2}$ electrons per atom for a

monovalent metal. Experimentally Shoenberg (1960) finds the periods of the 'belly' orbits in copper to be consistently less than calculated for free electrons, giving the total volume of the apparent Fermi surface to be about $5\% \pm 1\frac{1}{2}\%$ too high. Allowing for the volume of the 'necks' would only increase this further. Thus if we assume there is no fundamental error in the calibration of the measurements, we would conclude firstly that the de Haas–van Alphen period does indeed contain a correction factor of e^*/e and secondly that $e^*/e \approx 0{\cdot}97 \pm 0{\cdot}01$ for copper.

Acknowledgments

We are indebted to many people for discussions over several years particularly Professor N. F. Mott, F.R.S. for originally focusing our attention on the problem, Professor L. van Hove for pointing out the significance of the work of Hugenholtz, and Professor A. B. Pippard, F.R.S. for many penetrating comments. Recently we have profited from the papers presented by Professor J. M. Luttinger and Professor E. A. Stern at the Conference on the Fermi Surfaces of Metals, and from the lively discussions there (Conference Report, to be published). One of us (L.M.F.) is indebted to the Buenos Aires University for a scholarship during the tenure of which this work was carried out.

APPENDIX

From (3.23) the number of electrons travelling in one quasi-particle is

$$\delta N = \Omega \lim_{\mathbf{q}\to 0} \sum_{\mathbf{k}i} \alpha^*(\mathbf{k}_i)\alpha(\mathbf{k}_i+\mathbf{q})B(\mathbf{k}_i, \mathbf{k}_i+\mathbf{q}) \quad . \quad . \quad . \quad \text{(A 1)}$$

where the symbols are defined in § 3.1. In this expression $\alpha(\mathbf{k}_i+\mathbf{q})$ can be chosen to be continuous and we can therefore put

$$\lim_{\mathbf{q}\to 0} \alpha(\mathbf{k}_i+\mathbf{q}) = \alpha(\mathbf{k}_i),$$

and $B(\mathbf{k}_i, \mathbf{k}_i+\mathbf{q})$ is a continuous function of $\mathbf{k}_i$ as can easily be seen from its definition. Due to the small region in which $\alpha(\mathbf{k}_i)$ is defined, we can take the value $B(\mathbf{k}_i, \mathbf{k}_i+\mathbf{q}) = B(\mathbf{k}_0, \mathbf{k}_0+\mathbf{q})$ and assume it is constant over the small volume in $\mathbf{k}$-space where $\alpha(\mathbf{k}_i) \neq 0$. Using (3.7) for the normalization of the wave packet, (A 1) is transformed into

$$\delta N = \Omega \lim_{\mathbf{q}\to 0} B(\mathbf{k}_0, \mathbf{k}_0+\mathbf{q}) \quad . \quad . \quad . \quad . \quad . \quad \text{(A.2)}$$

which is the limit we now evaluate. It is not incidentally equal to $B(\mathbf{k}_0, \mathbf{k}_0)$ which is just the mean density $N(+1)\,\Omega$. There is a genuine discontinuity in this function at $\mathbf{q}=0$. To calculate the limit we study the commutator

$$\Delta^{\mathrm{op}} = \rho^{\mathrm{op}}\mathscr{H} - \mathscr{H}\rho^{\mathrm{ob}}, \quad . \quad . \quad . \quad . \quad . \quad . \quad \text{(A 3)}$$

where ρ^{op} is given by (3.5) and $\mathscr{H}$ by (2.1). Using the usual anticommutation relations of the operators $a_{\mathbf{k}}^*$, $a_{\mathbf{k}}$, it follows after a long but straightforward calculation

$$\Delta^{\mathrm{op}} = \frac{\hbar^2}{m\Omega} \sum_{\boldsymbol{\varkappa},\, \mathbf{q}} \{\boldsymbol{\varkappa}\,.\,\mathbf{q} + \tfrac{1}{2}\mathbf{q}^2\} a_{\boldsymbol{\varkappa}}^* a_{\boldsymbol{\varkappa}+\mathbf{q}} \exp(i\mathbf{q}\,.\,\mathbf{r}). \quad . \quad . \quad \text{(A 4)}$$

We now use the definition (A3) and assume that $\mathbf{k}_i$ is sufficiently near the Fermi surface that we can treat $|\mathbf{k}_i\rangle$ as an eigenvector of $\mathscr{H}$:

$$\begin{aligned}\langle \mathbf{k}_0, t|\Delta_{\mathrm{op}}|\mathbf{k}_0+\mathbf{q}, t\rangle &= [\epsilon(\mathbf{k}_0+\mathbf{q}) - \epsilon(\mathbf{k}_0)]\rho_{\mathbf{k}0,\ \mathbf{k}0+\mathbf{q}} \\ &= \frac{\hbar^2}{m\Omega} \exp(i\mathbf{q}\,.\,\mathbf{r}) \sum_{\boldsymbol{\varkappa}} \{\boldsymbol{\varkappa}\,.\,\mathbf{q} + \tfrac{1}{2}\mathbf{q}^2\} \langle \mathbf{k}_0, t|a_{\boldsymbol{\varkappa}}^* a_{\boldsymbol{\varkappa}+\mathbf{q}}|\mathbf{k}_0+\mathbf{q}, t\rangle. \\ &\quad . \quad . \quad . \quad . \quad . \quad \text{(4 5)}\end{aligned}$$

Taking $\mathbf{q} \neq 0$ and using the Taylor expansion for $\epsilon(\mathbf{k}_0+\mathbf{q})$ as well as the definition (3.11), (3.12) of $B(\mathbf{k}_0, \mathbf{k}_0+\mathbf{q})$, (A 5) reduces to

$$\begin{aligned}&\mathbf{q}\left\{\left(\frac{\partial\epsilon}{\partial\mathbf{k}}\right)_{\mathbf{k}0} + \tfrac{1}{2}\left(\frac{\partial^2\epsilon}{\partial\mathbf{k}\partial\mathbf{k}}\right)_{\mathbf{k}0} \mathbf{q} + \ldots\right\} B(\mathbf{k}_0, \mathbf{k}_0+\mathbf{q}) \\ &\quad = \mathbf{q}\left\{\frac{\hbar^2}{m\Omega} \sum_{\boldsymbol{\varkappa}} \boldsymbol{\varkappa}\langle \mathbf{k}_0|a_{\boldsymbol{\varkappa}}^* a_{\boldsymbol{\varkappa}+\mathbf{q}}|\mathbf{k}_0+\mathbf{q}\rangle + \tfrac{1}{2}\mathbf{q}B(\mathbf{k}_0, \mathbf{k}_0+\mathbf{q})\right\}, \quad \text{(A 6)}\end{aligned}$$

and from this, using (3.2) and (A 2)

$$\begin{aligned}&\mathbf{v}(\mathbf{k}_0)\delta N \\ &\quad = \lim_{\mathbf{q}\to 0} (\hbar/m) \sum_{\boldsymbol{\varkappa}} \boldsymbol{\varkappa}\langle \mathbf{k}_0|a_{\boldsymbol{\varkappa}}^* a_{\boldsymbol{\varkappa}+\mathbf{q}}|\mathbf{k}_0+\mathbf{q}\rangle. \quad . \quad . \quad . \quad \text{(A 7)}\end{aligned}$$

It is lengthy but not difficult to prove that the function on the right-hand side is continuous for $\mathbf{q} = 0$ so that the limit is simply given by putting $\mathbf{q} = 0$. One way of proving the continuity is by expanding $|\mathbf{k}_0\rangle$ in the perturbation series

$$|\mathbf{k}_0\rangle = A'|\mathbf{k}_0) + \sum A''(\mathbf{k}_i, \mathbf{k}_\kappa)|\mathbf{k}_i, \mathbf{k}_0 - \mathbf{k}_i + \mathbf{k}_\alpha;\ \mathbf{k}_\alpha) + \ldots \quad . \quad \text{(A 8)}$$

and similarly for $|\mathbf{k}_0+\mathbf{q}\rangle$. Evaluating the right-hand side of (A 7) we see that crossed terms (due to matrix elements between unperturbed states with different number of quasi-particles) are all at least proportional to $\mathbf{q}$, and terms coming from matrix elements between states of equal number of quasi-particles can be expressed as

$$(1/m)\langle \mathbf{k}_0|\mathbf{P}|\mathbf{k}_0\rangle + \mathrm{O}(\mathbf{q}), \quad . \quad . \quad . \quad . \quad . \quad . \quad \text{(A 9)}$$

where $\mathbf{P}$ is the momentum operator

$$\mathbf{P} = \hbar \sum_{\boldsymbol{\varkappa}} \boldsymbol{\varkappa} a_{\boldsymbol{\varkappa}}^* a_{\boldsymbol{\varkappa}}. \quad . \quad . \quad . \quad . \quad . \quad \text{(A 10)}$$

Thus in the limit as $\mathbf{q} \to 0$, we obtain from (A 7)

$$\mathbf{v}(\mathbf{k}_0)\delta N = (1/m)\langle \mathbf{k}_0|\mathbf{P}|\mathbf{k}_0\rangle, \quad . \quad . \quad . \quad . \quad . \quad . \quad \text{(A 11)}$$

which proves that $\mathbf{v}$ is parallel to $\langle \mathbf{P}\rangle$, and by comparison with (3.18), (3.19) that $\delta N = e^*/e$.

Similarly to prove that the background gives no contribution to the current, we evaluate the expectation value of the current density operated for the wave packet (3.6):

$$\mathbf{J}(\mathbf{r}, t) = \langle \mathbf{k}_0, \alpha, t | \mathbf{J}^{\mathrm{op}}(\mathbf{r}) | \mathbf{k}_0, \alpha, t \rangle \quad . \quad . \quad . \quad . \quad . \quad . \quad \text{(A 12)}$$

$$\mathbf{J}^{\mathrm{op}}(\mathbf{r}) = \frac{he}{m\Omega} \sum_{\varkappa, \mathbf{q}} \varkappa a_{\varkappa}^{*} a_{\varkappa + \mathbf{q}} \exp(i\mathbf{q} \cdot \mathbf{r}). \quad . \quad . \quad . \quad \text{(A 13)}$$

We obtain

$$\mathbf{J}(\mathbf{r}, t) = \sum_{\mathbf{k}i, \mathbf{k}j} \alpha^{*}(\mathbf{k}_i) \alpha(\mathbf{k}_j) J_{\mathbf{k}i, \mathbf{k}j} \quad . \quad . \quad . \quad . \quad . \quad \text{(A 14)}$$

$$J_{\mathbf{k}i, \mathbf{k}i + \mathbf{q}} = \frac{he}{m\Omega} \exp i\mathbf{q}[\mathbf{r} - \mathbf{v}(\mathbf{k}_i)t] \times \sum_{\varkappa} \varkappa \langle \mathbf{k}_i | a_{\varkappa}^{*} a_{\varkappa + \mathbf{q}} | \mathbf{k}_i + \mathbf{q} \rangle. \quad . \quad . \quad . \quad . \quad . \quad \text{(A 15)}$$

We have proved before that the summation on the right-hand side of (A 15) is a continuous function of $\mathbf{q}$. Consequently the coefficients of the Fourier series (A 14), (A 15) are continuous for the value $\mathbf{q} = 0$ and the current density packet represented by (A 14) is completely localized and similar to fig. 11 (*a*). Therefore no contribution to the total current comes from the background and the spatial transference of charge is only made by the localized quasi-particle.

References

Abrahams, E., 1954, *Phys. Rev.*, **95,** 839.

Baber, W. S., 1937, *Proc. roy. Soc.* A, **158,** 383.

Bloch, C., and de Dominicis, C., 1958, *Nuclear Physics*, **1,** 459.

Brueckner, K. A., 1958, *The Many Body Problem*, Cours donnés à l'Ecole de Physique Theorique, Les Houches (London : Methuen), 47, 164.

Brueckner K. A., and Sawada, K., 1958, *Phys. Rev.*, **112,** 328.

Chen C. S., and Chow S. H., 1958, *J. exp. theor. Phys., Moscow*, **34,** 1566. Translation : *Soviet Physics J.E.T.P.*, **7,** 1080.

Feynman, R. P., 1949, *Phys. Rev.*, **76,** 749.

Fletcher, J. G., and Larson, D. C., 1958, *Phys. Rev.*, **111,** 455.

Gaumer, R. E., and Heer, C. V., 1960, *Phys. Rev.*, **118,** 955.

Gell-Mann, M., 1957, *Phys. Rev.*, **106,** 369.

Gell-Mann, M., and Brueckner, K. A., 1957, *Phys. Rev.*, **106,** 364.

Gell-Mann, M., and Low, F., 1951, *Phys. Rev.*, **84,** 350 (Appendix).

Goldstone, J., 1957, *Proc. roy. Soc.* A, **239,** 267.

Heine, V., 1960, *Group Theory in Quantum Mechanics* (London : Pergamon Press).

Herring, C., 1960, *J. appl. Phys.*, **31,** *Suppl.*, 35.

Hubbard, J., 1957, *Proc. roy. Soc.* A, **240,** 539; 1958 a, *Ibid.*, **243,** 336 ; 1958 b, *Ibid.*, **244,** 199.

Hugenholtz, H. M., 1957, *Physica*, **23,** 481; 1958, *The Many Body Problem*, Cours donnés a l'Ecole de Physique Theorique, Les Houches (London : Methuen), 1.

Hugenholtz, N. M., and Van Hove, L., 1958, *Physica*, **24,** 363.

Kittel, C., 1956, *Introduction to Solid State Physics* (New York : Wiley).

Kohn, W., and Luttinger, J. M., 1960, *Phys. Rev.*, **118,** 41.

Landau, L. D., 1956, *J. exp. theor. Phys., Moscow*, **30,** 1058. Translation : *Soviet Physics J.E.T.P.*, **3,** 920 (1957).

Landsberg, P. T., 1949, *Proc. phys. Soc., Lond.*, **62,** 806.

Lee, T. D., and Yang, C. N., 1960, *Phys. Rev.*, **117,** 22.

Lien, W. H., and Phillips, N. E., 1960, *Phys. Rev.*, **118,** 958.

LINDHARD, J., 1954, *Kgl. Danske Videnskab. Selskab, Mat-Phys Medd.*, **28,** No. 8.
LUTTINGER, J. M., 1960, *Phys. Rev.* (to appear) ; also *Conference on the Fermi Surfaces of Metals* (Report, to be published),
LUTTINGER, J. M., and WARD, J. C., 1960, *Phys. Rev.*, **118,** 1417.
MENDELSSOHN, K., 1956, *Canad. J. Phys.*, **34,** 1315.
MIGDAL, A. B., 1957, *J. exp. theor. Phys., Moscow*, **32,** 399. Translation: *Soviet Physics J.E.T.P.*, **5,** 333.
MONTROLL, E. W., and WARD, J. C., 1958, *Phys. Fluids*, **1,** 55.
MORTON, V., 1960, Thesis, University of Cambridge.
MOTT, N. F., 1956, *Nature, Lond.*, **178,** 1205.
MOTT, N. F., and JONES, H., 1936, *The Theory of the Properties of Metals and Alloys* (Oxford : University Press).
NOZIÈRES, P., and PINES, D., 1958, *Phys. Rev.*, **111,** 442.
PINES, D., 1955, *Solid State Physics*, **1,** 368 (New York : Academic Press).
PIPPARD, A. B., 1957, *Phil. Trans.* A, **250,** 325 ; 1960, *Rep. Prog. Phys.*, **23,** 176.
PRATT, G. W., 1960, *Phys. Rev.*, **118,** 462.
QUINN, J. J., and FERRELL, R. A., 1958, *Phys. Rev.*, **112,** 812 ; 1959, Technical Report (to be published ?).
RENEKER, D. H., 1959, *Phys Rev.*, **115,** 303.
SAMPSON, J. B., and SEITZ, F., 1940, *Phys. Rev.*, **58,** 633.
SCHUMACHER, T. R., and SLICHTER, C. P., 1956, *Phys. Rev.*, **101,** 58.
SEITZ, F., 1940, *The Moderm Theory of Solids* (New York : McGraw-Hill).
SHOENBERG, D., 1957, *Prog. Low Temp. Phys.*, **2,** 226 ; 1960, *Phil. Mag.*, **5,** 105 : also *Conference on the Fermi Surfaces of Metals* (Report, to be published).
SKINNER, H. W. B., 1940, *Phil. Trans.* A, **239,** 95.
SPECTOR, H. N., 1960, *Phys. Rev.* (to appear).
STERN, E. A., 1960, *Conference on the Fermi Surfaces of Metals* (Report, to be published).
WILSON, A. H., 1953, *The Theory of Metals.* 2nd edition. (Cambridge : University Press).
WOLFF, P. A., 1959, *Phys. Rev.*, **116,** 544.
ZIMAN, J. M., 1960, *Electrons and Phonons* (Oxford : University Press).

FOR USERS OF CALCULATORS

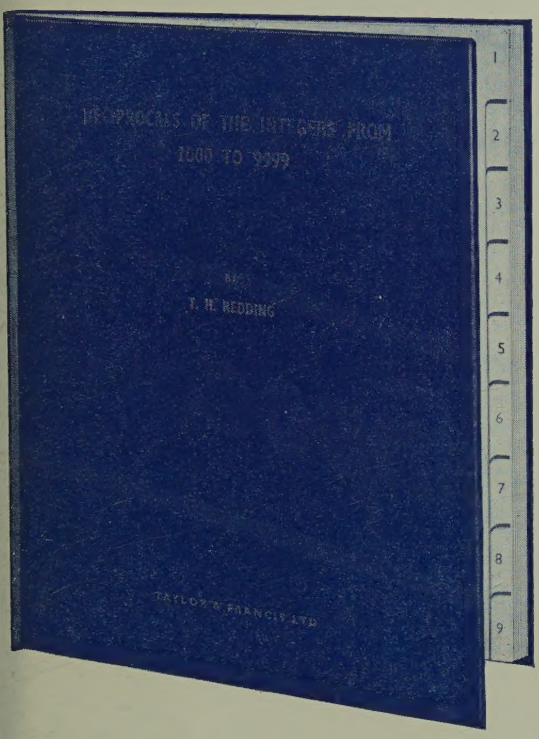

RECIPROCALS OF THE INTEGERS FROM 1000 TO 9999

By T. H. Redding
M.Sc.(Lond.), A.M.I.Mech.E., A.F.R.Ae.S.

Arranged for use with mechanical calculating machines to facilitate the evaluation of quotients and compound fractions

With an Appendix on mechanical barrel-setting calculators

These tables list the 10^6 multiples of the reciprocals of the integers 1000 to 9999 and are displayed as 1000 entries on each of nine double-page spreads which are thumb-indexed (1000 . . . , 2000 . . . , 3000 . . . , . . . etc) to facilitate rapid manipulation with one hand only. The entries are direct reading and are correct to the nearest integer in the third place of decimals.

Although suitable for general use, the tables have been prepared and arranged in a manner particularly suitable for use in conjunction with mechanical computing machines of the "barrel-setting" type in the evaluation of quotients and compound fractions. Equally the tables find application in effecting the evaluation of quotients on adding and listing machines when these incorporate a mechanism for automatically evaluating simple products.

In the first instance it was anticipated that an Appendix dealing with the advantages to be gained by the use of the reciprocal function in conjunction with such machines—and particularly with barrel-setting machines—would suffice to ensure the best use being made of the tables. The present 22-page *Appendix*, however, goes further than this, since the discussion of the tables is prefaced by a description of barrel-setting machines and their (simplest) method of operation in the evaluation of products, quotients and compound fractions. Thus, the description of each calculating procedure is followed by a numerical example with accompanying diagrams to illustrate the keyboard-displays at the beginning, the end, and at intermediate stages in the calculation. The machine-evaluation of series comprising the sum of a number of product or quotient-terms is also discussed. Generally it is hoped that the Appendix will serve as an introduction to mechanical methods of computation and that it will materially assist prospective purchasers in the choice of a machine.

A valuable guide to all users of Computers. Bound in blue publishers case, lettered on the front, with an 18 page table index. Printed on good quality paper for constant use.

Size 10 in. × 8 in.

Price 18s. 6d. *plus postage and packing* 1s. 3d.

Printed and Published by

TAYLOR & FRANCIS LTD

RED LION COURT, FLEET STREET, LONDON, E.C.4

Announcing the new publication

INSTRUMENT CONSTRUCTION

Translated from the Russian

SIRA BRITISH SCIENTIFIC INSTRUMENT RESEARCH ASSOCIATION

Приборостроение

Editor-in-chief: M. E. Rakovskii. Sub-editor: Yu. I. Shendler

The Russians describe their publication as a ' scientific, technical and production ' journal. It covers industrial instruments and instrumentation, automatic control, and production engineering for precision work. The articles which it presents not only introduce new instruments and techniques, they also afford a valuable insight into current Russian practice.

Subscription £6 yearly post free ($17.10 U.S.A. and Canada). A special rate of £3 yearly post free ($8.55 U.S.A. and Canada) is available to University and Technical College libraries.

Single copies 15*s*. each ($2.15 U.S.A. and Canada) plus postage

Orders should be sent to the Subscription Department, Taylor & Francis Ltd.

Produced for the Department of Scientific and Industrial Research by the British Scientific Instrument Research Association, ' Sira ', South Hill, Chislehurst, Kent

Printed and Published for B.S.I.R.A. by

TAYLOR & FRANCIS LTD

RED LION COURT, FLEET STREET, LONDON, E.C.4